ENERGY MINES AND RESOURCES CANADA

DEVELOPMENT OF TOUGH CERAMICS

FINAL REPORT

BY

Dr.D.Ghosh, Mr.L.Leo-Miza, Mr.F.Y.Ibrahim
Dr.J.Jacobs and Dr.S.Das Gupta
The Electrofuel Manufacturing Company Limited

Work on the project was conducted under the auspices of the **Canada Centre for Mineral and Energy Technology, Energy, Mines and Resources Canada**

MICROMEDIA

DSS File No : 06SQ.23440-6-9100
DSS Contract Serial No : 23440-6-9100/01-SQ
CANMET Scientific Authority : Dr.A.K.Kuriakose
: Dr.T.A.Wheat
Dated : 31st March 1988

181 pp

THE ELECTROFUEL MANUFACTURING CO.
9 Hanna Avenue, Toronto, Ontario, Canada M6K 1W8 Tel. (416) 535-1114 Fax. (416) 535-2361

Executive Summary

On behalf of Canmet-Energy, Mines and Resources, the Electrofuel Manufacturing Co. conducted this research and development program in the area of zirconia toughened ceramics for structural applications. The program objectives of developing transformation toughened ceramics and processing techniques to produce them have been achieved with successful development of the following materials :

- Yttria modified tetragonal zirconia polycrystals.
- Ceria modified tetragonal zirconia polycrystals.
- Alumina toughened zirconia.
- Zirconia toughened alumina with yttria additions.
- Zirconia toughened alumina without yttria additions.

The process and composition optimization has been carried out to yield products with good density, hardness and toughness values. Depending on the application, an optimum combination of properties and cost can be engineered based on data generated in this program.

It is suggested that transformation toughened ceramics could have near term applicability in a number of wear and structural applications, such as nozzles, wear parts and cutting tools.

Sommaire Executif

De la part du Centre Canadien de la Technologie des Minereaux et de l'Energie(Energie Mines et Ressources), la Compagnie Electrofuel Manufacturing a dirigé ce programme de recherche et de développement sur le sujet des ceramiques qui sont rendues plus resistantes par la zirconia .

Les objectifs de ce programme consistaient à développer (a) des céramiques qui par la transformation et le traitement étaient rendues plus résistantes (b) les tecaniques necessaires pour les fabriquer. Ces objectifs ont été realisés avec succes dans avec le developpement des matereaux ci-dessous :

1. Les polycrystals de la zirconia tetragonal qui sont modifiés par l'yttria .
2. Les polycrystals de la zirconia tetragonal qui sont modifiés par le ceria .
3. La zirconia qui est rendue plus resistante par l'alumina .
4. L'alumina qui est rendu plus resistante par la zirconia avec une addition de l'yttria .
5. Alumina qui est rendu plus résistants par la zirconia sans l'addition de l'yttria.

Le traitement et la composition optimums étaient réalisés pour obtenir des produits de bonne densité et de bonne dureté . Avec les données et les informations engendrées par ce programme. il est bien possible d'obtenir une combination optimum des propertes et du prix. Il est prévu que les céramiques rendues plus resitantes par la transformation vont avoir des applications presque matures dans le futur prochain. avec des applications structurales et d'usure telles que les tuyères, les pièces d'usure et les outils coupants.

TABLE OF CONTENTS

Chapter	Description	Page
1.	Introduction	1
	1.1 Background	1
	1.2 Program Objectives	2
	1.3 Literature Review	3
	1.4 Zirconia Toughened Ceramics	6
	1.5 Selection of Systems	8
	1.6 Applications	17
2.	Powder Characterization	20
	2.1 Alumina	21
	2.2 Zirconia	26
	2.3 Silicon Carbide Whiskers	31
3.	Processing	38
	3.1 Grinding	40
	3.2 Mixing	41
	3.3 Drying	48
	3.4 Slip Casting	50
	3.5 Cold Pressing	50
	3.6 Sintering	54
	3.7 Hot Pressing	57

Chapter	Description	Page
4.	Experimental Procedures	59
	4.1 Density	60
	4.2 Shrinkage	60
	4.3 XRD Phase Analysis	63
	4.4 Hardness	76
	4.5 Fracture Toughness	78
	4.6 Microstructure	97
5.	Results and Discussions	98
	5.1 Zirconia Based Materials	98
	5.2 ZTA with Yttria	112
	5.3 ZTA without Yttria	120
	5.4 ZTA with SiC Whiskers	127
	5.5 Hardness	127
	5.6 Hardness-Fracture Toughness Relationship	130
	5.7 Toughness vs Cost	132
6.	Conclusions	134
7.	Future Directions	140

Chapter	Description	Page
8.	Appendices	141
A.	Applications	141
	1. Cutting Tools	143
	2. Dies for Extrusion, Deep Drawing & Pressing	148
	3. Textile Thread Guides	149
	4. Wire Drawing Step Cones	149
	5. Paper Machine Parts	151
	6. Pump Seals and Bearings	153
	7. Printed Circuit Industry	155
	8. Armour	156
	9. Engine Components	156
	10. Nozzles for Slurries, Sand Blasting, etc.	159
B.	Bibliography	161

1. INTRODUCTION

The following is a report on the work that has been completed under the contract No. 06SQ.23440-6-9100 entitled "DEVELOPMENT OF TOUGH CERAMICS" carried out on behalf of CANMET - Energy, Mines and Resources, Canada.

Under this contract, The Electrofuel Manufacturing Company Limited conducted Research & Development work in the area of zirconia (transformation) toughened ceramics intended for structural applications.

1.1 Background

Ceramic materials have a number of intrinsic advantages over metals, such as higher hardness, wear resistance, high temperature stability and strength, corrosion/erosion resistance, etc. In spite of these favourable properties, they have not found widespread use as structural material due to one major overiding weakness : low fracture toughness. Low fracture toughness of ceramic materials makes it sensitive to processing flaw size, and hence, unreliable in service. Over the years, attempts to toughen ceramics by generating surface compressive stresses and introducing second phase particles enjoyed modest success. However, since mid 1970's, a new class of composite materials based on phase transformation from tetragonal to monoclinic zirconia has been discovered. This has led to the development of ceramic materials with high strength, toughness and reliability, in some cases approaching hard metals and cermets.

Recognizing the commercial importance of developing tough ceramics, the Department of Energy, Mines and Resources initiated a program at The Electrofuel Manufacturing Company Limited to develop advanced ceramic materials for structural applications based on zirconia transformation toughening.

1.2 Program Objectives

With the general objective of developing tough ceramic materials for structural applications, the immediate objectives of the program were :

* Conduct a comprehensive up-to-date literature survey on the zirconia toughened ceramics, and, based on this survey and consultation with the Scientific Authority select the most promising system for study.

* Prepare test materials in these systems by different ceramic processing techniques.

* Characterize these materials in terms of phase compositions, microstructure, strength and fracture toughness.

1.3 Literature Review

A comprehensive up-to-date literature review was done in this program, and, summarized in a 86-page report entitled "Literature Review on Tough Ceramics", which was submitted to Energy, Mines and Resources in August 1987. Table 1.1 shows the "Table of Contents" of that report and it can be seen that topics reviewed included zirconia phase transformations, toughening mechanisms, processing, microstructural aspects, zirconia toughened systems and conclusions and recommendations on systems.

There is a vast amount of published literature and patents in this area in the last 13 years. Since the publication of the article "Ceramic Steel ?" in Nature in 1975 by Garvie and co-workers, zirconia transformation toughening has been the subject of intense worldwide research. In addition to 58 papers reviewed in the above Report, the important sources of technical papers gathered on this subject are contained in the following :

Source	No.of papers
1.Proc.First Int.Conf.on Sci.& Tech. of Zirconia, Cleveland 1980 Advances in Ceramics,3,A.H.Heuer & L.W.Hobbs(Ed.)	30
2.Proc.Second Int.Conf.on Sci.& Tech. of Zirconia, Stuttgart 1983 Advances in Ceramics,12,N.Claussen,M.Ruhle & A.H.Heuer	77

TABLE OF CONTENTS

1. Introduction 1

2. Zirconia structure and phase transformation 4
    2.1 General Background 4
    2.2 Phase transformation 4

3. Toughening mechanism 14
    3.1 Transformation toughening 16
    3.2 Microcracking toughening 21
    3.3 Crack deflection toughening 25

4. Microstructural aspects 27

5. Processing 35
    5.1 Powder processing 35
    5.2 Sintering 41

6. Zirconia toughened systems 45
    6.1 Ceramics based on PSZ 45
        6.1.1 Conventional PSZ 45
        6.1.2 Fine grained PSZ 48
        6.1.3 TZP 52

    6.2 Zirconia toughened ceramics 59
        6.2.1 Mullite 60
        6.2.2 Alumina 61
        Applications 67
        6.2.3 Spinels 71
        6.2.4 Aluminum titanates 72
        6.2.5 Silicon carbide 74
        6.2.6 Silicon nitride 78
        6.2.7 Titanium diboride 78
        6.2.8 Applications 79

7. Conclusions 82

8. References 83

Table 1.1. Table of Contents from "Literature Review on Tough Ceramics"

3.Proc.Third Int.Conf.on Sci.& Tech. of Zirconia, Tokyo 1986 Advances in Ceramics,24	—
4.Journal, American Ceramic Society Special Issue on Zirconia, March 1986 Special Issue on Zirconia, July 1986	53
5.Proc.Int.Symp.on Engineering Ceramics (Dec.1984) Engineering Ceramics 1984,M.Ish-Shalom & D.G.Brandon (Ed.)	15

In addition to Journal of American Ceramic Society, papers on zirconia toughened ceramics frequently appear in the following publications :

* Journal of Materials Science
* Journal of Materials Science Letters
* Journal of Austr.Ceram.Soc.
* Yogyo-Kyokai-shi
* Ber.Dtsch.Keram.Ges.

A list of most recent publications, in addition to the above papers, is given in Appendix B under "Bibliography".

1.4 Zirconia Toughened Ceramics (ZTC)

As discussed above, zirconia toughened ceramics (ZTC) represent a new class of high performance ceramics with spectacular strength and toughness properties. The strengthening and toughening of zirconia and other ceramic matrices are achieved by utilizing the tetragonal (t) to monoclinic (m) martensitic phase transformation of zirconia, with its associated large volume increase (3-5%). While the exact mechanisms of toughening still remain subject of active discussions, it is generally recognized that the predominant mechanisms include :

* microcrack toughening
* stress induced transformation toughening
* crack deflection toughening

These mechanisms can act singly or in combination, and are discussed in detail in the Report on "Literature Review".

Following Claussen, the different ZTC microstructures can be schematically grouped into three classes (Fig.1.1) :

* Ceramics based on partially stabilized zirconia (PSZ)
* Dispersed zirconia ceramicss
* Complex zirconia systems

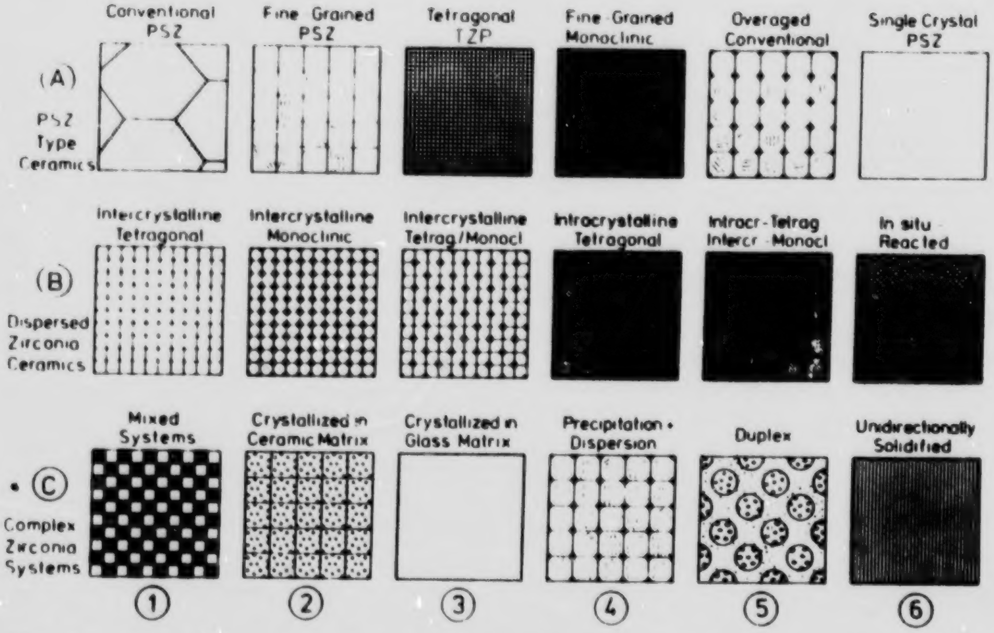
Conventional PSZ
Fine Grained PSZ
Tetragonal TZP
Fine Grained Monoclinic
Overaged Conventional
Single Crystal PSZ
(A)
PSZ Type Ceramics
Intercrystalline Tetragonal
Intercrystalline Monoclinic
Intercrystalline Tetrag/Monocl
Intracrystalline Tetragonal
Intracr-Tetrag Intercr-Monocl
In situ Reacted
(B)
Dispersed Zirconia Ceramics
Mixed Systems
Crystallized in Ceramic Matrix
Crystallized in Glass Matrix
Precipitation + Dispersion
Duplex
Unidirectionally Solidified
• (C)
Complex Zirconia Systems
①
②
③
④
⑤
⑥

Fig. 1.1 Classification of ZrO_2-toughened ceramics (ZTC) based on typical microstructural features. The different ZTC types are presently being produced or studied.

Not all microstructures shown are technologically important, some being laboratory curiosity only. Nevertheless, the classifications given by Claussen does provide an excellent tool to the materials scientists to explore new and useful combinations of the described microstructures.

1.5 Selection of Systems

Based on the above Report on "Literature Review on Tough Ceramics", and extensive discussions with Professor David Green (consultant to the project) and the Scientific Authority, it was decided to concentrate on the following systems :

System 1 : Based on zirconia matrix : such as partially stabilized zirconia (PSZ), tetragonal zirconia polycrystals (TZP), alumina toughened zirconia (ATZ).

System 2 : Based on alumina matrix (with stabilizer additions) : zirconia toughened alumina (ZTA) with yttria stabilizer additions.

System 3 : Based on alumina matrix (without stabilizer additions) : ZTA without yttria additions.

System 4 : Based on alumina matrix : with addition of zirconia and silicon carbide whiskers.

System 1 : Zirconia based matrix

As described in Table 1.2, conventional zirconia ceramics partially stabilized by the addition of MgO or CaO are usually sintered in the c solid solution range at relatively high temperatures, and hence, consist of large c grains (50-100 um) within which are dispersed t precipitates. Mg-PSZ is fairly mature material and is commercially available for applications such as metal forming tools, dies, pump seals and bearings, etc.However its strength is limited to 700-800 MPa due to its coarse grain size. On the other hand, 100% tetragonal zirconia (TZP), partially stabilized by yttria or rare earth oxides, can be obtained with very fine microstructure which results in exceedingly high strength and toughness. Strengths in excess of 2 GPa and toughness over 15 MPa.m^{½} are achievable in zirconia systems, although these exceptional strength and toughness cannot be currently realized in the same material. Swain and Rose (1986) have summarized strength and toughness data for Y-TZP,Ce-TZP, Mg-PSZ and Y-TZP/Al_2O_3 systems as shown in Figure 1.2. It can be seen that in Mg-PSZ system, the strength increases with increasing K_{Ic} reaching a maximum at ~10-11 MPa.m^{½} before decreasing for higher toughness materials. The maximum strength is 800 MPa. The figure identifies two regimes of toughness/strength relationship. Below K_{Ic} = 11 MPa.m^{½}, the maximum strength is flaw size dependent and the strength is virtually as predicted by critical flaw size C_f = 100 um. Above K_{Ic} = 11 MPa.m^{½}, the strength is transformation controlled. Y-PSZ shows a similar trend to Mg-PSZ with the maximum occuring

Table 1.2 PRECIPITATED ZIRCONIA CERAMICS

TYPE	MATERIAL	MICRO-STRUCTURE	PROCESSING	PROPERTIES AND COMMENTS
A1	PSZ Convent.	Large grain (50-100 um) cubic with dispersed precipitates of tetragonal	Sintering 1600 - 1900 C Needs Ageing to Optimize Transformation	Strength 700-800MPa Used as Metal Forming Tools, Dies, bearings. Being tested for Automotive components
A2	FINE GRAINED PSZ	Contains Cubic and Tetragonal Precipitates < 10 um	Refind Powder Processing Technique. Rapid Densification to avoid grain Growth or Grain Growth Inhibitors	RT Strength >1000 MPa after inducing surface compressive Stresses. Applications same as A1.
A3	TETRAGONAL ZrO_2 POLYCRYST	-Fine Grained -Single Phase Material with Yttria rare earths, retain t form due to Constrains 0.1 - 1 um	Similar to A2. With 1.5-3.5 Mol % Yttria sinter at 1300 -1450 C	Toughest Material Stronger than all zirconia ceramics At medium Temp. loses Strength Presently tested heat engine and metal forming applications
A4	FINE GRAINED <15% MgO	1-5 um Grain With Highly Dispersed MgO Cracking at Grain Bounds.	Hydro-thermal Synthesis Aged to achieve desired grain size	Low Strength Good thermal Shock Properties.
A5	OVERAGED CONVENTIONAL	Three Phase Material Complex MIcrostruct. Modificat. of A1 and A4	Subeutectoid Ageing of Presintered Conventional Mg - PSZ	Excellent Thermal Shock Prperties
A6	SINGLE CRYSTAL PSZ	Single Cryst. With t Precipitates	Skull Melting	High Strength > 1400 MPa 700 MPa at 1500 C Can be Shaped

Table 1.3 DISPERSED ZIRCONIA CERAMICS

TYPE	MATERIAL	MICRO-STRUCTURE	PROCESSING	PROPERTIES AND COMMENTS
B1	Dispersed t Zirconia in a Ceramic Matrix. (Alumina)	Reduced Matrix Grain Size. Zirconia mainly in t form.	Homogenizing Techniques. Wet Milling Narrow Partc. Size Distrib.	Increase Fracture Toughness. Very High Strength as compared to Matrix alone.
B2	Dispersed mZirconia in Ceram. Matrix. (Zircon)	Particle Size Larger than that of B1	Prepared Similar Way as B1	Microstructure Induc. Stable Crack Growth. Improved Therm.Shock Resist. - Nozzles for Continous Casting
B3	Dispersed m and t Zirconia	Most Common Microstruct. of the Dispsion Type ZTC	Conventional Ceramic Mix. Technique.	Properties between B1 and B2. Alumina Based ZTC Cutting Tools
B4	tZirconia in Coarse Grained Ceramics			Prepared only for TEM Analysis.
B5	Medium Grained t Partc. Intercrat & m Part. at Grain Boundars.		Sol-Gel Tech. Alumina & Zirconia	Properties Similar to A5 PSZ
B6	In- Situ Reacted Microstructure	B-Type & C-Type Simpler to Prepare	Dispersed Zircon or Zr Compounds Fabrication Techniques	

Table 1.4 PRECIPITATED ZIRCONIA CERAMICS

TYPE	MATERIAL	MICRO-STRUCTURE	PROCESSING	PROPERTIES AND COMMENTS
A1	PSZ Convent.	Large grain (50-100 um) cubic with dispersed precipitates of tetragonal	Sintering 1600 - 1900 C Needs Ageing to Optimize Transformation	Strength 700-800MPa Used as Metal Forming Tools, Dies, bearings. Being tested for Automotive components
A2	FINE GRAINED PSZ	Contains Cubic and Tetragonal Precipitates < 10 um	Refind Powder Processing Technique. Rapid Densification to avoid grain Growth or Grain Growth Inhibitors	RT Strength >1000 MPa after inducing surface compressive Stresses. Applications same as A1.
A3	TETRAGONAL ZrO_2 POLYCRYST	-Fine Grained -Single Phase Material with Yttria rare earths, retain t form due to Constrains 0.1 - 1 um	Similar to A2. With 1.5-3.5 Mol % Yttria sinter at 1300 -1450 C	Toughest Material Stronger than all zirconia ceramics At medium Temp. loses Strength Presently tested heat engine and metal forming applications
A4	FINE GRAINED <15% MgO	1-5 um Grain With Highly Dispersed MgO Cracking at Grain Bounds.	Hydro-thermal Synthesis Aged to achieve desired grain size	Low Strength Good thermal Shock Properties.
A5	OVERAGED CONVENTIONAL	Three Phase Material Complex MIcrostruct. Modificat. of A1 and A4	Subeutectoid Ageing of Presintered Conventional Mg - PSZ	Excellent Thermal Shock Prperties
A6	SINGLE CRYSTAL PSZ	Single Cryst. With t Precipitates	Skull Melting	High Strength > 1400 MPa 700 MPa at 1500 C Can be Shaped

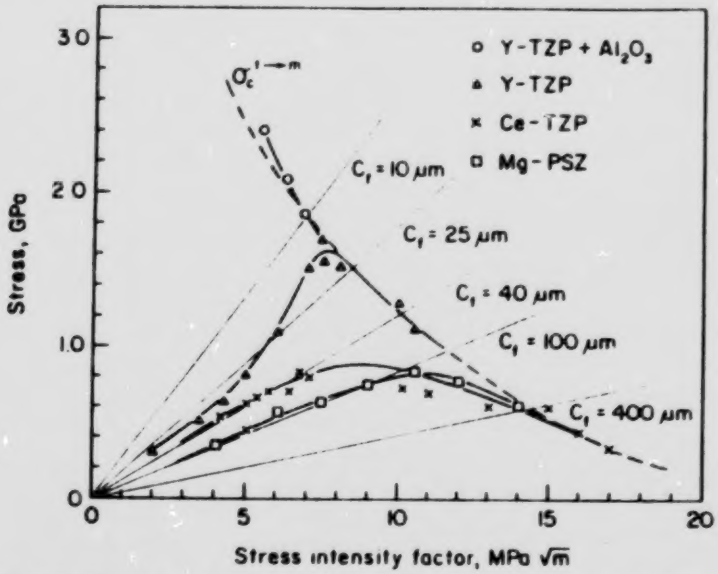

Fig. 1.2 Plot of strength vs toughness for transformation-toughened ceramics. This figure is discussed in more detail in this issue by Swain and Rose.

at $\sigma \sim 1.5$ GPa and $K_{Ic} = 8$ MPa.m$^{1/2}$. Upto $K_{Ic} = 5$ MPa.m$^{1/2}$, the strength of Y-PSZ is predicted by a critical flaw size $C_f = 25$ µm, indicating that the fine grained materials have much smaller critical flaw size. Above $K_{Ic} = 5$, the strength is in excess of this flaw size. The higher strengths are probably related to surface compressive stresses resulting from grinding which are more effective in fine grained than coarse grained PSZ materials. However, Y-PSZ also show a transition from flaw controlled strength to transformation limited strength at $K_{Ic} > 8$ MPa.m$^{1/2}$.

Exceptionally strong PSZ can be made by addition of alumina to Y-PSZ. Figure 1.2 shows data for 3 mole% Y-PSZ to which upto 20 wt% of alumina has been added, resulting in strength as high as 2.4 GPa. However, this increase in strength is accompanied by a reduction in K_{Ic} from 9 to 6 MPa.m$^{1/2}$. The criticcal flaw size can be calculated to be < 5 µm which agrees with SEM observations. Alumina thus appears to decrease the critical defect size of these TZP materials. This material has been called "alumina toughened zirconia" (ATZ).

Finally, Figure 1.2 also gives the data for Ce-TZP system which has a maximum strength of only about 700 MPa at $K_{Ic} \sim 6$-7 MPa.m$^{1/2}$. However, in this system high toughness of > 17 MPa.m$^{1/2}$ can be achieved, with specimens to the right of the peak displaying non linear stress strain curves and permanent strain at failure (pseudoductility).

It was decided to manufacture all these zirconia based materials at Electrofuel from commercially available powders, with the exception of Mg-PSZ which is well known mature material.

System 2 : ZTA with yttria additions

The intercrystalline dispersion of t-ZrO_2 particles in a fine-grained matrix usually leads to very high strengths compared to the matrix alone. The inter-crystalline dispersion can be obtained either by homogenizing techniques, i.e.fine grinding and mixing (attrition milling), or by wet chemical techniques. The retention of all ZrO_2 particles in their t-form is however difficult to achieve, unless great care is taken to achieve a narrow particle size distribution. For ZrO_2 volume fractions higher than 0.15, small amounts of stabilizers, e.g. 0.5 - 2 mole% Y_2O_3 are usually required to have most particles retain their t-symmetry at room temperaure. In reality, the microstructure consists of the matrix phase (s) with most of the zirconia retained in tetragonal form by matrix constraint, while some are converted to monoclinic state depending on grain size and stabilizer content.

The material most often tested as a candidate for improved performance through transformation toughening by the addition of tetragonal zirconia is alumina. Combination of the two materials are being widely varied to find the optimum composition for strength, fracture toughness, and wear properties.

One of the primary advantages, by combining these materials, that was noted was the effect of alumina in suppressing the tetragonal to monoclinic transformation of zirconia because of the higher modulus of elasticity of alumina. Conversely with zirconia addition to alumina, grain growth that normally occurs in sintering alumina is suppressed.

It was decided to work on the alumina-zirconia system wherein the second phase zirconia particles contained the optimum content of stabilizer to retain it in the tetragonal phase.

System 3 : ZTA without yttria additions

As mentioned above, upto a certain critical size and volume fraction, the zirconia particles can be retained in tetragonal form just by alumina matrix constraint. Below 10 volume percent almost all zirconia can be retained in tetragonal form in alumina matrix, without any stabilizer additions, if the zirconia grains can be maintained below the critical size of about 2 µm. This may be feasible by attrition milling very fine powder or by chemical route. This system can potentially yield a high performance cost ratio, as expensive yttria additions are eliminated and smaller zirconia additions are required.

System 4 : ZTA with SiC whiskers

Unfortunately all zirconia toughened systems lose its strength and toughness at elevated temperatures (>800° C). Fibre reinforcement seems to be promising strategy to strengthen zirconia toughened ceramics at higher temperatures as reported by Claussen, Weisskopf and Rühle (1986). Figure 1.3 shows strength of 3Y-TZP and 3Y-TZP-30 v% SiC whisker material as a function of temperature. It can be seen that SiC containing material retains higher strength at 1000° C. Only selected number of heats were hot pressed in this system.

1.6 Applications

A number of applications of zirconia toughened ceramic materials appropriate for commercialization in the Canadian context has been identified from literature, patents and discussions with users and ceramic vendors :

1. Cutting tools
2. Dies (for extrusions, drawing, pressing, etc.)
3. Textile thread guides
4. Wire drawing
5. Pulp and paper
6. Pump seals and bearings
7. Printed circuit industry
8. Armour
9. Engine components
10. Nozzles for slurries, sand blasting, etc.

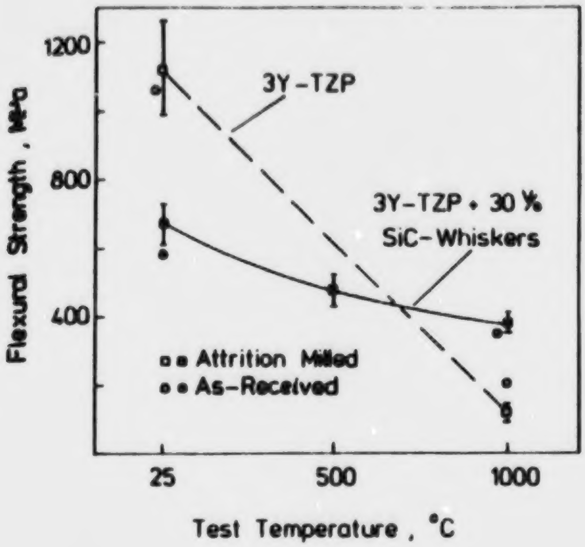

Fig. 1.3 Flexural strength of TZP with and without SiC whisker reinforcement. Thermal mismatch stresses reduce strength at room temperature, whereas modulus load transfer becomes effective at 1000°C.

These applications are described in detail in Appendix A. In many of these applications, high purity alumina is presently being used, and, we believe use of zirconia toughened alumina will further improve the performance cost ratio. There is a great incentive to address the high end alumina market where its performance at the present time is only marginal.With cost effective System 3, it may be possible to address even low cost alumina market.

2. POWDER CHARACTERIZATION

Starting powder characteristics have a profound effect on the processing and the final properties of the sintered product. The general quality requirements for powder in the manufacture of advanced ceramic components are shown in Table 2.1. The powder purity, fineness, morphology, crystal structure and sinterability are important considerations when selecting powders for any application. Considerable amount of this data is supplied by the producers. In this program, a selected number of commercially available alumina and zirconia powders were characterized by X-ray diffraction and SEM techniques, and evaluated by experimentation.

2.1 Alumina Powders

A number of high purity, fine alumina powders are commercially available. Large tonnages of alumina are produced by the Bayer's process from Bauxite ore, most of which is consumed in the production of metallic aluminium. While Bayer alumina is relatively inexpensive (less than $0.50/lb), they are not of sufficient purity and fine particle size to be appropriate for the manufacture of advanced structural components.

TABLE 2.1 QUALITY REQUIREMENTS FOR CERAMIC POWDER.

Quality	Requirements
Powder Fineness	Submicron size
	Narrow size distribution
	High surface area (10-20 m^2/gm)
Powder Morphology	Spherical shape
	Mono size
	Required crystalline phases
	Required crystallite size
	High lattice defects
Powder Purity	Very high purity
	Minimum concentration of undesirable impurities (ppm)
Physical State	Minimum agglomeration
	High packing density
Sinterability	Shrinkage
	Density

There are six commercial processes for the production of high purity alumina :

i) modified Bayer process
ii) thermal cracking of ammonium alum
iii) thermal cracking of ammonium Al carbonate
iv) hydrolysis of organometallic compounds
v) ethylene chlorohydrin process
vi) spark discharge process

These processes are summarized in Figure 2.1 (reproduced from "Advanced Ceramics" Ont. Min. Northern Dev.& Mines)and the qualities of the powders produced by these processes are listed in Table 2.2. and Table 2.3. The quality of powders from modified Bayer process, in which harmful impurities like Na are reduced, has been improving steadily, such that submicron powder with purity better than 99.95% are now available at a price less than $3.0/lb. Alum or other chemical routes normally yield high purity (> 99.99%), high surface area (BET 5-30 m^2g)reactive powder. However, they are sold at a premium price (~$20-30/lb), and are considered in critical applications only.

In this program we have evaluated the following grades of powders :

1. Alcoa A-16SG (Modified Bayer process), $1.50/lb
2. Ceralox HPA (Chemical), $8.0/lb
3. Sumitomo AKP-30 (Organometallic), $20.0/lb
4. Baikowski CR-10 (Alum process), $30.0/lb

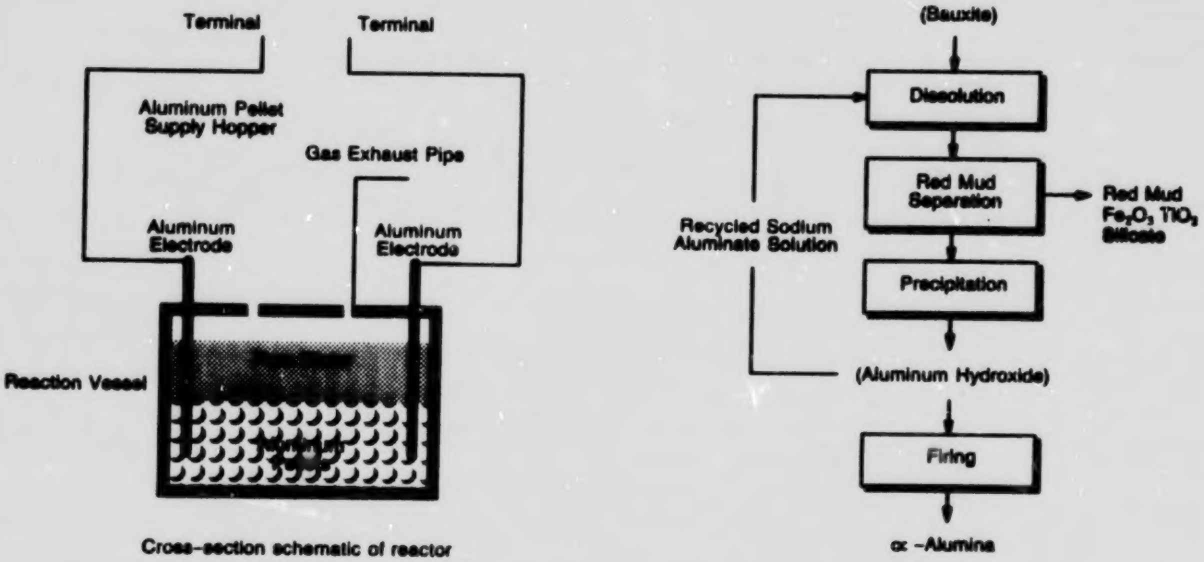
Terminal
Terminal
Aluminum Pellet Supply Hopper
Gas Exhaust Pipe
Aluminum Electrode
Aluminum Electrode
Reaction Vessel
Cross-section schematic of reactor
(Bauxite)
Dissolution
Red Mud Separation
Red Mud
Fe₂O₃ TiO₂
Silicate
Recycled Sodium Aluminate Solution
Precipitation
(Aluminum Hydroxide)
Firing
α -Alumina

Thermal Cracking Of Ammonium Alum

$$Al_2(SO_4)_3 + (NH_4)_2SO_4 + 24H_2O \rightarrow 2\ NH_4Al(SO_4)_2 \cdot 12H_2O \xrightarrow[\text{heat}]{} 2\ Al_2O_3$$

Thermal Cracking Of Ammonium Aluminum Carbonate

$$8\ NH_4HCO_3 + (NH_4)nAl_2(SO_4)_4 \rightarrow 2\ NH_4AlO(OH)HCO_3 + 4\ (NH_4)_2SO_4 + 6\ CO_2 + 2\ H_2O \xrightarrow[\text{heat}]{} 2\ Al_2O_3$$

Hydrolysis Of Organometallic Compound

$$2\ AlR_3 + 6\ H_2O \rightarrow Al_2O_3 \cdot 3H_2O + 6\ RH \xrightarrow[\text{heat}]{} Al_2O_3$$

$$2\ Al(OR)_3 + 6\ H_2O \rightarrow Al_2O_3 \cdot 3H_2O + 6\ ROH \xrightarrow[\text{heat}]{} Al_2O_3$$

(R = alkyl group such as CH3 or C_2H_5)

Ethylene Chlorohydrin Process

$$2\ NaAlO_2 + 2\ ClCH_2CH_2\ OH \rightarrow Al_2O_3 \cdot nH_2O + 2\ \underset{\diagdown O \diagup}{CH_2-CH_2} + 2\ NaCl$$

$$Al_2O_3 \cdot nH_2O \xrightarrow[\text{heat}]{} Al_2O_3 \cdot 2H_2O$$

$$\underset{\diagdown O \diagup}{CH_2-CH_2} + HCl \rightarrow ClCH_2CH_2OH$$

Figure 2.1 *Production processes for high purity alumina: spark discharge process (left), Bayer process (right).*
Source: Japan Fine Ceramics Association, Annual Report, 1986.

TABLE 1,7. PROPERTIES OF HIGH PURITY ALUMINA POWDERS PRODUCED BY VARIOUS PROCESSES.

	Sumitomo Chem. Co.						Showa-Keikinzoku Co.			Iwatani Chem.			Sin-Nihon Chem. Co.
Production Process	Hydrolysis of organo-metallic compound			Modified Bayer			Thermal cracking of alum			Spark Discharge			Ethylene Chlorohydrin
Grade	AKP-20	AKP-30	AKP-HP	A-HPS40	A-HPT	A-HPT-F	UA-5035	UA-5055	UA-5105	RA-40	RG-40	RK-40	L-30
Crystal Phase	α	α	α	α	α	α	α	α	α	α			α
Purity %	>99.99	>99.99	>99.995	>99.99	>99.99	>99.99				>99.99	>99.99	>99.99	99.98–99.995
Average particle size μm	0.5	0.4	0.4	0.4	0.4	0.3	0.4*	0.3*	0.25*	0.83	0.51	0.78	0.4**
BET m^2g	4–6	5–10	4–10	6–8	5–6	5–8	3	5	10	5.3	48.0	282.0	5–40
True density g/cc							3.97	3.97	3.88	3.93	3.70	3.14	
Bulk density	0.7–1.1	0.7–1.0	0.6–1.0	0.8	0.5	0.5	0.6	0.6	0.6	0.40	0.39	0.46	0.20–0.40
Tapped density g/cc	1.1–1.5	1.1–1.5	0.9–1.3	1.2	1.2	1.2	1.0	1.0	1.0	0.95	0.93	0.95	0.40–0.80
Impurities (ppm)													
Si	<40	<40	<8	10	8	8		6			20		40 <10 <10
Na	<10	<10	<3	20	15	15		10			6		65 50 10
K								5					
Mg	<10	<10	<3	<10	4	2		<1					
Ca				10	2	2		<2					
Fe	<20	<20	<8	7	7	7		4			25		60 10 10
Cu	<10	<10	<3										
Ga								<2					25 <10 <10
Cr								<2					

*α–*Grain size*

** *by SEM*

Source: Japan Fine Ceramics Association, Annual Report, 1986.

Table 2.2

Table 2.3 Commercial ceramic grade alumina

Alumina	Grade	Major phase	Particle size, m	Surface area BET, m²/gm	Overall purity %	Chemical analysis wt% ppm Na	Si	Fe	Notes
Baikowski	CR-10	Alpha	0.15	10 + 1	99.99	30	10	20	Alum process-1000 lbs
Baikowski	CR-30	Alpha	0.05	30 + 1	99.99	30	10	20	Alum process-1000 lbs
Linde	A	Alpha	0.3	10 - 18	99.98				Alum process-1000 lbs
Linde	C	Alpha	1.0	1.0-4.0	99.98				Alum process-1000 lbs
Reynolds	RC-122		2.0		99.7				Bayer process-40,000 lbs
Reynolds	RC-152		1.5		99.7				Bayer process-40,000 lbs
Reynolds	RC-172		0.65		99.7				Bayer process-40,000 lbs
Reynolds	RC-HP	Alpha	0.55	6 - 8	99.95	<0.008	0.016	0.004	Bayer process-40,000 lbs
Reynolds	RC-HP DBM				99.95				Bayer process-40,000 lbs
Reynolds	RC-20	Alpha	2.0		99.3	0.5	0.02	0.03	Bayer process-40,000 lbs
Reynolds	RC-20DF	Alpha	2.0		99.3				Bayer process-40,000 lbs
Reynolds	RC-23	Alpha	1.0		99.3	0.3	0.02	0.03	Bayer process-40,000 lbs
Reynolds	RC-23DM	Alpha	1.0		99.3	0.3	0.02	0.03	Bayer process-40,000 lbs
Kaiser	SA	Pseudoboeh		300		0.03	0.10	0.06	Bayer process-40,000 lbs
Kaiser	WAGN	Pseudoboeh		300		0.03	0.10	0.06	Bayer process-40,000 lbs
Kaiser	B-201	c-p-e			93.6				Bayer process-40,000 lbs
Kaiser	C-SRW	Alpha	4-6	<1	99.2	0.45	0.02	0.02	Bayer process-40,000 lbs
Kaiser	C-SRG	Alpha	4-6	<1	99.2	0.45	0.02	0.02	Bayer process-40,000 lbs
Kaiser	C-SRGB	Alpha	4-6	<1	99.2	0.45	0.02	0.02	Bayer process-40,000 lbs
Sumitomo	AKP-20	Alpha	0.4-0.6	5-10	99.99+	10	40	20	Chem process-66,000 lbs/yr
Sumitomo	AKP-HP50	Alpha	0.1-0.3	4-16	99.995	3	8	8	Chem process-66,000 lbs/yr

$30/lb

$0.5-3/l

$20/lb

The characteristics of these powders are given in Table 2.4. From the Table it is clear that all the chemically derived powders are somewhat superior to modified Bayer alumina (Alcoa A-16 SG) with respect to purity and reactivity (surface area). Although the manufacturer claims average crystallite size 0.3-0.5 µm for A-16 SG, a considerable fraction of "hard" agglomerates were observed in the as received condition after pH dispersion and ultrasonication. These "hard" agglomerates required over 16 hours of ball milling to be broken down. Alcoa A-16 SG also contained substantial harmful impurities like NaO_2 and SiO_2. However, its price is attractive and hence it should be considered in non-critical room temperature applications. Of the chemical powders, Ceralox HPA is attractive due to its favourable price to performance ratio. However, it also contains some "hard" agglomerates and requires some milling before use. In view of the practical thrust of this program we have essentially concentrated on Alcoa A-16 SG and Ceralox HPA grades.

2.2 Zirconia Powder

Zirconia powders are commercially recovered from two mineral sources : baddeleyite, the m-oxide form, and zircon, the silicate $ZrSiO_4$. Most zirconia is produced in arc furnaces by melting zircon sands to yield monoclinic zirconia which is calcined with dolomite to stabilize the tetragonal or cubic phase. Zircon can also be dissociated in a plasma arc furnace to yield uniform zirconia particles with low silica content. A third method involves disolving zircon sand in NaOH, separating

Table 2.4 Alumina powders evaluated in this program

PROPERTY \ POWDER GRADE	ALCOA A-16SG	CERALOX HPA	SUMITOMO AKP-30	BAIKWOSKI CR-10
Major Phase	Alpha	Alpha	Alpha	Alpha
Purity Al_2O_3 (min)	99.5	99.7	99.99	99.90
Na_2O (ppm max)	800	14	10	30
SiO_2 (")	250	25	40	45
Fe_2O_3 (")	100	13	20	20
Av.particle size (μm)	0.3-0.5*	0.6	0.4	0.15
Surface area m^2g	–	8.6	5-10	10
Price	1.50	8.0	20	30

* Crystal size : larger "hard" agglomerates present

the silica and precipitating zirconia. There are three major variations of this method as shown in Figure 2.2. Toyo Soda, producer of fine high purity zirconia powder for ceramic applications, uses the oxychloride process.

Zirconia powder is available in various grades. Pure zirconia powder with monoclinic structure is available as an additive to the other ceramic matrices (Al_2O_3 , Si_3N_4 , mullite, etc.) for toughening, grain refining, sintering, etc. Due to destructive t-m transformation, it cannot be used by itself, but require "stabilizing" additives such as CaO, MgO, Y_2O_3 , rare-earth oxides,etc. A host of commercial zirconia powders with various stabilizer additives in various concentrations are available, as shown in Table 2.5. The arc furnace zirconia is of low purity and too coarse for structural ceramic components. It is mainly used for refractory and other applications. Zirconia made by precipitation from a soluble salt (such as oxychloride) or organometallic compounds is fine, high surface area, high purity powder which is suitable for ceramic applications.

In this program we have evaluated both the pure zirconia (monoclinic) powders and zirconia with various concentrations of yttria (Y_2O_3) and ceria (CeO_2) additives. Table 2.6 gives the important characteristics of pure monoclinic zirconia powders used. It can be seen that both the quality and the price varies considerably between the different producers. While Toyo Soda TZ-0 is the most expensive, it is not the finest or the purest available. On the other hand, the least pure or the coarseest powder, Magnesium Electron, SC15, is not the cheapest. It

Figure 2.2

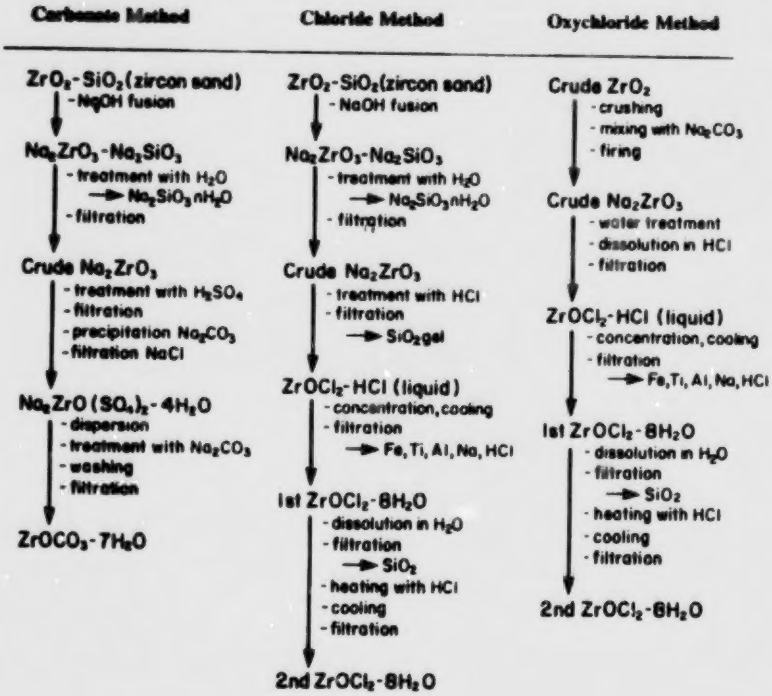
Carbonate Method
Chloride Method
Oxychloride Method
ZrO2-SiO2(zircon sand)
-NaOH fusion
Na2ZrO3-Na2SiO3
-treatment with H2O
Na2SiO3nH2O
-filtration
Crude Na2ZrO3
-treatment with H2SO4
-filtration
-precipitation Na2CO3
-filtration NaCl
Na2ZrO(SO4)2-4H2O
-dispersion
-treatment with Na2CO3
-washing
-filtration
ZrOCO3-7H2O
ZrO2-SiO2(zircon sand)
-NaOH fusion
Na2ZrO3-Na2SiO3
-treatment with H2O
Na2SiO3nH2O
-filtration
Crude Na2ZrO3
-treatment with HCl
-filtration
SiO2gel
ZrOCl2-HCl (liquid)
-concentration, cooling
-filtration
Fe, Ti, Al, Na, HCl
1st ZrOCl2-8H2O
-dissolution in H2O
-filtration
SiO2
-heating with HCl
-cooling
-filtration
2nd ZrOCl2-8H2O
Crude ZrO2
-crushing
-mixing with Na2CO3
-firing
Crude Na2ZrO3
-water treatment
-dissolution in HCl
-filtration
ZrOCl2-HCl (liquid)
-concentration, cooling
-filtration
Fe, Ti, Al, Na, HCl
1st ZrOCl2-8H2O
-dissolution in H2O
-filtration
SiO2
-heating with HCl
-cooling
-filtration
2nd ZrOCl2-8H2O

Carbonate and chloride methods for producing pure zirconia from ores.

Table [illegible]5 Commercial zirconia

Zirconia	Grade	Major phase	Particle size, μ	Surface area BET, m²/gm	Overall purity %	Chemical analysis Si	Fe	Notes	
TAM	[illegible]	mono				0.15	0.02	Arc Furnace	~$2/lb Unacceptable
TAM	CP [illegible]11	mono				0.15	0.02	Arc Furnace	
TAM	Z[illegible]250	mono		2.5		0.7	0.06	Arc Furnace	
TAM	Z[illegible]120	mono		4.2		0.9	0.06	Arc Furnace	
TAM	Z[illegible]70	mono		6.5		1.0	0.06	Arc Furnace	
TOK	TZ-0							Precipitation	$25-40/lb
TOK	TZ-3Y	mono	0.025	15		0.02	0.005	Precipitation	
TOK	TZ-2Y							Precipitation	
TOK	TZ-2.5Y							Precipitation	
TOK	TZ-4Y							Precipitation	
TOK	TZ-6Y							Precipitation	
TOK	TZ-8Y							Precipitation	
Zircar	ZYP unst	mono	0.1	40*	99.3	0.1%		Chloride Salt-100 lbs	$30/lb
Zircar	ZYP [illegible]Y	mono	0.1	40*	99.3	0.1%		Chloride Salt-100 lbs	
						SiO_2	Fe_2O_3		
Harshaw	Electro	mono	50%<0.5	19	99.7	0.03	<0.015%	225* lbs	$8/lb
Harshaw	103	mono	50%0.8-1.	11-14	99.7	0.15	<0.02%	225* lbs	
Mag Elek	S	mono	14.0	2-4	99.0*	0.20		Precipitation-bulk	$5/lb
Mag Elek	SC15	mono	<2.0	4-6	99.0*	0.15		Precipitation-bulk	
Mag Elek	SC101	mono	2.0	15-20	99.0*	0.05		Precipitation-bulk	
Mag Elek	SC4m/oY	psz	25.0	2	99.0*	0.15		Precipitation	$10-15/lb
Mag Elek	SC8m/oY	psz	25.0	2	99.0*	0.15		Precipitation	
Mag Elek	SC5.2m/oY	psz	<0.5	20	99.0*	<0.1		Precipitation	

appears that two powders, Harshaw Electronic Grade and Daiichi Kigenso DK-1, show the best cost to performance ratio of the six powders evaluated. These are submicron powders, with BET surface area 20-25 m^2/g, purity better than 99.6% and priced at $6-8/lb range.

Zirconia powders were mixed with the matrix phase by wet co-milling. Some of the powders required longer milling in order to break down "hard" agglomerates. Especially in case of coarse Mag. Electron SC 15, ball milling as long as 72 hours were required. Other powders were finer and normally required 8 to 16 hours of ball milling.

Table 2.7 gives the various zirconia powders with additives used on this program. All powders except Unitec PSZ-Ce 14 have been made by co-precipitation process which yields fine homogeneous, high purity powders. Unitech powder is made by electrofusion, refining, controlled solidification and grinding process. It also yields high purity fine powder.

2.3 Silicon Carbide Whiskers

Ceramic-ceramic composites reinforced by whiskers or fibres are subject of intense international R&D effort in order to improve the toughness and reliability of monolithic materials. Single crystal silicon carbide (SiC) whiskers are emerging as an important reinforcement material for ceramic (alumina, Si_3N_4, PSZ, etc.) and metal (Al alloys) matrices. A number of

NAME/GRADE-PROPERTIES	Mag.Elctr SC15	Dynamit Nobel-F	Daiichi DK-1	Harshaw Elec.Gr.	Z-Tech SS-Ultra	Toyo Soda TZ-0
STRUCTURE	mono.	mono.	mono.	mono.	mono.	mono.
COMPOSITION						
(Wt%) ZrO_2	99	bal.	99.6	99.7	99.95	99.9
SiO_2	0.15	<0.05	0.02	0.03	0.008	0.09
TiO_2	0.15	0.011	0.10	-	0.018	-
Fe_2O_3	0.02	0.02	0.03	<0.015	0.005	0.03
L.O.I.	0.15	0.90	0.50	0.48	-	-
BET SURF.AREA (M2/g)-	4-6	50-60	25	19	15-20	14
GRAIN SIZE (mm)-	-	0-5	0-5	-	-	-
d50-	2.0	0.7	1.0	0.5	0.2	0.4
PRICE($/lb)-	15	-	6.75	8	15	~35

Table 2.6 Pure zirconia powders used in this program.

NAME/GRADE-PROPERTIES	Zircar ZYP	Toyo Soda TZ-2Y	Daiichi HSY-3	Daiichi HSY-3	Toyo Soda TZ-3Y 20A
STRUCTURE	M	M+T	M+T	T+C	M+T+α
COMPOSITION					
(Wt%) ZrO_2	bal.	bal.	bal.	bal.	75.7
Y_2O_3	1.8	3.74	5.4	10.5	4.2
SiO_2	.2	.09	.2	.2	.1
Fe_2O_3	.04	.03	.05	.05	.03
Al_2O_3	.02	.07	.25	.25	20
BET SURF.AREA (M2/g)-	30-45	14-18	8	~8	15
GRAIN SIZE d50(mm)-	-	0.3	-	-	0.3
PRICE ($/lb)-	61	60	20	25	60

Table 2.7 Zirconia - yttria powders used .

producers make SiC whiskers by the rice hulk or VLS (vapour-liquid-solid) process :

1. Tokai Carbon (Japan)
2. Tateho Chemicals (Japan)
3. Advanced Composite Materials Co. (USA)
4. American Matrix (USA)
5. Alcan (Canada, recent announcement)

SiC whiskers are manufactured in a variety of diameters from 0.3 µm to 3.0 µm, and their length vary from 10 µm to 100 µm. During this program, only Japanese whiskers (Tokai and Tateho) were available to us, and, these have been characterized and tested. Advanced Composite Materials (formerly ARCO Chemicals) reputedly produces the best quality whiskers for use in alumina and other ceramic matrices. However, this whisker is not available in the open market, and, is only sold in pre-mixed form to limited customers. American Matrix and Alcan have made recent entry into this market.

Table 2.8 gives some data on the whiskers used in this program. The impurities Ca, Mg, Fe shown in Table are found in the whiskers as inclusions. Their origin and effect on their properties are not well known. Neither is there any correlation between the bulk oxygen and free carbon analysis and the properties of ceramic composites made from the whiskers. However, a number of studies have established that there is a good correlation between the surface analysis and the properties of the composite. Presence of surface oxide has been demonstrated to adversely affect the whisker pull out and hence

	ARCO	Tateho	Tokai
Crystalline phase	or mixed		
Diameter (m)	0.7	0.4	0.5
Length (m)	30	20-200	40-200
Ca (ppm) (1)	300	800	
Mg	100	80	
Fe	300	400	
Mn	30	200	
Total Carbon (%) (2)	28.7	28.6	
Free Carbon (%)	0.30	0.60	
Oxygen (wt%) (3)	2.3	1.6	
Oxygen (wt%) (4)	1.2	0.6	

(1) Emission Spectroscopy
(2) Leco WR-12; stoichiometric total carbon - 29.96%
(3) Neutron Activation
(4) Inert Gas Fusion

Table 2.8 Reported data for various SiC whiskers

reduce toughness. On the other hand, presence of free carbon on the surface was shown to be beneficial for whisker pull out.

Figures 2.3-2.5 are SEM, micrographs of ARCO, Tateho and Tokai SiC whiskers. It can be seen that there is considerable variation in diameters and lengths, the average diameter being about 0.5 µm. It can also be seen that Japanese whiskers contain more "shots" or non-whisker materials with low aspect ratio. Some cleaning of this non-whisker materials and debris is possible by "washing" i.e. settling procedure. In the literature there are references to pretreatment of whiskers by acid washing (HF), thermal treatment in argon or vacuum, coating, etc. In this program only "cleaning" by settling was tried.

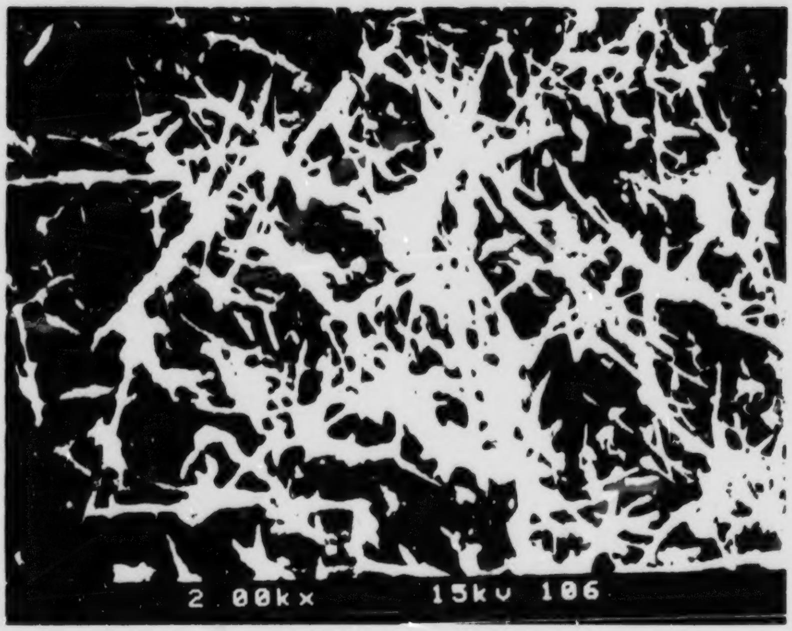
2 00kx
15kv 106

Fig.2.3.

S.E.M. micrograph of Arco SiC whisker

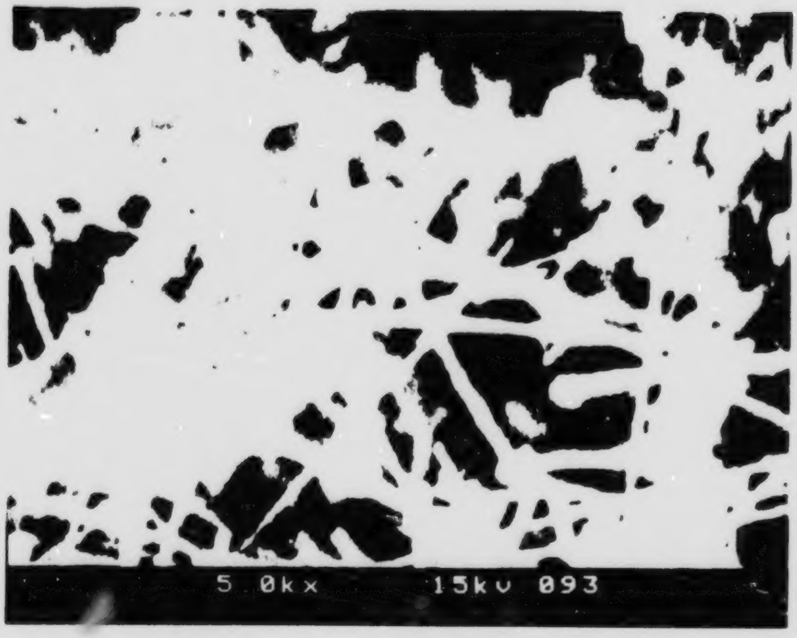
5 0kx
15kv 093

Fig.2.4 . SEM micrograph of Tateho SiC_W

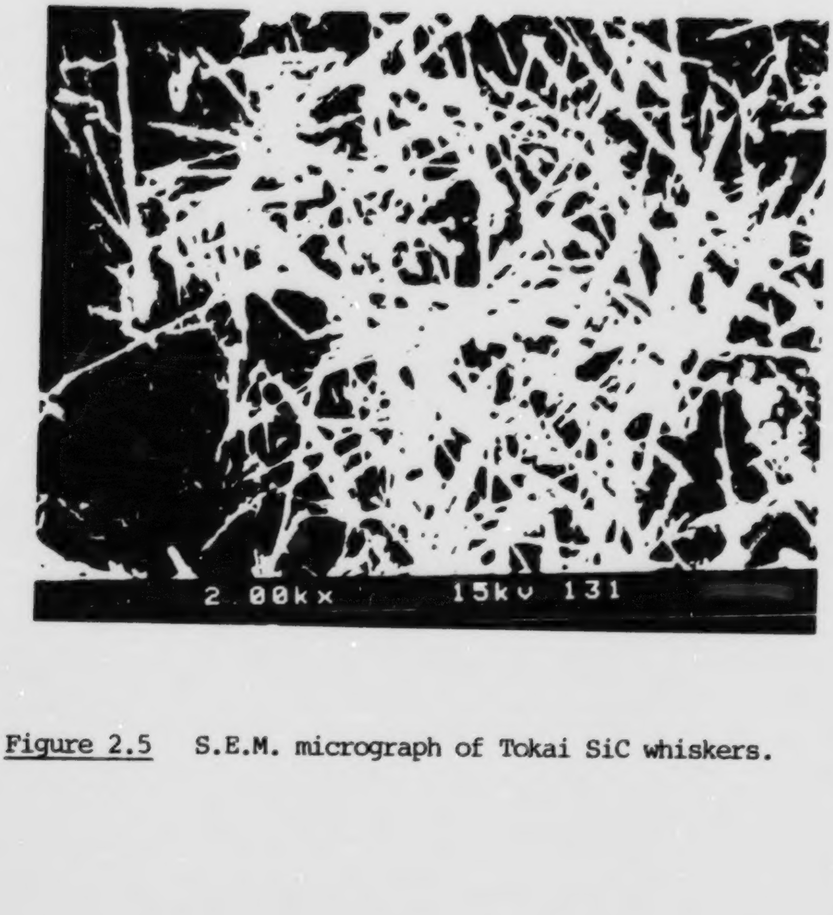
2.00kx 15kv 131

Figure 2.5 S.E.M. micrograph of Tokai SiC whiskers.

3. PROCESSING

In consultation with Scientific Authority and Prof.David Green it was decided to start with commercially available powders and to concentrate on composition development on this project. It was felt that developing our own powder manufacturing process would require considerable effort which would not be justified on this limited program, especially since a number of high quality fine powders are commercially available.

Figure 3.1 illustrates generalized processing techniques used in this program. Preprocessed commercial powders, spray dried to yield free flowing powders, were directly cold pressed and sintered or hot pressed. However, most powders required some form of pretreatment before they could be formed and sintered. Figure 3.1 illustrates the various routes taken. This chapter gives a short description of the following processing steps :

1. Grinding
2. Mixing
3. Drying
4. Slip casting
5. Cold pressing
6. Sintering
7. Hot pressing

Fig.3.1 PROCESS FLOW CHART

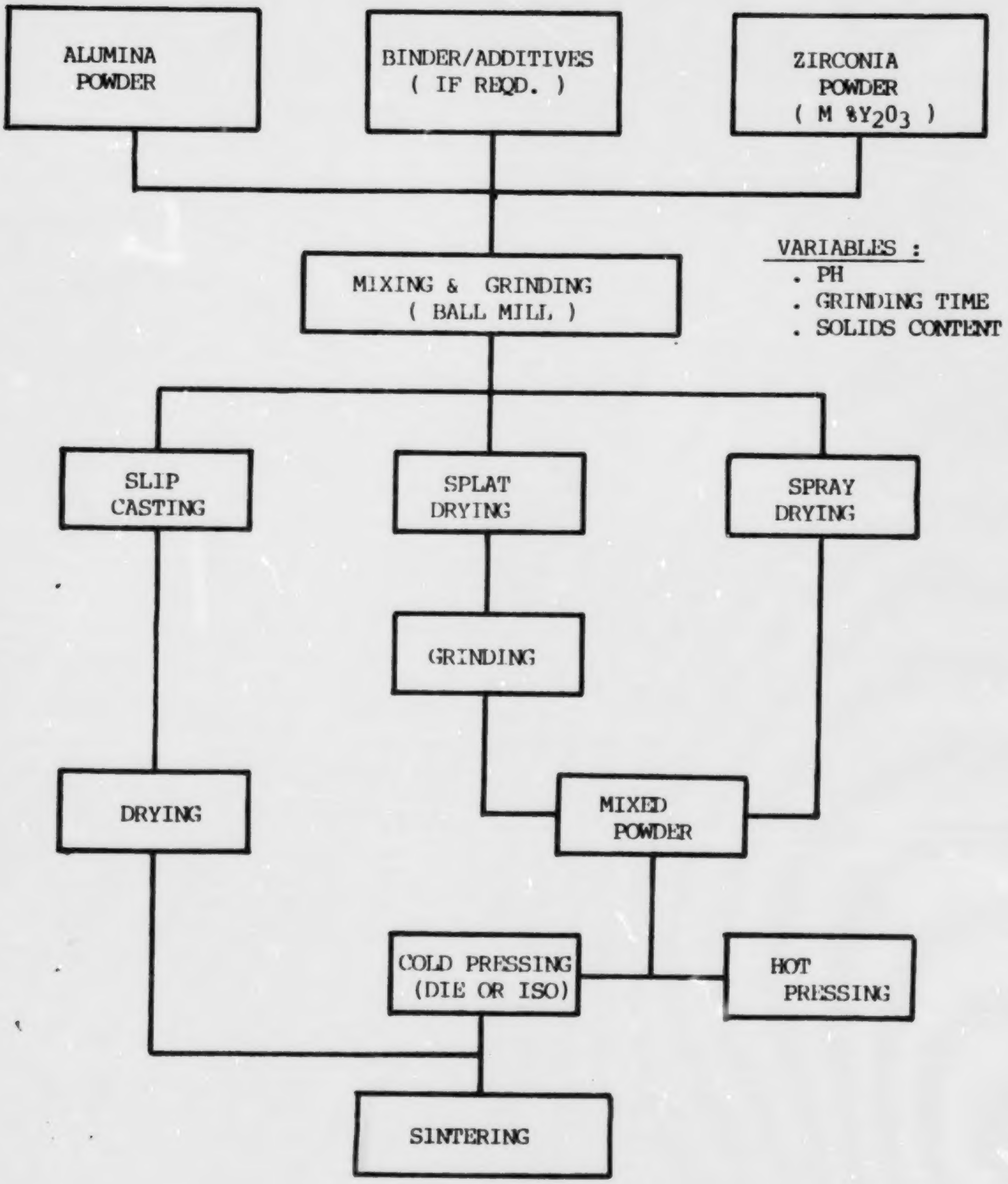
ALUMINA POWDER
BINDER/ADDITIVES (IF REQD.)
ZIRCONIA POWDER (M %Y_2O_3)
MIXING & GRINDING (BALL MILL)
VARIABLES :
. PH
. GRINDING TIME
. SOLIDS CONTENT
SLIP CASTING
SPLAT DRYING
SPRAY DRYING
GRINDING
DRYING
MIXED POWDER
COLD PRESSING (DIE OR ISO)
HOT PRESSING
SINTERING

Title	Scale	Date	Initial	Dwg.No.	Rev.

3.1 Grinding

As described in the previous chapter, the manufacturers of the commercial powders purchased claimed very fine particle or crystallite sizes. However, most of them contained large agglomerates which could not be dispersed just by the action of colloidal (electrostatic repulsive) forces or by ultrasonication. These "hard" agglomerates required considerable amount of wet attrition milling to disperse them as fine particles. Wet ball milling using partially stabilized zirconia balls was used for grinding operation. Ball milling was carried out in either rubber lined or alumina lined mills, and, in case of small lots,it was also carried out in polyethylene jars. The mill speed was optimized to 65-80% of the critical speed, which was calculated from the formula :

$$N_c = \frac{42.3}{\sqrt{D}}$$

where, N_c is the critical speed in R.P.M.
and, D is the mill diameter in metres

The bulk volume of the ball charge was usually between 40-50% of the volume of the mill and the charge volume (solids plus water) was varied between 20 to 35%, so that material-to-void ratio was about one. The solids content of the charge was optimized for each material so that the resulting slurry had the right consistency (viscosity) for efficient grinding. The solids content generally varied between 20 vol% to 55 vol%, the higher contents being used for slip casting.

3.2 Mixing

It is important to uniformly disperse zirconia into the matrix material as fine particles in order to obtain the benefits of its toughening. In this program, wet mixing was mainly carried out in the ball mill (along with grinding) using colloidal chemistry. The powders which had only "soft" agglomerates were also mixed wet in the colloidal state by high shear mixers.

Stable dispersion of powders is of critical importance in the wet mixing process. Otherwise, powders will tend to agglomerate due to Van der Waal's forces and there will be segregation of the constituents. In order to disperse powders, repulsive forces must be created on the particles to overcome the attractive Van der Waal's forces. This can be done by : a) electrostatic repulsion of like charges on the surface of the particles, or, b) stearic hindrance. Strong electrostatic repulsion can be created either by controlling the surface double layer or by adsorbing charged species (polyelectrolyte) on the surface.

In this program, powders were mainly dispersed in water, and, only pH control was used to vary the surface charge for maximum dispersion.When particles are dispersed in polar liquids like water, a double layer is formed on the surface. The charge of this surface double layer depends on the surface properties of the solid and on the concentrations of charged species in the liquid. Thus, by changing pH (i.e. concentration of H^+ ions) the surface charge of particles can be changed as shown in Figure 3.2, which gives the zeta-potential diagram for one of the commercial aluminas (grade AKP 30 from Sumitomo). It demonstrates that at low pH the surface charge on alumina is positive, and, this charge decreases in neutral solution to zero at the iso-electric point of pH≈7.5. At higher pH, the surface charge is reversed and alumina can again be dispersed. Thus alumina can be dispersed in either the acid or basic region, as long as the pH is sufficiently far from its iso-electric point of pH≈7.5.

Similar considerations are important when mixing two or more components. It is important to know the zeta potential diagrams of individual components in order to determine the working range of pH. From theoretical considerations, isoelectric point can be predicted from the charge (z) and ionic radius (R) of the surface species. Figure 3.3 shows the iso-electric point of various solid oxides and hydroxides as a function of the z/R, and, the line predicted from the theory. It can be seen that data for many oxide materials lie close to the predicted line. According to this figure, alumina has isoelectric point of about pH=8.5 and zirconia about pH=6.5. However, as noted earlier, these values are a function of the surface phase (not the bulk phase), which often vary depending on previous processing, reactions with electrolyte, etc. Thus, powders with same bulk analysis from different suppliers may have different zeta potential curve, as demonstrated in Figure 3.4. This figure

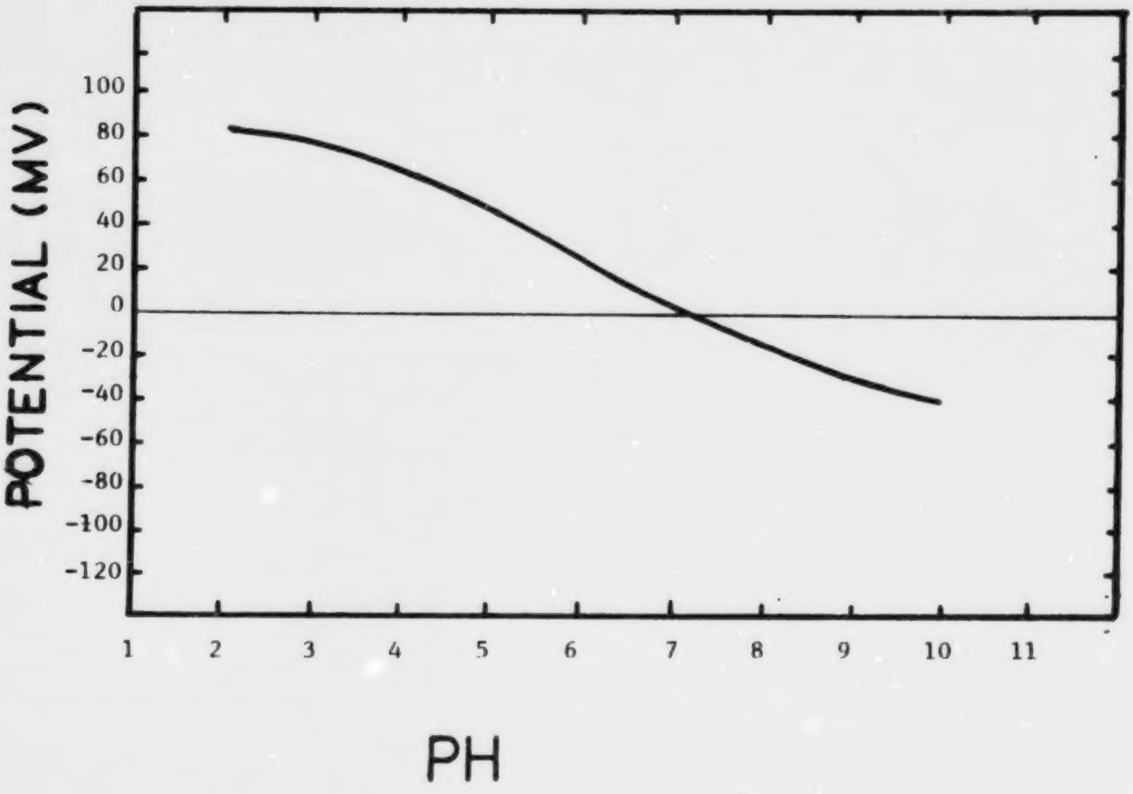

Figure 3.2. Zeta-potential diagram for alumina Sumitomo AKP-30.

ISOELECTRIC POINTS OF SOLID OXIDES AND HYDROXIDES

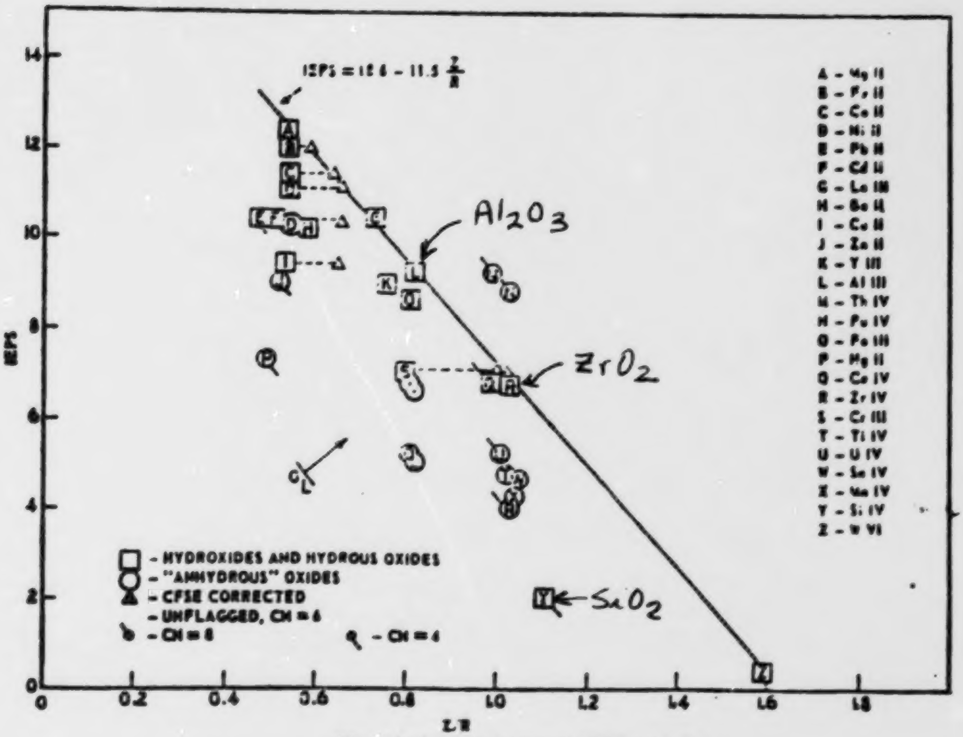

The relationship between IEPS and Z/R.

Figure 3.3

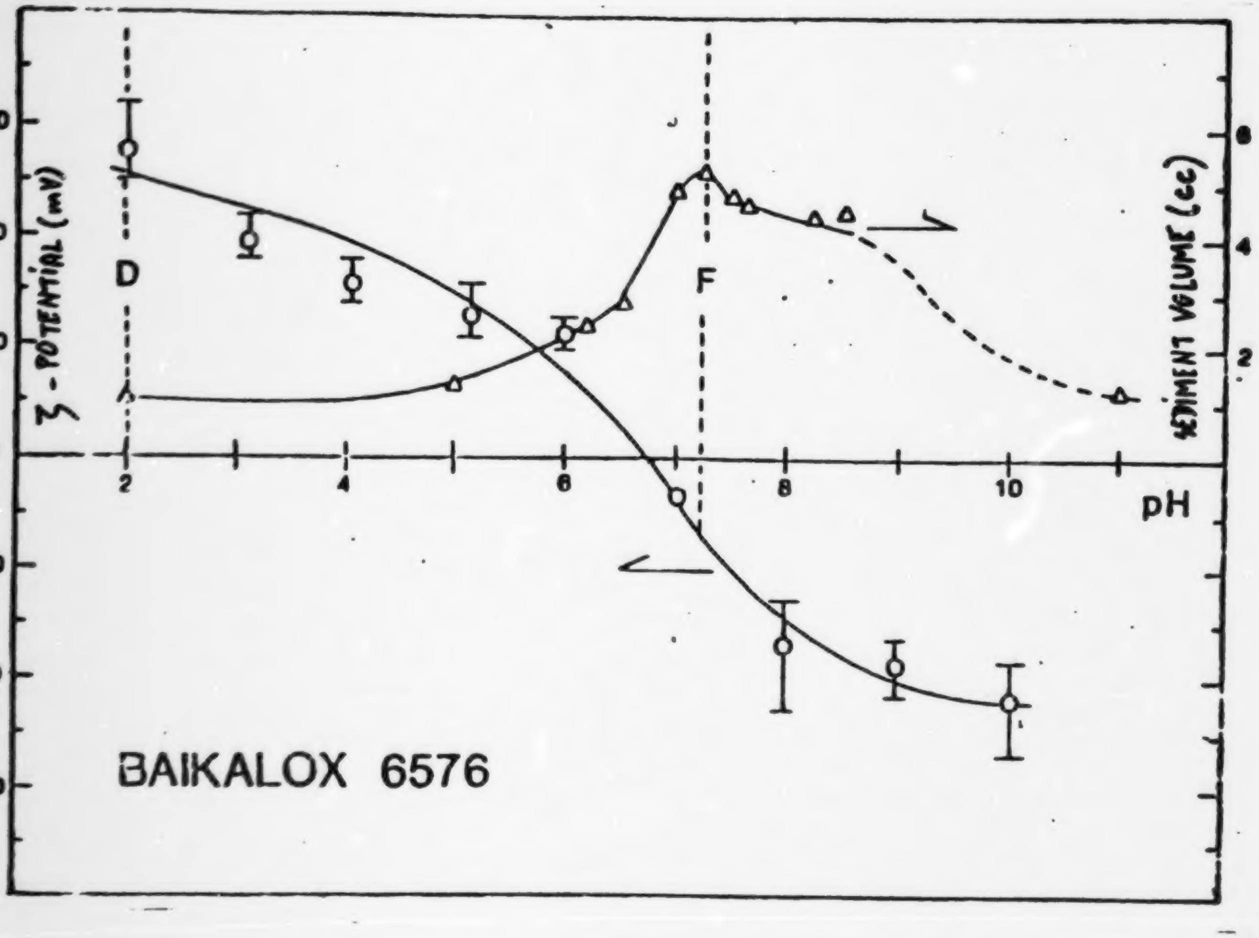

Figure 3.4 Zeta potential of Baikowski's CR10 alumina

gives the data for alumina Grade CR10 manufactured by Baikowski, showing an I.E.P. of pH≈6.7, which is somewhat different from data in Figure 3.2 and 3.3.

The fact that reactions change the nature of surface is amply demonstrated by the "aging" process that occurs in slips on standing. The slips which have been well dispersed can flocculate and visa versa on standing due to surface reaction. This often leads to a change of pH on standing and may require readjustment for optimum dispersion.

Zirconia is a typical example wherein the surface reaction affect the zeta potential diagram (see Figure 3.5). Instead of a single I.E.P. of pH=6.5 shown in Figure 3.3, in practice it shows three isoelectric points at pH~3, pH~5.5 and pH~6.5. This is believed to be caused by stability of different surface species as a function of pH.

When mixing two or more components, it is necessary not only that they be dispersed at the chosen pH, but, also they must have the same sign of surface charge. Thus, by comparing Figures 3.2, 3.4 and 3.5, it is clear that alumina and zirconia can be mixed together in a colloidal solution under the following range of pH :

1. pH < 3 Alumina/zirconia +ve surface charge
2. 5.5 < pH < 6.5 Alumina/zirconia +ve surface charge
3. pH > 8.5 Alumina/zirconia -ve surface charge

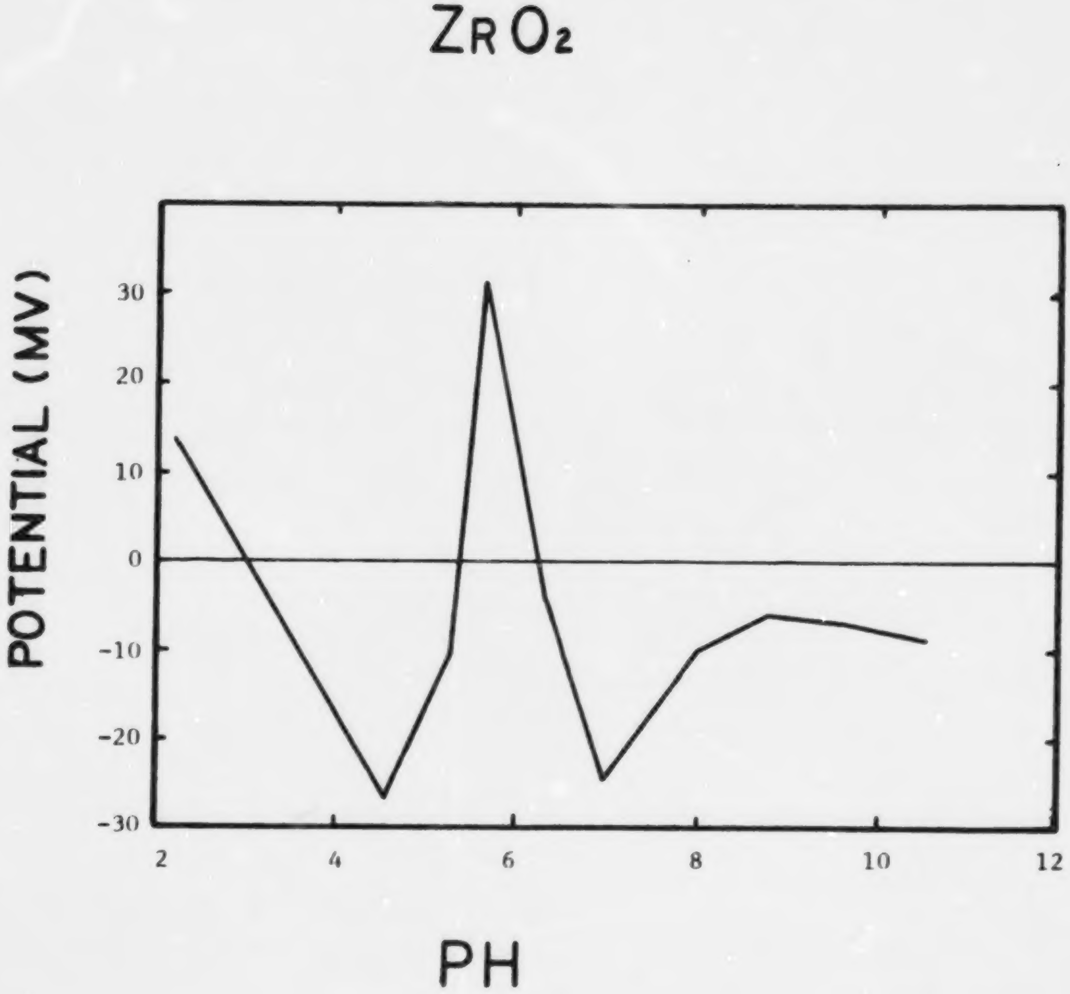

Figure 3.5. Zeta potential diagram for zirconia.

The region of pH between 5.5 and 6.5 is too narrow for control and good dispersion. Hence, these two materials can be mixed in the colloidal state in the acid region (pH < 3) or in the basic region (pH > 8.5). Both regimes were tried, and, it was experimentally determined that acid region with pH = 2.5 gave the best results for alumina-zirconia system.

However, the picture is different when mixing alumina, zirconia and silicon carbide whiskers. Figure 3.6 illustrates the zeta potential curve for SiC whiskers, showing an iso-electric point of about pH ≈ 4. This I.E.P. is probably determined by surface oxide phase present on whiskers,the I.E.P. of SiO_2 being around pH=2 (see Figure 3.3). This makes the mixing of SiC whiskers, alumina and zirconia in the acid range not very efficient. The three component system could only be mixed well at pH ≈ 10.5.

3.3 Drying

After the components have been mixed by attrition milling or high shear mixing, the colloidal solution was either slip cast or dried before further processing (see Figure 3.1). Drying can be most efficiently performed by "spray drying" technique, which produces "soft" agglomerates of about 100 µm. Spray dried powders have good flow properties, which fill the mold uniformly, and, result in green compacts with no density variations. However, spray drying equipment was not available at Electrofuel, and hence the solution was splat dried.

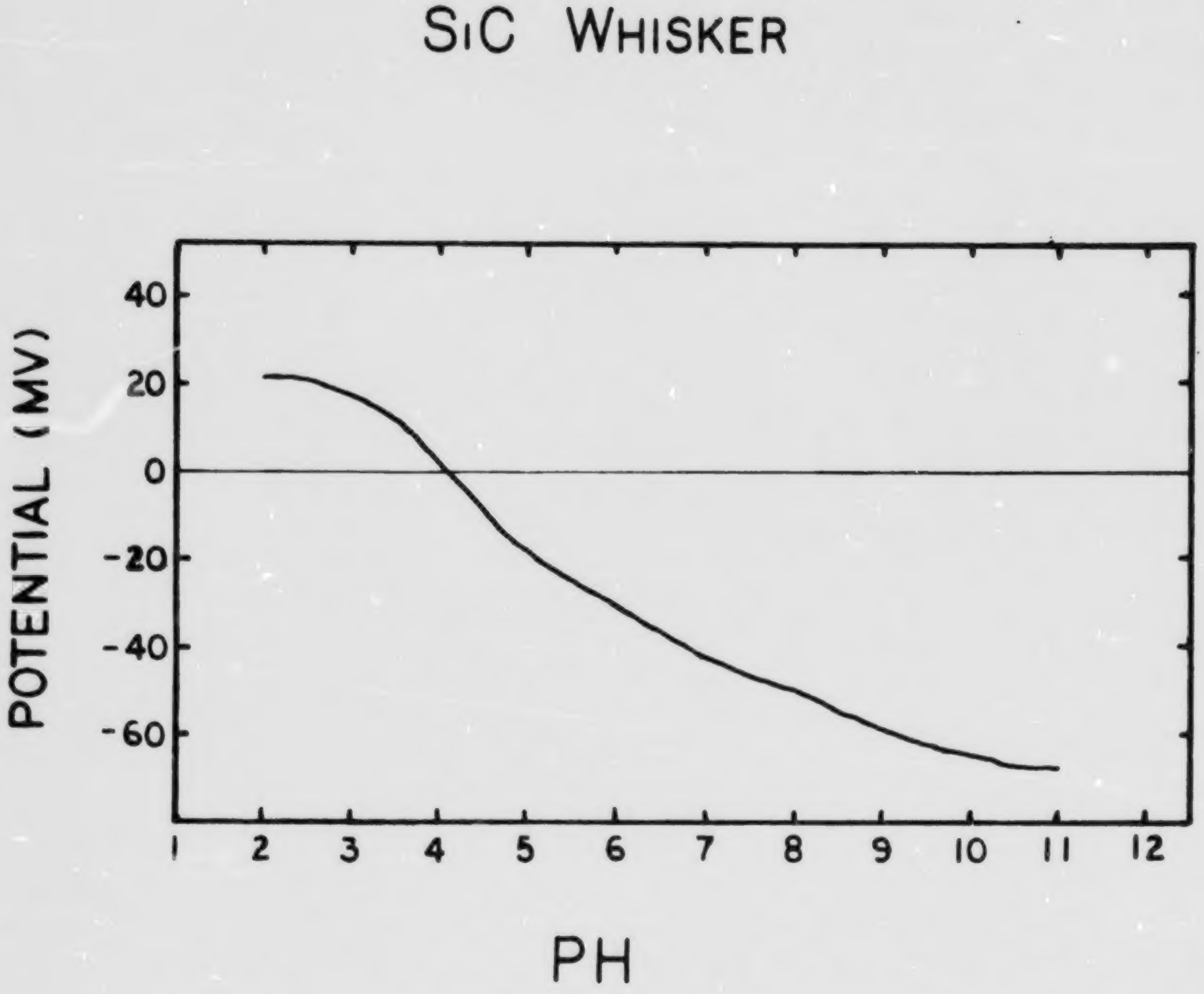

Figure 3.6 Zeta-potential diagram for SiC whiskers.

Splat drying technique consisted of heating an aluminum plate to about 120° C and pouring a thin layer of solution, which dried quite rapidly. The material was then scraped off and further dried in an oven at 200° C for 16 hours. The dried material was then ground in an alumina mortar and pestle and screened through 20 mesh before further processing.

3.4 Slip Casting

Only a limited number of pieces were made by slip casting in order to gain some experience with this forming technique for zirconia toughened alumina materials. Slip casting is a low capital cost process for forming a limited number of reasonably complicated shapes with thin wall thickness. In this program, however, only a simple cylindrical shape was cast using a plaster of paris mold shown in Figure 3.7. It consisted of a plaster of Paris block which was machined to fit a plastic tube of internal diameter 1.34 inches. The slip was cast into this tube, and, excess liquid was drained off after a given time. After air drying, the casting was recovered, slowly dried upto 200°C and then sintered. The cast must be dried very carefully in order to prevent cracking. The green density of cast made in this way approached 60%, when the slip was made well.

3.5 Cold Pressing

Dry mixed powder, after grinding and screening, was cold pressed in a tool steel die to make cylindrical compacts, which were then sintered. It is important to make good flowing powders for cold pressing, otherwise, density variations in the cold pressed pellet give rise to cracks in the sintered product.

SLIP CASTING MOLD

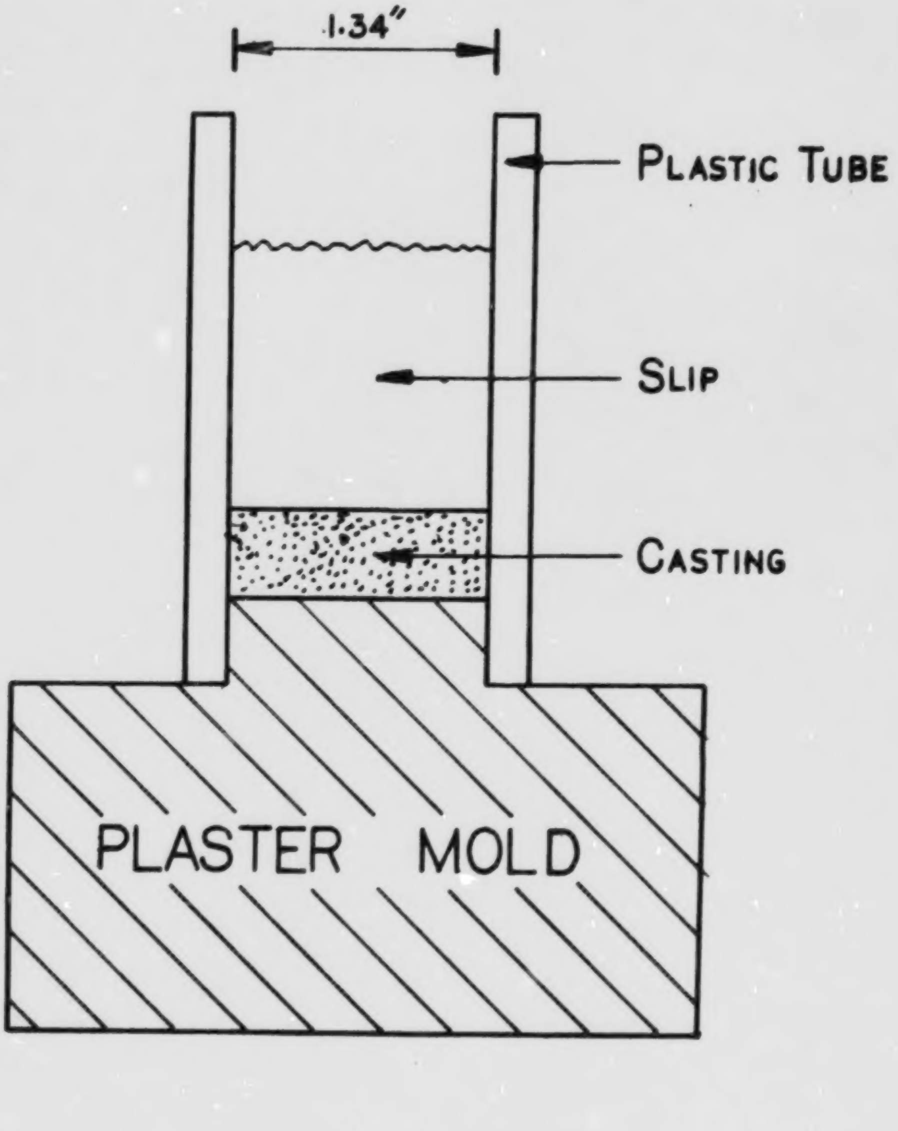
1.34"
PLASTIC TUBE
SLIP
CASTING
PLASTER MOLD

Figure 3.7 . Slip casting mould.

THE ELECTROFUEL MANUFACTURING CO. 9 Hanna Avenue Toronto, Ontario, Canada **M6K 1W8**

Title	Scale	Date	Initial	Dwg.No.	Rev.

Another important factor is the length-to-diameter (L/D) ratio in the pellet. In uniaxial pressing, density variations in the pressed body is caused by powder friction with die walls and between particles. This density variation gets worse with increasing L/D ratio, and, practical limit for many ceramic powders, when a single ram is moving, is L/D ratio between 1 and 2. This may be doubled for double acting rams. In this program we have used only single acting ram, and, with alumina-zirconia powders we could get good results with L/D ratio upto 1.

The uniaxial pressure applied during cold pressing is an important process variable. Too little pressure results in a low density green body, which generally yields a low density final sintered product. On the other hand, too high a pressure results in cracks, end capping, laminations and other pressing defects in the green compact. Figure 3.8 shows the relationship between the relative density and uniaxial pressure during cold pressing of an alumina-20 vol% zirconia powder mixture. The results were determined from the ram position with pressure. It can be seen that the relative density of the powder compact rises rapidly with pressure first and then levels off. Thus, after 10 ksi pressure, very little density was gained, but chances of pressing defects, such as end caps and laminations, increased.

These pressing defects in uniaxial cold pressing are caused by the fact that, when the ram pressure is released, the axial stresses are relieved without relieving the radial stresses. This gives rise to cracks originating at the corners, which ultimately causes end capping. On the other hand, cold isostatic

GREEN DENSITY ON COLD PRESSING

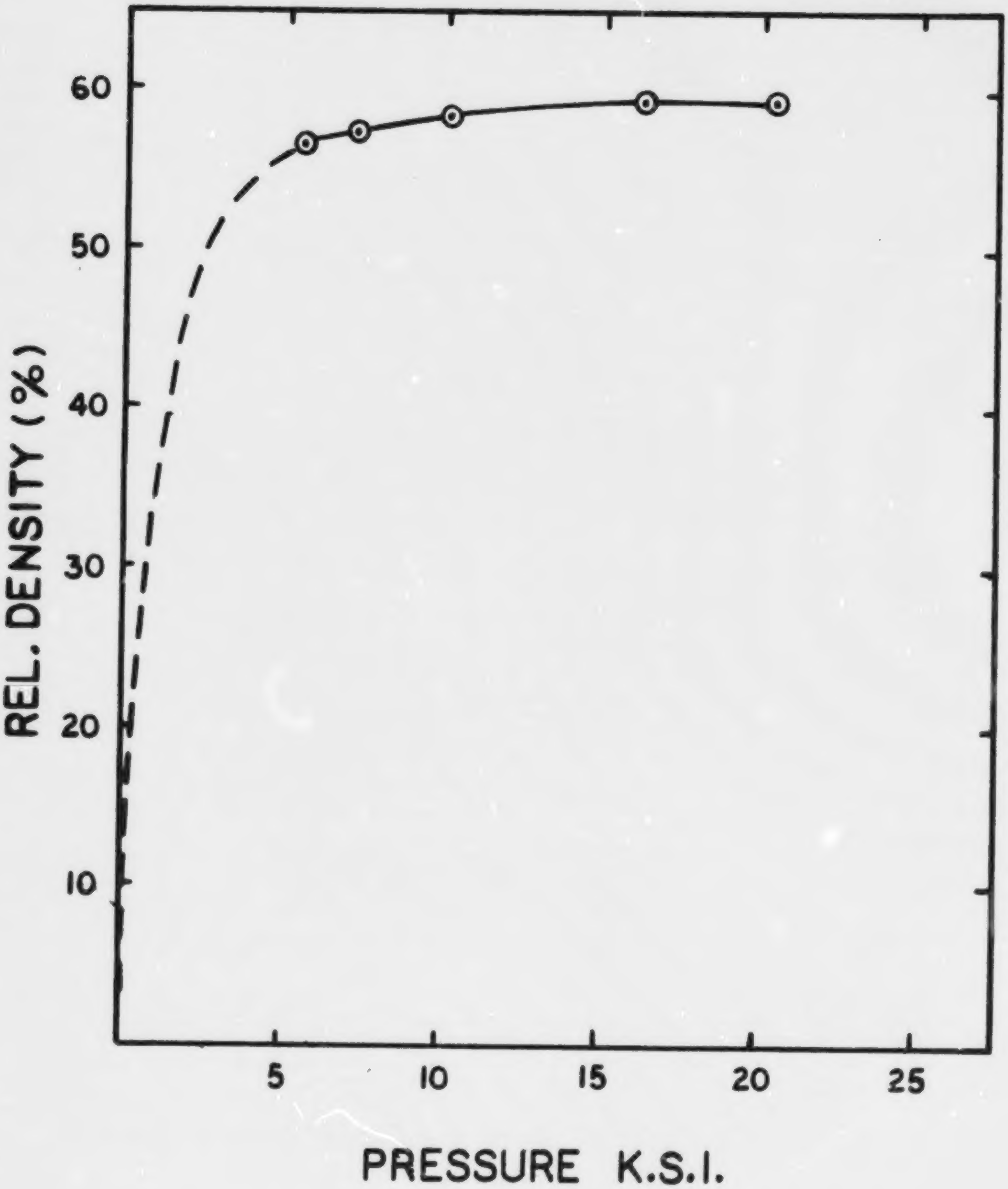

Figure 3.8

Title	Scale	Date	Initial	Dwg.No.	Rev.

pressing (CIP) imposes and relieves pressure from all directions, and hence, is free of such defects. Thus, much higher pressures and green densities are feasible with CIP and is recommended for some applications. However, during the course of this program, CIP was not available at Electrofuel, and, the samples have been uniaxially cold pressed.

3.6 Sintering

Pressureless sintering of PSZ, alumina and ZTA were carried out in a molybdenum disilicide furnace capable of operating in air upto 1700°C. The furnace is insulated using low mass alumina fibre boards on the hot face, with high alumina alumino-silicate fibre boards as back up insulation. This construction allows rapid temperature cycling, if required, using $MoSi_2$ heating elements. The furnace is equipped with a SCR power pack (Eurotherm Model 830) driven by a multisegment programmable temperature controller (Eclipse Model 560).

A number of sintering schedules were tried with with PSZ, ZTA and alumina materials. Figures 3.9 a,b and c shows examples of three optimized sintering cycles. Figure 3.9 a was used to sinter alumina, zirconia and ZTA parts without binder/additives to densities higher than 96%.The sintering temperature (T_s) used for fine-grained zirconia based materials varied between 1400° and 1500°C, while, for alumina based materials it was in the range of 1500°-1650°C. When organic binder or electrolyte was added, they require a long burn out cycle, in which temperature was raised at the rate of 15°C/hr upto 800°C, followed by 2 hour hold at 800°C, as shown in Figure 3.9 b. For thin samples when organic binders/additives are not being used, much higher heating and cooling rates can be used as shown in Figure 3.9 c.

Figure 3.9a & b. Sintering schedule.

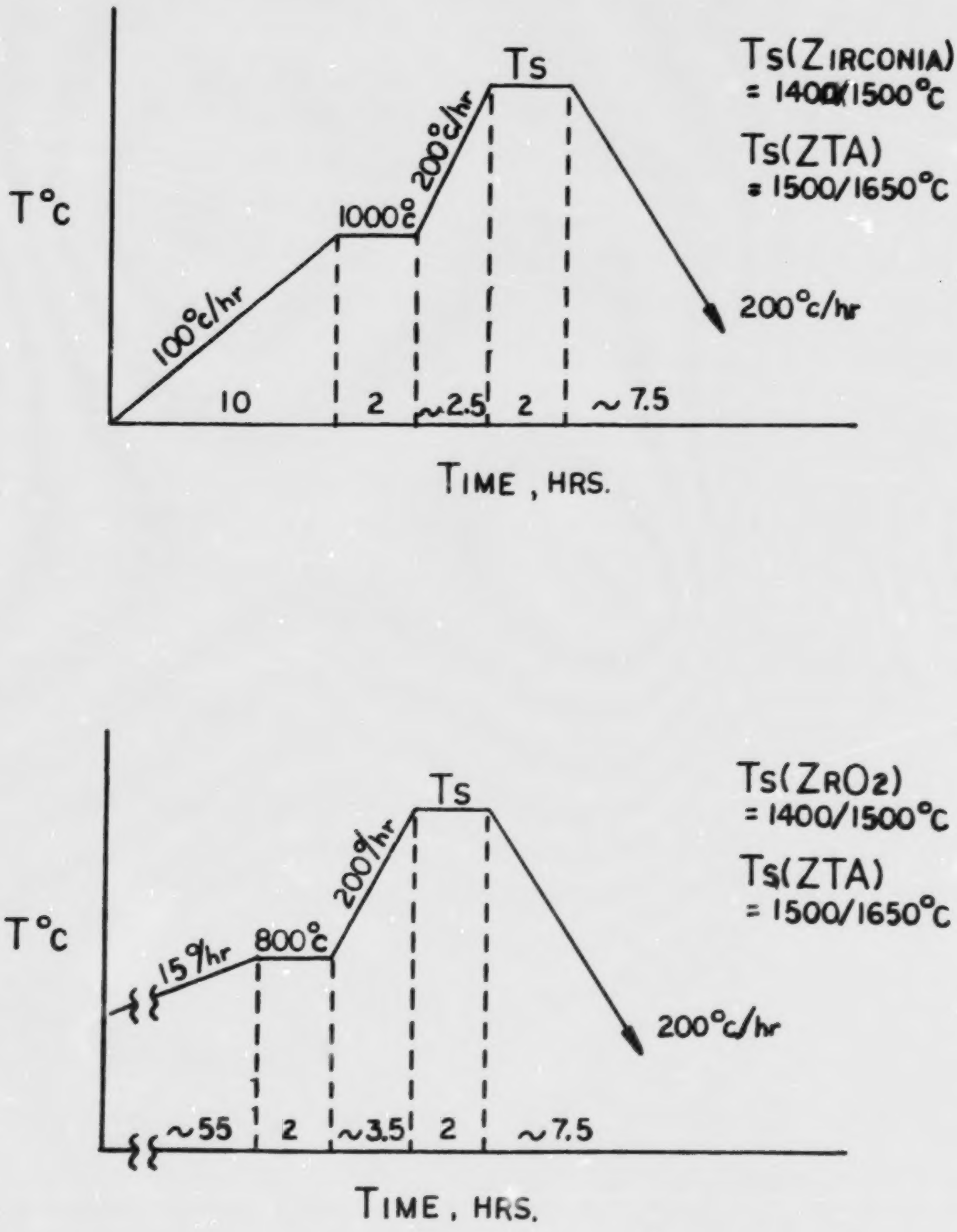
Ts(Zirconia)
= 1400/1500°C
Ts(ZTA)
= 1500/1650°C
Ts
T°C
1000°C
100°C/hr
200°C/hr
200°C/hr
10
2
~2.5
2
~7.5
Time, hrs.
Ts(ZrO2)
= 1400/1500°C
Ts(ZTA)
= 1500/1650°C
Ts
T°C
800°C
15°/hr
200°/hr
200°C/hr
~55
2
~3.5
2
~7.5
Time, hrs.

Figure 3.9c. Sintering schdule

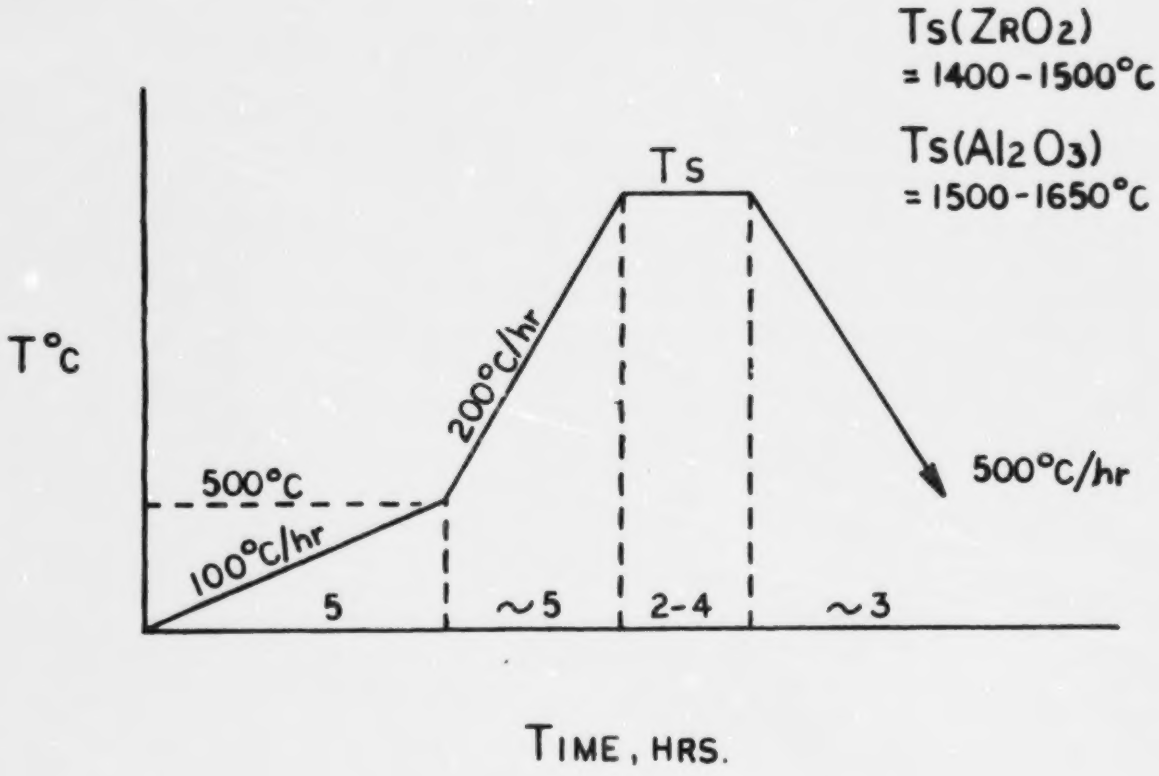

Title	Scale	Date	Initial	Dwg.No.	Rev.

Figure 3.10 gives the realtionship between the final sintered density as a function of initial green density of the pellet for the ZTA system. While there is some scatter, it is clear that the final sintered density increases rapidly with the green density and then it somewhat levels off. Thus, in order to make ZTA with > 96% sintered density, it is necessary to cold press (or form in any other way) a green body with density greater than 55%.

3.7 Hot Pressing

Hot pressing is a pressure assisted sintering technique which normally leads to higher densities, finer grain sizes and finer flaws resulting in improved properties. However, it can produce only simple shapes and hence, products made by hot pressing require expensive machining afterwards. However, for making composite materials containing whiskers or fibres, it may be the only practical process of fabrication. Hot pressing was used in this program to produce a limited number of SiC whisker reinforced ZTA materials and a few PSZ and ZTA heats for comparative studies.

All hot pressing was done at Electrofuel's 400 T hot press in small graphite molds with 2.5 inch diameter rams (part size).

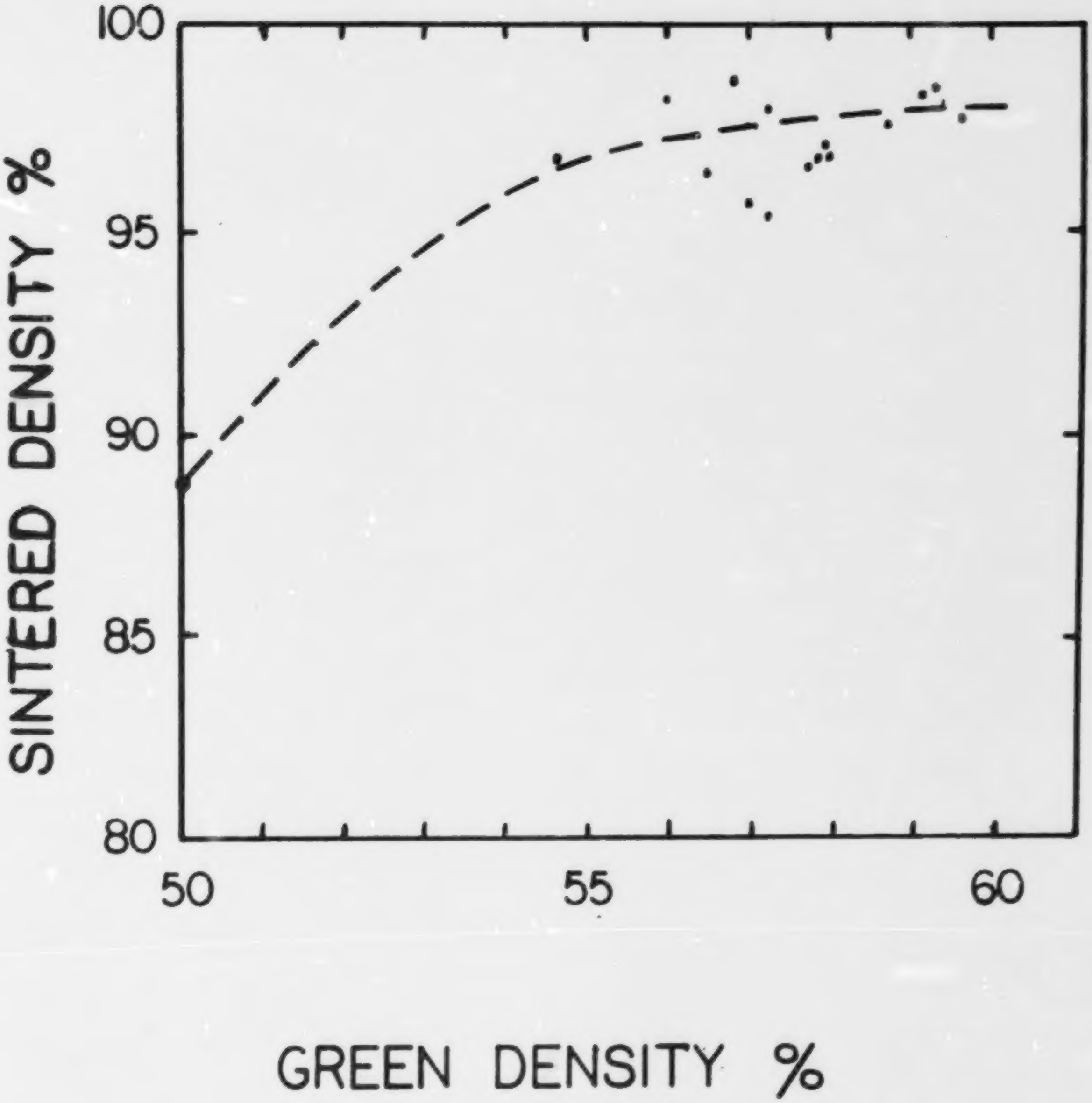

Figure 3.10. Sintered density as a function of green density.

Title	Scale	Date	Initial	Dwg.No.	Rev.

4. EXPERIMENTAL PROCEDURES

As the primary objective of this program was to develop and evaluate a number of promising zirconia toughened ceramics, the experimental procedure consisted of characterizing the raw materials, processing the powders to sintered bodies and evaluating the properties and microstructures obtained. The following measurements were performed :

1. Density : both in green and in sintered state
2. Shrinkage : during sintering
3. XRD phase analysis of sintered material
4. Hardness
5. Fracture toughness
6. Microstructure : both optical and SEM

Although fracture strength is an important mechanical property, it was decided not to measure it due to the following reasons :

- Strength is not characteristic material property, but depends to a large extent on flaws generated at each stage of processing - from powder blending upto grinding the finished part. As the aim of the study was to develop new promising materials rather than fine tune processing, it was decided to concentrate on fracture toughness (characteristic material property) rather than strength.

* The above reasoning is valid in case of all ceramic materials, but, in case of transformation toughened material it is even more significant due to surface compressive stresses that can be generated during grinding. The strength of zirconia toughened ceramics would depend to quite an extent on whether the tensile surface of the specimen was as sintered, ground or polished (also on the grinding or polishing conditions). Unless the surface preparation during testing reflects the conditions of a component under service, the strength data is not relevant.

4.1 Density

The green density of the cold pressed compact was determined from the measured weight and physical dimensions. The physical dimensions were very carefully determined using a digital micrometer. The error in density values is estimated to be ±1%.

The final sintered density was determined by :

a) measurement of physical dimensions and weight, and
b) Archimedes principle (weight loss in water)

An average density was recorded. In case of a substantial difference, Archimedes density was used.

4.2 Shrinkage

The shrinkage on sintering was measured from the dimensions of the green part before sintering and the final part after sintering.

Table 4.1a gives data on typical shrinkage observed in various zirconia toughened ceramics. While shrinkage varies with powder preparation, cold pressing conditions, sintering conditions, etc.,it can be essentially related to the green body density and final sintered density through the relationship :

$$S = 1 - \sqrt{\frac{\rho_g(1 - c/100)}{\rho_f}}$$

where, S = Shrinkage

ρ_g = Green Density

ρ_f = Final density after sintering

and, c = Content of plasticizers in wt%

Material	Composition	Shrinkage (%)
Alumina	100% Al_2O_3	16
Ce-PSZ	ZrO_2, 14% CeO_2	20
Y-PSZ	ZrO_2, 2 m% Y_2O_3	26
Y-PSZ	ZrO_2, 3 m% Y_2O_3	21
Y-PSZ/Alumina	ZrO_2, 3 m% Y_2O_3, 20 wt% Al_2O_3	20.5
ZTA	Al_2O_3, 10 v% ZrO_2 (2 m% Y_2O_3)	16.0
ZTA	Al_2O_3, 20 v% ZrO_2 (2 m% Y_2O_3)	16.2
ZTA	Al_2O_3, 30 v% ZrO_2 (2 m% Y_2O_3)	17.0

Table 4.1a : Typical shrinkage observed in various zirconia toughened materials

From Table 4.1a, it can be seen that shrinkage depends on the zirconia content of the composite. This is due to the fact that zirconia powder contains certain fraction of low density monoclinic particles which is retained as high density tetragonal phase in the sintered product. Thus as volume fraction of zirconia in ZTA increases, so does shrinkage on sintering.

4.3 XRD Phase Analysis

In zirconia toughened ceramics, it is important to identify and determine the content of three important zirconia polymorphs (monclinic, tetragonal and cubic), as the properties are strongly affected by these phases. The presence of the phases can be identified by the standard x-ray diffraction techniques, although distinguishing between the tetragonal and cubic phases are difficult due to overlapping peaks. Since the a and c axes of the t-ZrO_2 are very similar to each other, as well as to the lattice parameter of c-ZrO_2, the t-zirconia would not be easily distinguishable from c-ZrO_2 if it were not for the presence of (112) reflection, which is not allowed for c-ZrO_2. Figure 4A shows a XRD pattern obtained from a ZTA with 10 v% unstabilized zirconia addition. It can be seen that in this sample, a part of the zirconia has been retained as t-ZrO_2 while the rest has transformed to m-ZrO_2.Table 4.1b gives the d-spacings and Miller indices for m- and t-ZrO_2 taken from literature. However, the d spacings vary depending on the type and content of stabilizer addition (MgO,

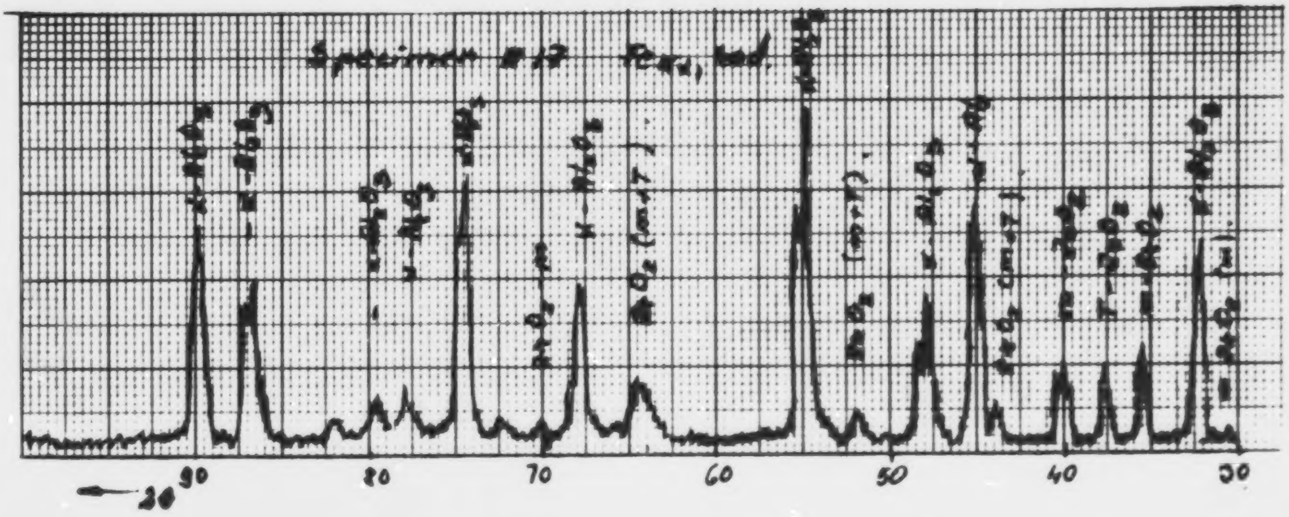

XRD pattern of unstabilized zirconia - alumina

Figure 4A

Calculated and Observed *d* Spacings for *m*- and *t*-ZrO_2

m-ZrO_2*			*t*-ZrO_2†		
hkl	d (Å)	d_{obsd} (Å)	hkl‡	d (Å)‡	d_{obsd} (Å)
100	5.079	5.08	111	2.996	2.98
011	3.694		002	2.635	
110	3.636	3.62	200	2.574	2.56
$\bar{1}11$	3.162	3.12	112¶	2.135¶	2.12¶
		2.93§	202	1.842	
111	2.839		220	1.821	1.82
002	2.621		113	1.582	
020	2.604	2.58	311	1.556	1.55
200	2.539	2.52	222	1.498	1.49

*JCPDS CARD 24–1165.

†G. Teufer, *Acta Crystallogr.* 15, 1187 (1962).

‡Based on double fct CaF_2-type cell.

¶Not allowed for face-centered cubic symmetry.

§Possible evidence of *t* phase.

Table 4.1B.

CaO, Y_2O_3, or rare earths, etc.) which goes into solid solution in different phases. This is demonstrated by XRD pattern, shown in Table 4.2, obtained from a ZrO_2-3 m% Y_2O_3 sample which was sintered to density > 98%. By comparing Table 4.1b and 4.2 it is clear that there are some differences in d-spacings.

Quantitative Phase Analysis

Following Garvie and Nicholson (1972), a XRD technique to analyze the volume fractions of m and (t+c) was developed using the XRD facilities at the Geology Department of the University of Toronto. The volume fraction of monoclinic phase (V_m) can be calculated based on integrated intensities of the $(111)_m$ and $(111)_t$ peaks, as given by :

$$V_m = \frac{I(111)_m + I(11\bar{1})_m}{I(111)_m + I(11\bar{1})_m + I(111)_{t,c}} \quad ....(4.2)$$

$$V_{t,c} = \frac{I(111)_{t,c}}{I(111)_m + I(11\bar{1})_m + I(111)_{t,c}} \quad ....(4.3)$$

In most of our samples in which only t- and m-zirconia phases were present (ZTA, TZP, ATZ), this analysis was sufficient. However, when substantial c-zirconia is present (e.g. PSZ), the t and c

Sample #19 Radiation Fe k
HV 40kV I 15mA
200 cps 1 s goniom. 1 /min
chart 600 mm/h

zirconia (T)					Comments
$d_{exp.}$	$I/I_{exp.}$	$d_{calc.}$	hkl	I/I	
2.952	100	2.96	111	100	
2.639	33	2.63	002	18	
2.598	20	2.59	200	25	
1.8251	45	1.83	202	65	
1.8048	35	1.81	220	35	
1.5601	25	1.564	113	25	
1.5538	25				reflection of coexisting cubic zirconia
1.5398	20	1.540	131	45	
1.4784	10	1.483	222	12	
1.2941	8	1.294	004	4	broad maximum including the reflection
1.2757	5	1.276	400	8	of cubic zirconia structure

Table 4.2. XRD pattern obtained from zirconia-3m% yttria sample.

zirconia must be resolved using $(400)_c$, $(400)_t$ and $(004)_t$ peaks, as given by :

$$V_c = \frac{I(400)_c}{I(400)_c + I(400)_t + I(004)_t} \qquad \text{........(4.4)}$$

These cubic and tetragonal peak separation occurs at high diffraction angles, and, since they overlap considerably (see Figure 4 b), a technique to resolve them is required.

Step-by-step x-ray intensity measurements were made every 0.04 degree (2θ) through monoclinic and tetragonal (111) peaks, as shown in Tables 4.3 a, b and c. These were plotted and areas under the curves were determined using a computer. Integral intensities were determined from the areas under the curve and half width of the peaks. Table 4.4 gives the results for 2 zirconia toughened samples using the integral and the absolute (maximum) intensities. Both methods give very similar results (column 1). Table 4.4 also gives the results of calculations based on intensities corrected for Lorentz polarization, multiplicities and structure factors (column 2) discussed below :

To calculate the required correction, Porter and Heuer proposed that :

$$I = (K\ R_i\ V_i\ )/2\ \mu_m \qquad \text{............(4.5)}$$

where K is a constant dependent only on the type of radiation used and the beam size, V_i is the volume fraction of phase i, μ_m

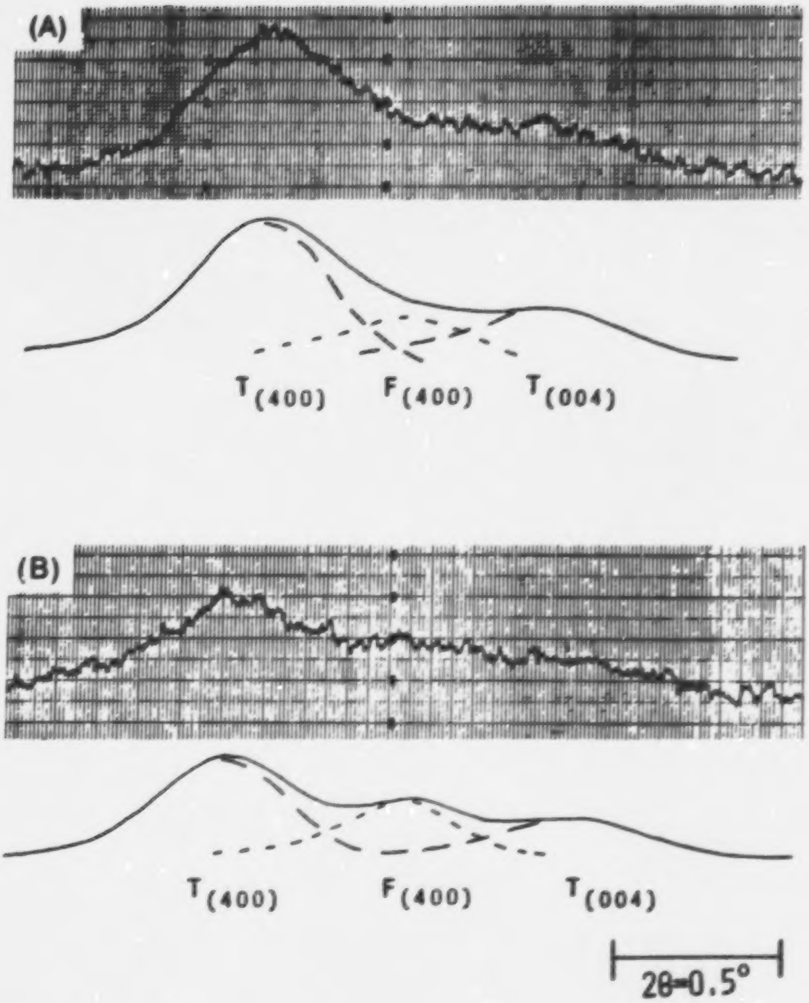

Figure 4B. Cubic and tetragonal peaks at high diffraction angles.

Table 4.3a. Step-by-step X-Ray intensities.

X-ray diffraction
Step by step recorded intensity

Sample: #8 Time 20 sec

Diffraction line: m $(11\bar{1})$ Radiation Cu k

HV(kV) 40 I(mA)

I max.	Area	Half-width	I int.
638.40	274.1346	0.52	527.18

Bragg angle	I ave.	I abs.
	530.4	
27.76	530.4	0.00
27.80	530.6	4.53
27.84	539.4	14.93
27.88	561.6	35.53
27.92	592.4	62.67
27.96	620.8	105.07
28.00	688.8	155.13
28.04	742.6	217.00
28.08	806.4	279.87
28.10	877.4	333.80
28.12	904.4	379.07
28.14	942.2	423.40
28.16	1010.4	468.53
28.18	1039.8	512.80
28.20	1075.0	537.27
28.22	1083.8	568.67
28.24	1134.0	589.20
28.26	1136.6	627.33
28.28	1198.2	638.40
28.30	1167.2	636.60
28.32	1131.2	610.40
28.34	1119.6	589.40
28.36	1104.2	574.60
28.38	1086.8	559.13
28.40	1073.2	533.80
28.42	1028.2	488.47
28.44	950.8	438.33
28.46	922.8	383.87
28.48	864.8	351.87
28.50	854.8	318.87
28.52	823.8	287.73
28.54	771.4	242.33
28.56	718.6	203.67
28.58	707.8	165.87
28.60	658.0	130.00
28.64	611.0	90.00
28.68	587.8	63.27
28.72	577.8	41.07
28.76	544.4	20.93
28.80	527.4	4.13
28.84	527.4	0.00

Table 4.3b X-ray diffraction
Step by step recorded intensity

Sample: # 8 Time 20 sec

Diffraction line: T (111) Radiation Cu k

HV(kV) 40 I(mA)

I max.	Area	Half-width	I int.
255.57	109.3853	0.47	232.73

Bragg angle	I ave.	I abs.
	492.0	
29.70	492.0	0.00
29.74	508.6	5.43
29.78	508.6	13.03
29.82	514.8	24.57
29.86	543.2	36.17
29.90	543.4	51.30
29.94	560.2	69.97
29.98	599.2	100.23
30.00	634.2	123.50
30.02	630.0	139.50
30.04	647.2	145.97
30.06	653.6	167.90
30.08	695.8	191.23
30.10	717.2	214.77
30.12	724.2	231.03
30.14	744.6	242.03
30.16	750.2	246.70
30.18	738.2	255.57
30.20	771.2	252.03
30.22	739.6	255.43
30.24	748.4	244.23
30.26	737.6	238.30
30.28	721.8	224.57
30.30	707.2	208.37
30.32	689.0	192.30
30.34	673.6	174.97
30.36	655.2	161.97
30.38	650.0	150.50
30.40	639.2	130.90
30.44	596.4	107.10
30.48	578.6	80.90
30.52	560.6	63.30
30.56	543.6	43.43
30.60	519.0	26.43
30.64	509.6	9.17
30.68	491.8	0.10
	491.8	

Table 4.3c. X-ray diffraction
Step by step recorded intensity

Sample: # 8 Time 20 sec

Diffraction line: m (111) Radiation Cu k

HV(kV) 40 I(mA)

I max.	Area	Half-width	I int.
338.73	141.2506	0.47	300.53

Bragg angle	I ave.	I abs.
	490.4	
31.00	490.4	0.00
31.04	494.2	5.73
31.08	506.2	19.00
31.12	530.2	29.27
31.16	525.0	44.27
31.20	551.2	61.60
31.24	582.2	99.47
31.28	638.6	134.67
31.30	656.8	171.20
31.32	691.8	190.73
31.34	697.2	208.87
31.36	711.2	221.20
31.38	728.8	249.00
31.40	780.6	270.40
31.42	775.4	293.33
31.44	797.6	304.87
31.46	815.2	322.60
31.48	828.6	327.13
31.50	811.2	336.40
31.52	843.0	333.87
31.54	821.0	338.73
31.56	825.8	331.93
31.58	822.6	326.47
31.60	804.6	313.47
31.62	786.8	288.40
31.64	747.4	255.80
31.66	706.8	224.27
31.68	692.2	196.33
31.70	663.6	167.07
31.74	619.0	127.00
31.78	572.0	80.53
31.82	524.2	49.40
31.86	525.6	23.27
31.90	493.6	12.33
31.94	491.4	0.60
31.98	490.4	0.00
	490.4	

		[1]		[2]	
		f_T	f_m	f_T	f_m
Sample #17	integral I	31.5%	68.5%	32.59%	67.41%
	absolute I	32.3%	67.7%		
Sample # 8	integral I	21.95%	78.05%	23.55%	76.45%
	absolute I	20.7%	79.3%		

Volume fraction of coexisting "t" and "m" zirconia.

Table 4.4

is the linear absorption coefficient of the mixture, and R_i is given as :

$$R_i = \frac{1}{v_2{}^2} \left[1F_i1^2 P_i \left(\frac{1 + \mathrm{Cos}^2 2\theta_i}{\mathrm{Sin}^2\theta_i \ \mathrm{Cos}\theta_i} \right) \right] (e^{-2M_i}) \qquad \text{.................. (4.6)}$$

where v_i is the volume of the unit cell, F_i is the structure factor, P_i is the multiplicity of the given reflection, θ_i its Bragg angle (the terms in the parenthesis comprise the Lorentz polarization factor, L_P). Thus, the ratio of volume fractions of phases is :

$$\frac{V_c}{V_m} = \frac{[\, R(111)_m + R(111)_m \,]\ I(111)_c}{[\, I(111)_m + I(111)_m \,]\ R(111)_c} \qquad \text{...........(4.7)}$$

The R factors were calculated and given in Table 4.5. Using these corrections based on structure factor, multiplicities and Lorentz polarization, the volume fraction of phases were recalculated and shown under column (2) in Table 4.4. It can be that these corrections do not significantly modify the results.

As automatic step motor and data acquisition system were not available, step-by-step analysis was very time consuming and

Table 4.5.

Correction data for phase analysis in Zirconia systems.

Material	Reflexion	P	L_p	$v(A^3)$	$/F/^2$	R
C + T ZrO_2	(111)	8	25.936	131.48	16.735	200.31
m ZrO_2	(111)	4	30.851	142.36	20.515	124.92
m ZrO_2	(111)	4	24.303	142.36	21.285	102.10

labourious. On the other hand, recording the x-ray intensity on a chart recorder at a goniometer speed of 0.25 degree/min is fast and simple. Figure 4c gives example of such a recording of the (111) m- and t-zirconia peaks. Using the area under the peaks (and peak half widths), the phase composition can be calculated using equations (4.2) through (4.3). The results of such calculations were found to be within 5% of those calculated from step-by-step data. For example, in case of sample #17, chart recording gave 29.6% tetragonal and 70.4% monoclinic phases, not far from 32.6% t- and 67.4% m-phase as shown in Table 4.4 by step-by-step analysis. Therefore, most of the data in this program was obtained by simple chart recording technique.

4.4 Hardness

The hardness of sintered materials were determined on polished samples using a Vickers diamond indenter. The Vickers hardness number (HV) was obtained by dividing the applied load in Kilograms-force by the surface area of the indentation in square millimeters computed from the mean of the measured diagonals of the indentation (ASTM E384-84), as :

$$\begin{aligned} HV &= P/A_s \\ &= 2P\,\mathrm{Sin}(\alpha/2)/d^2 \\ &= 1.8544\,P/d^2 \quad \ldots\ldots\ldots\ldots\ldots\ldots(4.8) \end{aligned}$$

where : P = load, Kgf

A_s = surface area of indentation, mm²

d = mean diagonal of indentation, mm

α = face angle of indenter = 136°

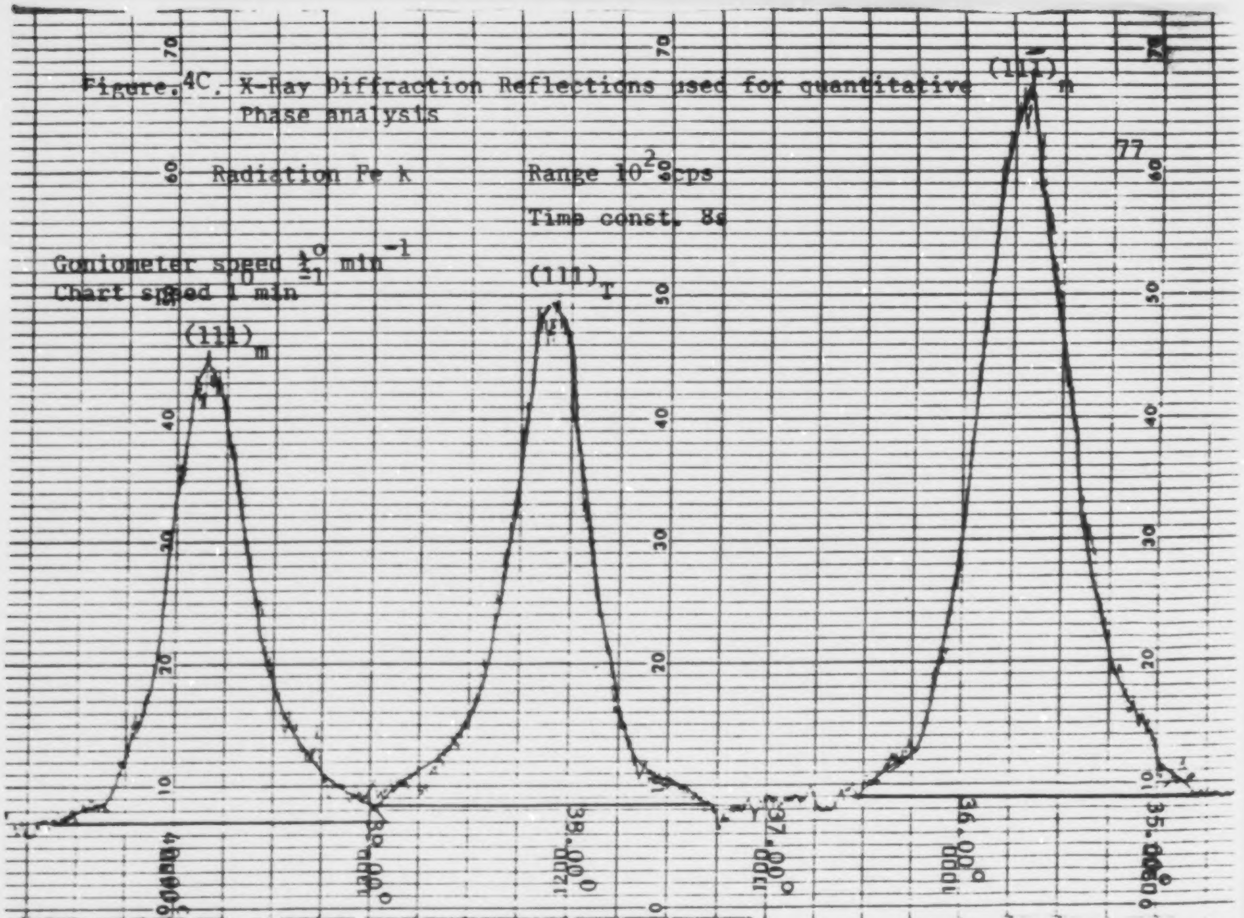

Figure. 4C. X-Ray Diffraction Reflections used for quantitative Phase analysis

Radiation Fe k

Range 10^2 cps

Time const. 8s

Goniometer speed $\frac{1}{4}^{o}$ min^{-1}

Chart speed 1 min^{-1}

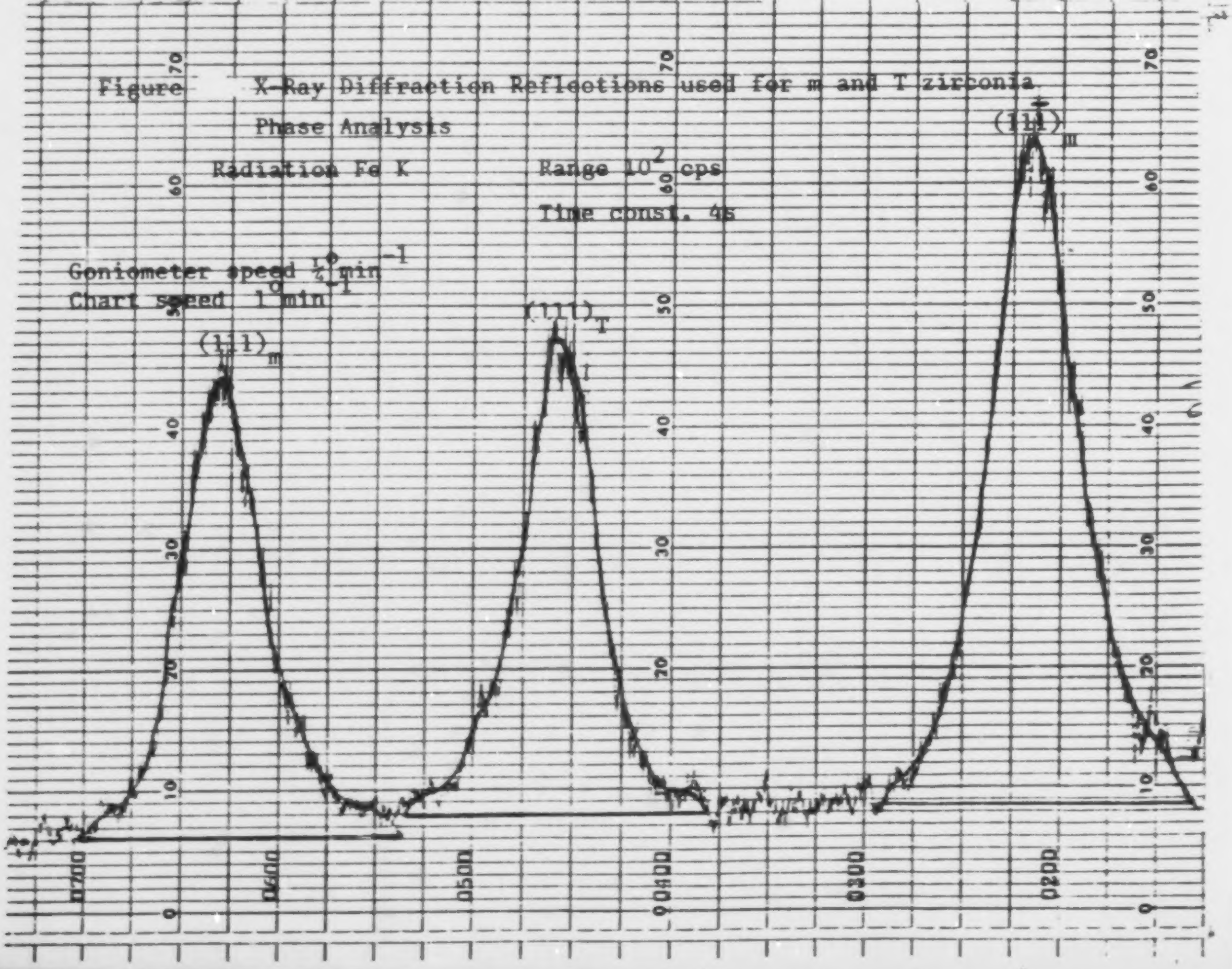

Figure X-Ray Diffraction Reflections used for m and T zirconia Phase Analysis

Radiation Fe K

Range 10^2 cps

Time const. 4s

Goniometer speed $\frac{1}{4}^{o}$ min^{-1}

Chart speed 1 min^{-1}

The Vickers hardness, as measured above, unfortunately is dependent on load applied. This dependence stems from the fact that when the load is applied there is both an elastic and plastic deformation taking place. However, the measurement is only made on the permanent (plastic) deformation left behind after the load is removed. Figure 4.1 illustrates this effect on alumina-25% silicon carbide whisker composite. It can be seen that Vickers hardness drops rapidly upto a load of about 5 Kg and then levels off. Therefore, it can be concluded that below 5 Kg load the elastic deformation is a significant proportion of the total deformation and this proportion decreases rapidly with load until about 5 Kg for this material. Thus, it is important to compare hardness under the same load conditions. It was decided to measure hardness at or above 5 Kg load.

4.5 Fracture Toughness

Plain strain fracture toughness (K_{Ic}) is an important property of a material as it relates failure stress (σ_c) with critical flaw size (a_c). At the present time there is no standardized method of K_{Ic} determination of brittle materials. Various types of specimens and testing have been used to measure this quantity, such as :

1. Single end notch bend (SENB)
2. Double cantilever beam (DCB)
3. Double torsion (DT) specimen
4. Chevron notch specimen
5. Micro-indentation technique

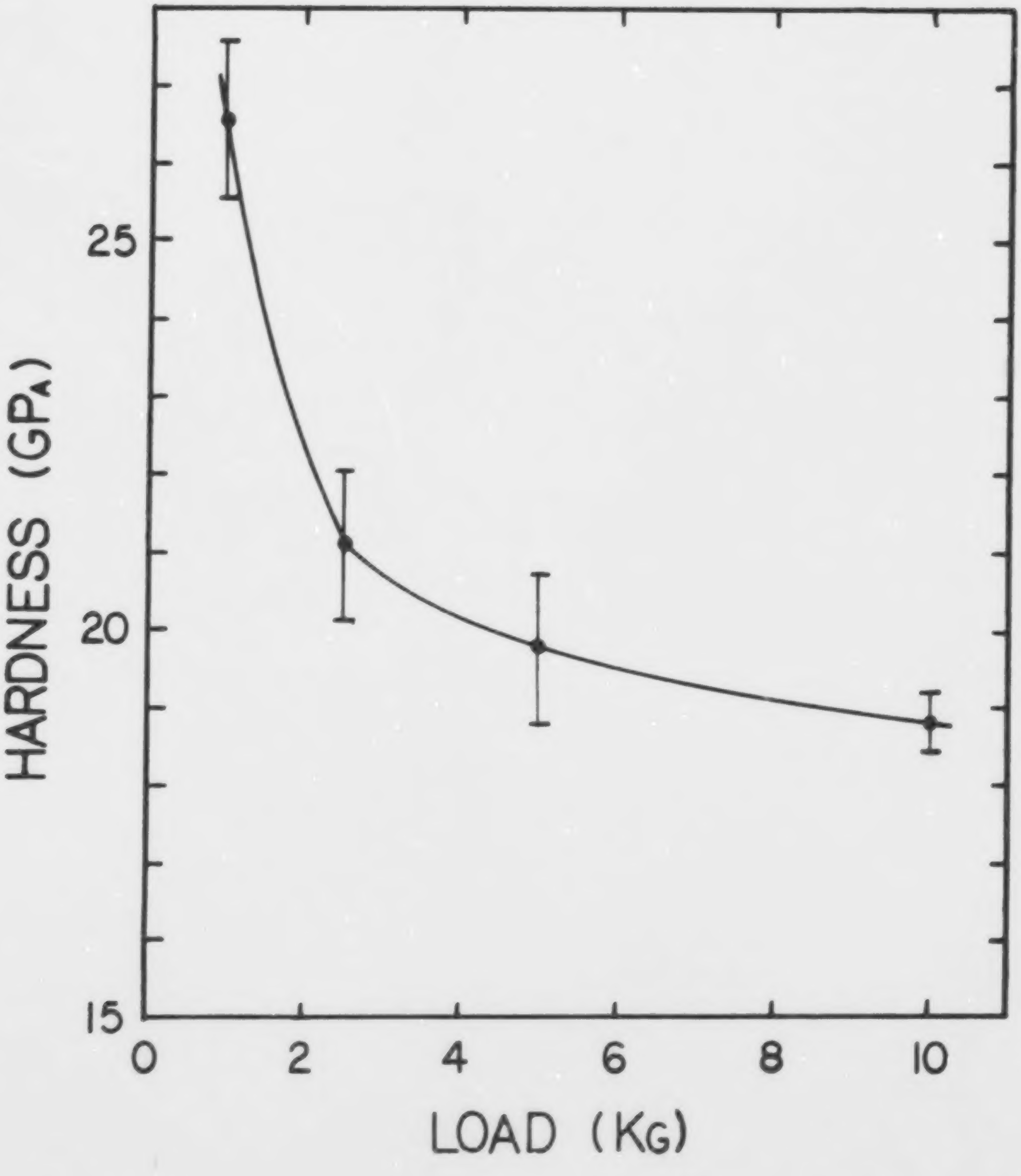

Figure 4.1. Vickers hardness as a function of applied load.

Title	Scale	Date	Initial	Dwg.No.	Rev.

Figures 4.2 and 4.3 illustrates the different types of samples used.

All the above techniques tend to give differing fracture toughness values for the same material. The main difficulties for the first three techniques are introducing a sharp crack and measuring the length of the sharp crack when it can be successfully introduced.

4.5.1 Micro-indentation Technique

Micro-indentation is a rapid and simple technique to measure K_{IC}, and, is particularly useful when a small volume of material is available (as is often the case during material development). As we will see below, a number of analytical formalae have been proposed in the literature for calculation of fracture toughness from indentation measurements, and, the technique is not strictly valid for composite materials. However, we believe it is nevertheless an useful technique for comparative evaluation of materials, and, most of the results presented in this study are based on this technique.

Micro-indentation is performed by applying a load through the tip of a diamond indenter (Vickers indenter used in this study) to the polished surface of a sample and measuring the radius of penny-like radial/median crack formed after the load has been removed. As

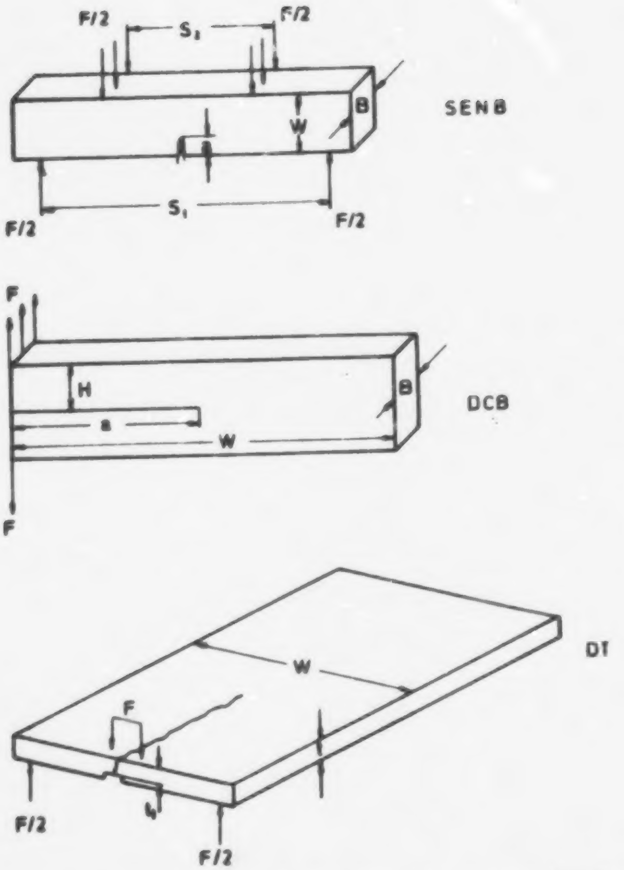
F/2
S₁
F/2
W
B
a
SENB
F/2
S₁
F/2
F
H
B
DCB
a
W
F
DT
W
F
F/2
t
F/2

Commonly used specimens for measuring K_{Ic}

Figure 4.2

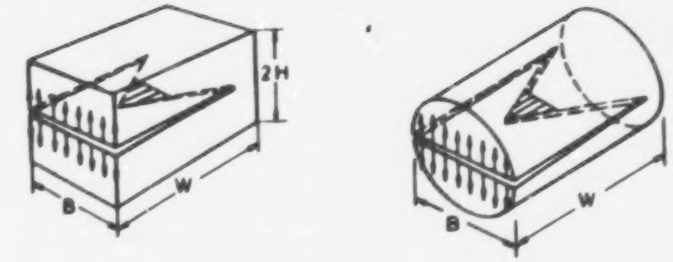

Short bar

Short rod

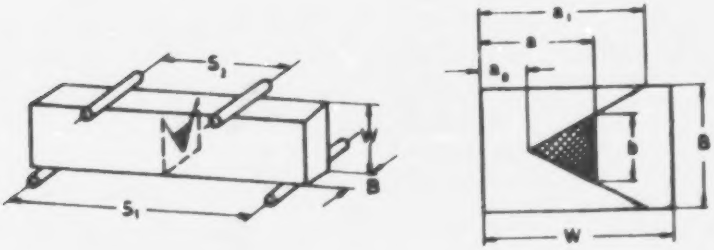
S2
W
B
S1
a1
a
a0
b
B
W

Four point bend

Chevron notch specimens

Figure 4.3.

shown in Figure 4.4, two kinds of cracks may occur : median (half-penny) and lateral (Palmqvist) cracks depending on the load and material. It is important to know which cracks have formed as the formulation is different for the two regimes.

Early analysis by Lawn and Swain (1975) used only the elastic component of the elastic/plastic field developed under loaded indenter for the median vent formation. They reported the equation :

$$K_c = \mu_a (P/C)^{1/2} \quad \ldots\ldots\ldots\ldots\ldots \quad (4.9)$$

where, μ_a is a dimensionless constant
P is indenter load
and, C is the radius of median crack

Lawn and Fuller (1975) used dimensional arguments for penny-shaped cracks to yield :

$$K_c = \psi_b P/C^{3/2} \quad \ldots\ldots\ldots\ldots\ldots \quad (4.10)$$

where, $\psi_b = 1/\pi^{3/2} \tan\psi$
ψ = Indenter cone half angle = 68°

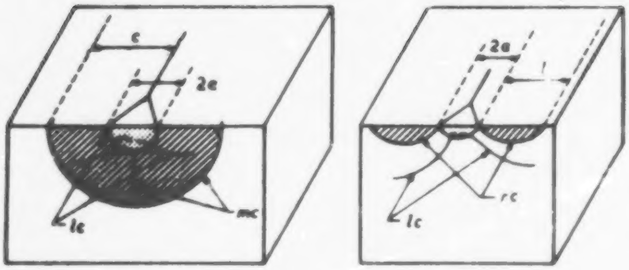

(a) (b)

Top and cross sectional views of median (half-penny), lateral and radial (Palmqvist) cracks, *mc*, *lc*, *rc*, respectively around Vickers indentations.

Figure 4.4

Substituting in equation 4.10, we get,

$$K_c = 0.073\ P/C^{3/2} \quad \ldots\ldots\ldots\ldots\ldots \quad (4.11)$$

A residual stress field forms about the plastic zone and it has been demonstrated that the residual stress field exerts an opening force on the median vents; fracture toughness values using cracks formed about indentations as starting flaws were found to be consistantly lower than fracture toughness values determined by more conventional methods. Evans and Charles and Evans and Wilshaw included the elastic/plastic field in their analyses through the hardness to modulus (H/E) ratio but derived only a semi-empirical equation. In addition, a detailed description of the mechanisms involved in the crack system evolution was avoided. Marshall and Lawn specifically dealt with both the elastic and residual components of the stress field in modifying equation 4.10. Unfortunately, their analysis contained empirical constants that had to be evaluated for each indenter/specimen system.

Recently, the approach of Marshall and Lawn was extended further by Lawn, Evans and Marshall. They argued the elastic component drives the downward extension of the median vent during the loading cycle but that it is the residual component that provides the primary driving force during the unloading sequence when the median vent forms its well-developed half-penny shaped geometry. What is unique about this analysis is that an expression was derived specifically for the surface trace of the median crack. This point is important since only the surface trace of the median vent crack can be measured in opaque materials. The exact expression obtained by Lawn et al for the radial crack was :

$$K_C = \frac{P\left[\xi_r^R \ (\mathrm{Cot}\,\psi)^{2/3} \ (E/H)^{1/2}\right]}{C_R^{\ 3/2}} \qquad ....(4.12)$$

where C_R is the radial (surface trace) crack and ξ_r^R is a constant evaluated to be 0.032 ± 0.002. A comparison of equation (4.12) to equation (4.11) shows that inclusion of the residual component of the elastic/plastic stress field into the indentation fracture mechanics analysis has led to the appearance of the ratio E/H in the expression.

On substituting for $\psi = 68°$ in equation (4.12) we get

$$K_c = 0.017 \ (E/H)^{1/2} (P/C^{3/2}) \ .... \ (4.13)$$

Anstis, Chantikul, Lawn and Marshall (1981) used the indentation technique on a number of ceramic systems (Si_3N_4, Al_2O_3, glass, glass-ceramic, WC-Co, SiC, etc.) and compared the results versus those determined by other techniques (DCB, DT, etc.). Figure 4.5 illustrates the data for the different materials and the "calibration" constant was determined to be 0.016 ± 0.004, which is quite close to 0.017 in equation (4.13).

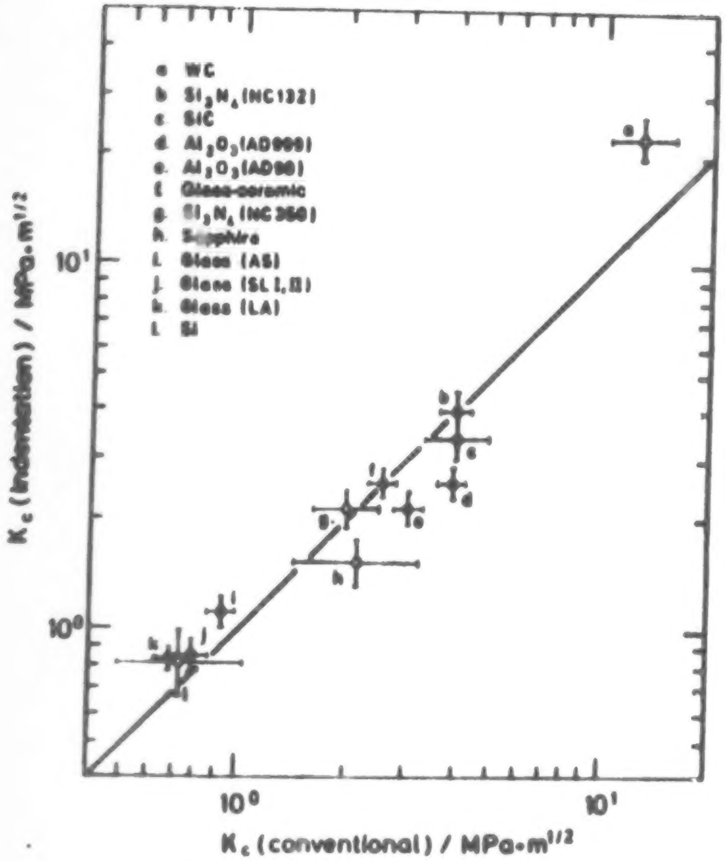

Plot demonstrating correlation between toughness values determined by indentation and by conventional means. Filled symbols denote reference materials used to evaluate constant ξ^R_V. Vertical error bars represent uncertainty (standard deviation) in parameter $P/c_0^{3/2}$ obtained [illegible] horizontal error bars nominal accuracy of K_c values

Figure 4.5.

Niihara, Morena and Hasselman (1982) considered two different regimes of cracks formed (median/penny and Palmqvist/lateral cracks), and proposed the following equations :

For the Palmqvist cracks ($0.25 \leq l/a \leq 2.5$)

$$(K_{Ic}\phi/Ha^{1/2}) (H/E\phi)^{2/5} = 0.035 (l/a)^{-1/2} \quad \text{........(4.14)}$$

For the median cracks ($c/a \geq 2.5$)

$$(K_{Ic}\phi/Ha^{1/2}) (H/E\phi)^{2/5} = 0.129 (c/a)^{-3/2} \quad \text{......(4.15)}$$

Thus it is important to determine which regime is applicable. In this study it was ensured that the load applied was sufficient to create median penny cracks, i.e. c was at least 2-2.5 times a. Due to the different functional relationship between load and crack length c (or l) in the above relationship, applicable load regime was established by plotting log (load) vs log (c) as shown in Figure 4.6. The slope of this plot was generally determined to be around 1.5 predicted for median penny cracks from the above theory.

On substituting for hardness H in equation (4.15) we get :

$$K_{Ic} = 0.031 (E/H)^{2/5} (P/C^{3/2}) \quad \text{.............(4.16)}$$

Notice the different power of (E/H) term in this equation compared to equation (4.13)

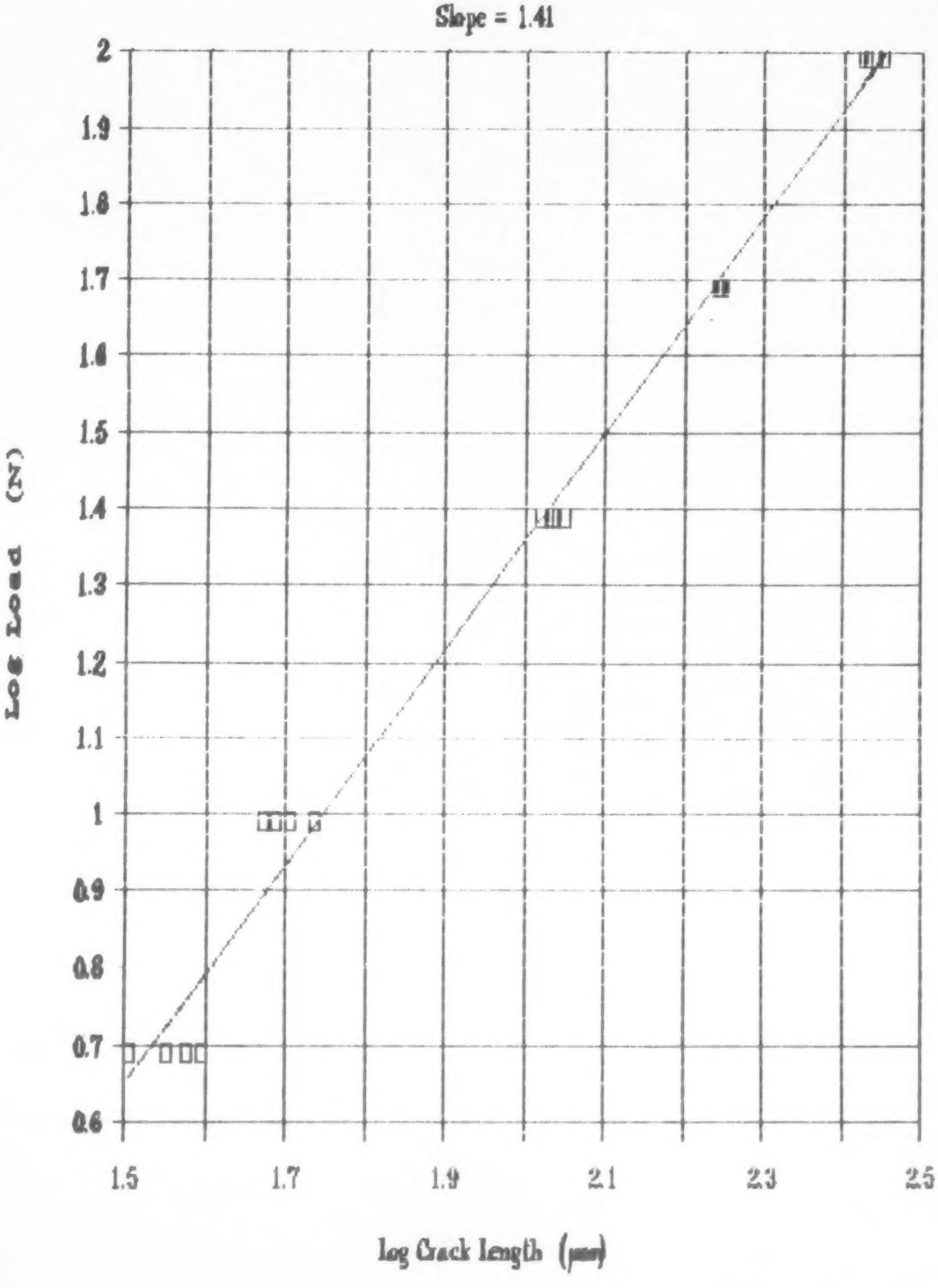

Figure 4.6. Log(load) vs log(crack length) relationship

Finally, Nihara et al (J.A.C.S., Jan.1984, C 13-14) have proposed the following equation, after normalizing with data from a number of materials :

$$K_{Ic} = 0.203 \; (Ha^{1/2}) \; (c/a)^{-3/2} \; .... (4.17)$$

Substituting for hardness H, it can be simplified to the equation:

$$K_{Ic} = 0.0941 \; P/C^{3/2} \; .... (4.18)$$

It is apparent the E/H term has been eliminated by "normalizing" the data from various materials. In this study we have used both formulations with and without E/H terms.

The above formulations give different K_{Ic} values for the same measurements. However, for comparative purposes, any one formula can be used. We have used equation (4.18) in reporting results in this report.

As mentioned above, the major advantages of the micro-indentation are :

i) very little sample required
ii) simple, and
iii) fast

The disadvantages are :

i) a well polished surface is required, otherwise crack length measurement is not accurate

ii) it is difficult to detect end of crack tip in an opaque material

iii) residual surface stress effects due to grinding and polishing introduce errors, and

iv) error due to lateral crack formation

A technique suggested by T.Troczynski of Electrofuel in which a diffuse indirect lighting is used instead of direct lighting in the optical microscope to highlight end of a crack tip in translucent materials such as alumina was found very useful, and, was used in most alumina matrix composites.

4.5.2 Chevron Notch Technique

Chevron notch technique was used for a few selected compositions as a comparison. The work was done by two final year students of the Metallurgy Department of the University of Toronto, R.Peters and S.Bywater, in conjunction with Electrofuel staff.

The Chevron notch configuration (Figure 4.7) has several desirable qualities :

i) Crack initiation is confined to the tip of the triangular notch,

ii) stable crack extension occurs up to, and beyond a maximum load point,

iii) a minimized notch width is not necessary, and,

iv) crack length measurement is not required to calculate K_{IC}.

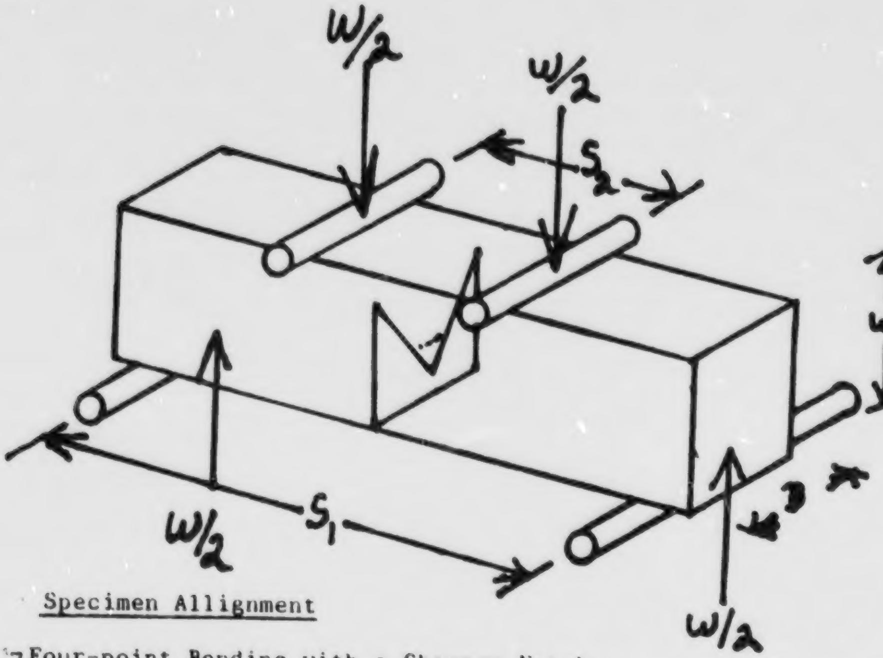

Specimen Allignment

Figure 4.7 Four-point Bending with a Chevron Notch

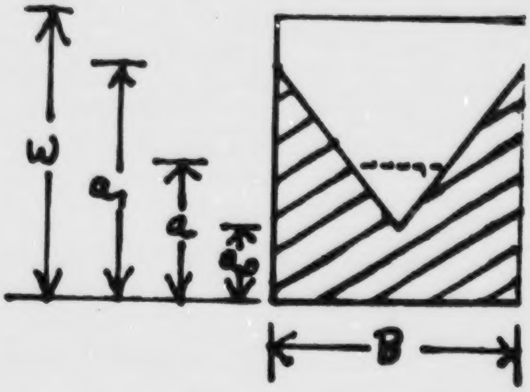

Detail of Chevron Notch

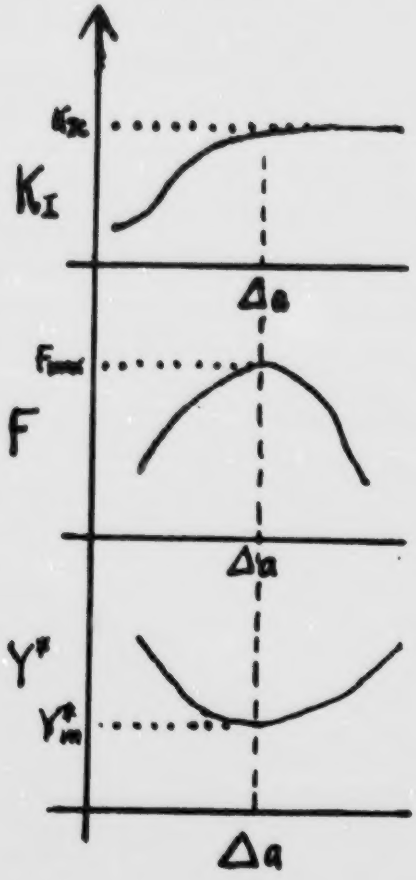

Figure 4.8 Graphs showing the relationship between i) K_I, the Stress Intensity Factor, ii) F, the Applied Load, iii) Y*, the Stress Intensity Factor Coefficient, and a, the Crack Extension.

For the notch configuration shown in Figure 4.7, the calculation for K_{Ic} is :

$$K_{Ic} = \frac{F_{max}}{P\sqrt{W}} Y^*_m \text{ ....(1)}$$

In this context, K_{Ic} is defined as the maximum stress intensity as complete fracture is approached. This occurs at maximum load, F_{max}, and at minimum Y* (see Figure 4.8). Y* is the stress intensity factor coefficient and is defined by Munz as :

$$Y^* = \frac{1}{2} \frac{d\,C^*tr}{d\alpha} \times \frac{\alpha_1 - \alpha_0}{\alpha - \alpha_0} \qquad \text{.............(2)}$$

where C*tr is the compliance for a trapezoidal crack front propagation through the Chevron notch. The expression is very important as it defines the minimum value of Y* (Y^*_m) as crack growth occurs.

Two major analysis have been performed to evaluate Y^*_m. The first and most common is the straight through crack assumption (STCA). This assumes that the change of compliance term, dC*tr/dα is the same for a single edge-straight crack front as a trapezoidal crack front in the Chevron notch.

The second analysis by Blum is the Slice Model. In this case, the compliance is deduced from the sum total of compliances of uniform straight through notch slices across the Chevron notch. Although the increased accuracy predicted of the Slice Model is questionable, the deviation of the results is lowered significantly.

Munz has evaluated closed-form analytical formulae for STCA and the Slice Model :

$$Y^{*}m\ (\text{STCA}) = [2.92 + 4.52\ \alpha_0 + 10.14\ \alpha_0^2]$$

$$Y^{*}m\ (\text{Slice Model}) = [3.08 + 5.00\ \alpha_0 + 8.33\alpha_0^2]$$

For the following range parameters :

$$0.12 \le \alpha_0 \le 0.24$$

$$0.90 \le \alpha_1 \le 1.00$$

$$1.00 \le W/B \le 1.25$$

These formulae were found to be accurate for a variety of ceramics.

Munz has also done detailed analysis on four-point bend specimens with Chevron notches using a wide range of parameter valves for AL_2O_3. The most consistent results were obtained for $\alpha_1=1$. These results were found to be independent of α_0.

Three samples were chosen for comparative and variety purposes. These were :

i) Sample #14 : 99.8% Al_2O_3
ii) Sample #20 : 20% Al_2O_3 , 80% ZrO_2
111) Sample #13 : 75% Al_2O_3 , 25% SiC whiskers

4.5.3 Four-Point Bending

Four-point bending was done using a four-point bending jig having four stainless steel load rollers, 1.2 cm in diameter and separated by 20 cm and 40 cm for each cell pair. The jig was mounted on an Instron 1000 lb tensile testing machine set at a cross-head speed of 1/2 inch per minute. The value for F max were read from the maximum point of the load-deflection curves graphed by the Instron plotter.

The results of the four-point bend/Chevron notch specimens are shown in Figure 4.9, along with K_{IC} values calculated by four different formulae given in section 4.5.1. It can be seen that Chevron STCA and Slice Model give comparable values for the three materials studied : alumina, alumina-zirconia and alumina-silicon carbide whisker composites. Some of the micro-indentation formulae also give results close to Chevron notch specimens, thus indicating fairly good correlation between methods.

Fig.4.9. , Plot of Micro-indentation and Four-Point Bend Results versus K_{IC}.

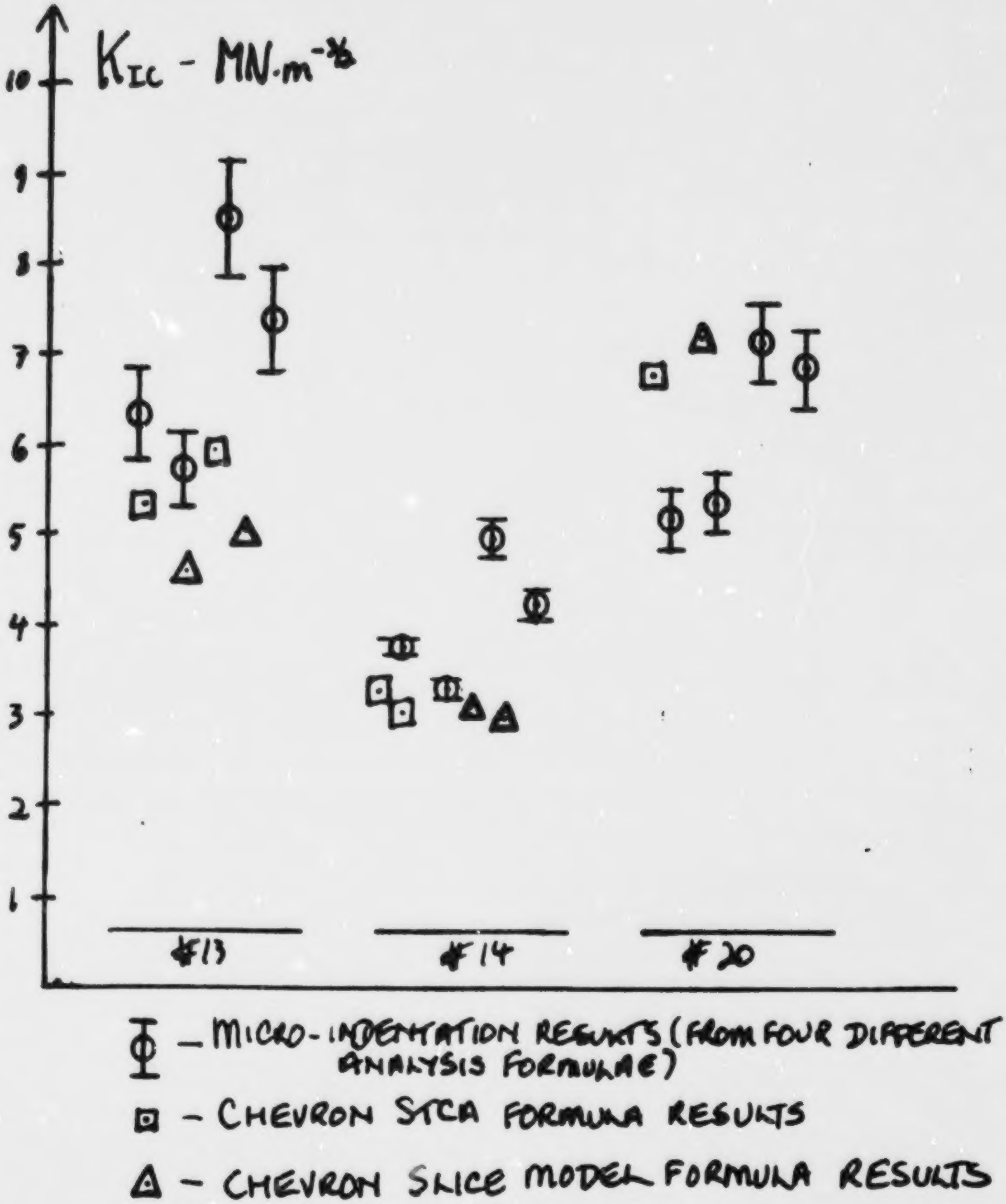

SAMPLE #13 - 75% Al_2O_3, 25% SiC

#14 - Al_2O_3

#20 - 20% Al_2O_3, 80% ZrO_2

4.6 Microstructure

As it is true in metals, microstructure is of critical importance in determining the properties of ceramic materials. In zirconia toughened ceramics, microstructural factors such as, size of matrix and zirconia grains, location of zirconia grains (whether intragranular or at grain boundaries), type and amount of zirconia phases present (m,t or c-zirconia), etc.,have a profound effect on mechanical properties such as strength and toughness. Therefore, microstructure was carefully studied using optical and scanning electron microscope (SEM). On the SEM, the backscatter electron mode is particularly useful in improving the contrast between a high atomic number element like Zr and light element like Al.

The effect of raw materials and processing variables on the microstructure was studied and this was correlated with its effect on the properties of the final sintered product. In this way, powders and processing were optimized to yield the desired combination of properties.

5. RESULTS AND DISCUSSIONS

As discussed in Section 1.5, it was decided to explore the following four promising systems on this program :

1. Zirconia based materials (PSZ, TZP, ATZ)
2. ZTA with Yttria additive
3. ZTA without Yttria additive
4. ZTA reinforced with SiC whiskers

This chapter summarizes the results obtained and the discussions.

5.1 Zirconia Based Materials (PSZ, TZP, ATZ)

A number of zirconia based materials were fabricated from commercially available powders. All of them were compacted by the cold press and sinter technique, although some were hot pressed for comparative studies. Other than one spray dried powder (Toyo Soda TZ-3YA with binder added), all of the commercial powders had very low bulk density and did not flow well. They were all dispersed in water and processed as described in Chapter 3.

5.1.1 Tetragonal Zirconia Polycrystals (TZP)

We have studied the following TZP materials :

1. ZrO_2 - 1 mole% Y_2O_3 (Zircar)
2. ZrO_2 - 2 mole% Y_2O_3 (Toyo Soda TZ-2Y)
3. ZrO_2 - 3 mole% Y_2O_3 (Toyo Soda TZ-3YA)
4. ZrO_2 - 6 mole% Y_2O_3 (Daiichi HSY-6)

The 1 mole% Y_2O_3 samples were cracked extensively, and XRD results indicated that all zirconia transformed into monoclinic phase, as shown in Table 5.1. This result is expected from the ZrO_2-Y_2O_3 phase diagram, (shown in Figure 5.1), as 1 mole% Y_2O_3 lies in the m-phase field. However, 2 mole% Y_2O_3 samples resulted in 100% tetragonal phase as shown in Table 6.1, although phase diagram (Figure 5.1) predicts m and c phases. The high temperature tetragonal phase is completely retained at room temperature due toáconstraints tetragonal grains place on each other. This phenomenon can also be thought of in the following manner : the M_s temperature, i.e. the temperature belowáwhich the martensitic t-->m transformation starts, is below room temperature. In the case of 1 mole% Y_2O_3 (above), both M_s and M_f (martensitic finish) are above room temperature, and hence, 100% transformation to m-phase took place.

Figure 5.2 shows the results of fracture toughness (K_{IC}) obtained. It can be seen that high toughness (above 10 $MPa.m^{½}$) is obtained with 2 mole% Y_2O_3 materials. For 3 mole% Y_2O_3 materials, again 100% t-phase is obtained (Table 5.1), but slightly lower fracture toughness around 8 $MPa.m^{½}$ is achieved. These results are in excellent agreement with literature data, shown in Figure 5.3 (from Tsukuma, Kubota and Tsukidate, 1983). This reduction in fracture toughness is related toáthe higher transformability of the 2 mole% Y_2O_3 compositions.

However, the 2 mole% Y_2O_3 material suffers from higher instability, as shown by ageing experiments reported in the literature (see Figure 5.4 - ibid). From Figure 5.4 it can be

Table 5.1 PHASE ANALYSIS BY XRD - ZTA

COMPOSITION		Relative Density %	% MONOCLINIC PHASE	% TETRAGONAL PHASE
Vol % ZrO_2	Mole % Y_2O_3			
100	1.0	91.9	100	-
100	2.0	98.7	-	100
100	3.0	98.8	-	100
80	3.0	98.9	-	100
20	0.0	96.9	100	-
20	1.0	97.1	88.1	11.9
20	3.0	98.1	-	100
10	2.0	97.4	6.8	100
20	2.0	98.0	-	100
30	2.0	97.4	-	100
5	0.0	98.2	12.9	87.1
10	0.0	98.9	57.4	42.6
15	0.0	97.0	90.6	9.4

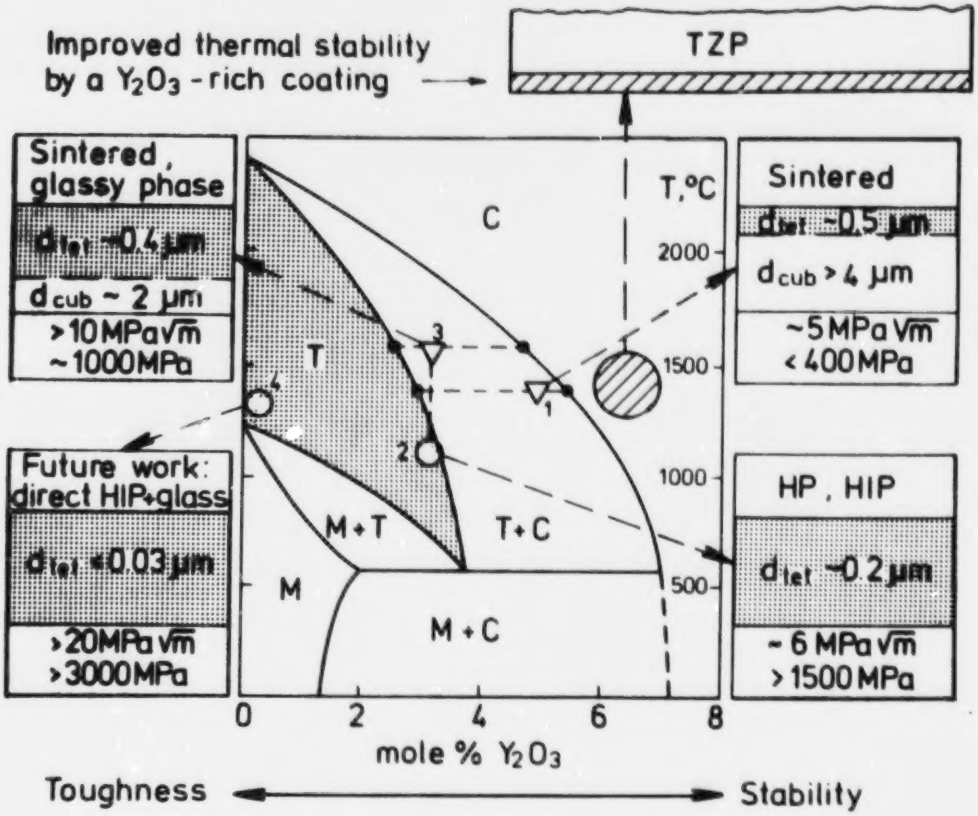
Improved thermal stability
by a Y2O3 - rich coating
TZP
Sintered, glassy phase
dtet ~0.4 µm
dcub ~ 2 µm
>10 MPa√m
~1000 MPa
Future work: direct HIP+glass
dtet <0.03 µm
>20 MPa√m
>3000 MPa
Sintered
dtet ~0.5 µm
dcub > 4 µm
~5 MPa√m
< 400 MPa
HP, HIP
dtet ~0.2 µm
~ 6 MPa√m
> 1500 MPa
C
T
M+T
T+C
M
M+C
1
2
3
4
T, °C
2000
1500
1000
500
0
2
4
6
8
mole % Y2O3
Toughness
Stability

Figure 5.1. Zirconia- yttria phase diagram.

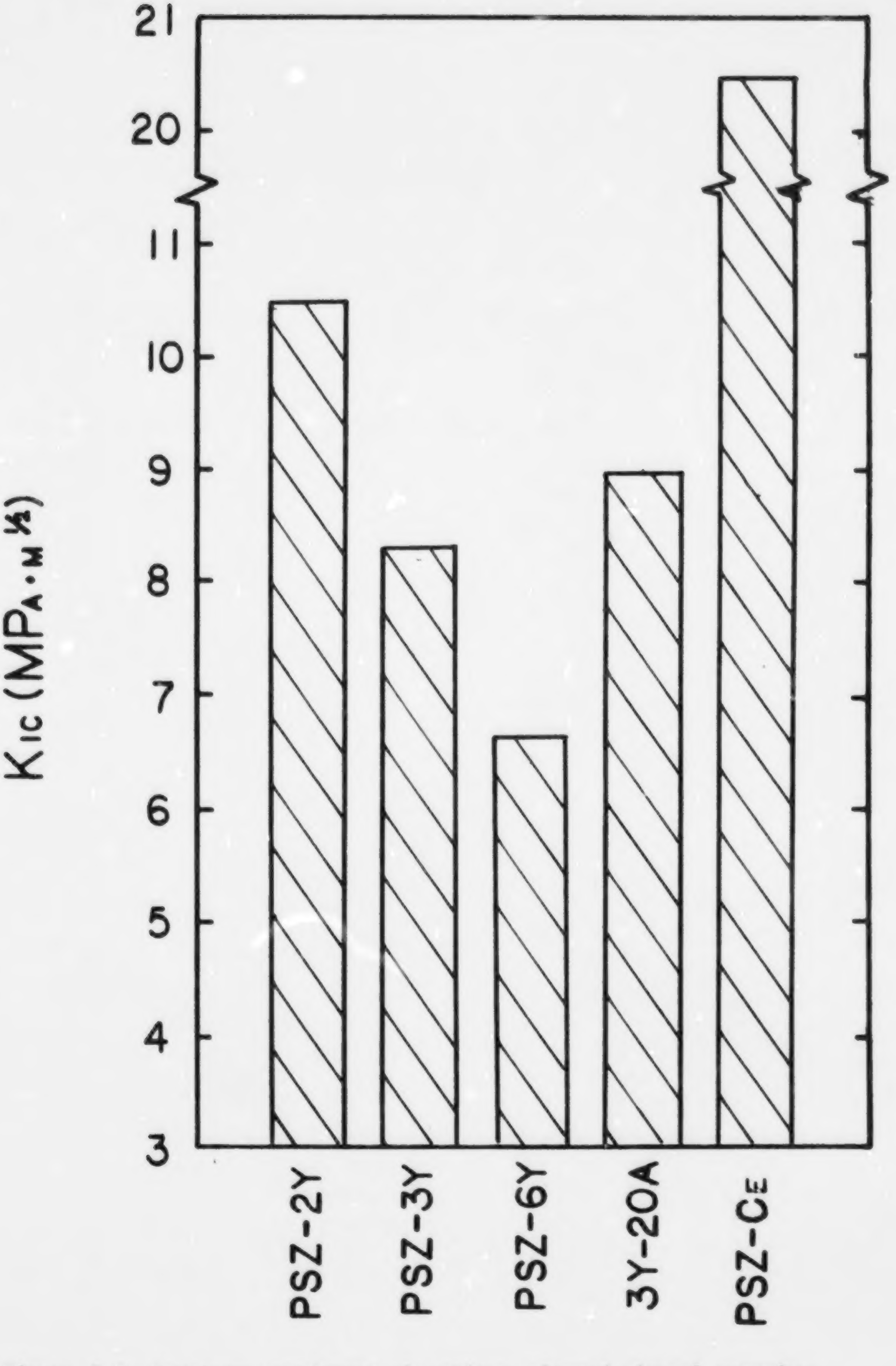

Figure 5.2. Fracture toughness of various zirconia based ceramics.

Title	Scale	Date	Initial	Dwg.No.	Rev.

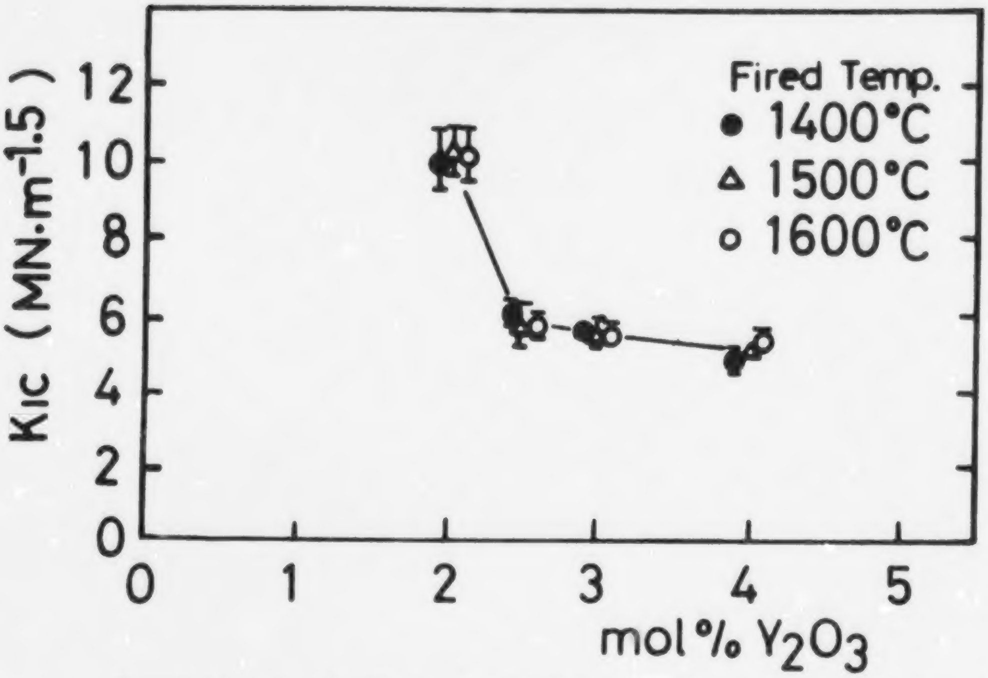

Dependence of fracture toughness on Y_2O_3 content (firing temperature: ●, 1400°C; △, 1500°C; ○, 1600°C).

Figure 5.3.

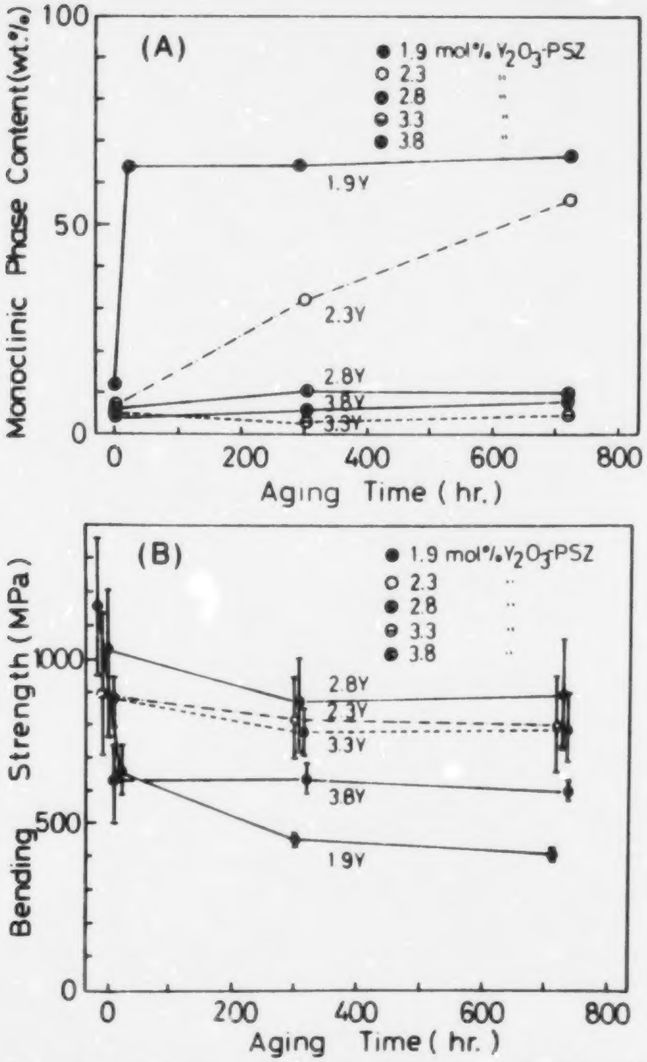

Relationship between Y_2O_3 content and 300°C aging time: (*A*) phase transformation dependence on Y_2O_3 content; (*B*) bending strength dependence on Y_2O_3 content.

Figure 5.4

seen that, for any composition below 2.8 mole% Y_2O_3, considerable fraction of m-phase appeared on ageing at 300°C, which resulted in a degradation of strength.

On further increasing the Y_2O_3 content to 6 mole%, the fracture toughness reduced even further to about 6 $MPa.m^{½}$, as the transformability of t-particles is reduced (see Fig.5.2). However, the stability of this material is further improved.

5.1.2 Ce-Modified TZP

Ce-TZP is an unique ceramic material with exceptional fracture toughness ($K_{IC} > 30$ $MPa.m^{½}$), which shows inelastic stress-strain behaviour (like metals) before failure. Furthermore, this material does not have medium temperature instability problem observed with Y-TZP. However, Ce-TZP has some weaknesses: its maximum strength and hardness are limited.

Figure 5.5a (Tsukuma, 1986) illustrates the mechanical properties of Ce-TZP as a function of CeO_2 content. Hardness increased with CeO_2 content upto 9 GPa at 16 mole% CeO_2. While the strength peaked at 14 mole% CeO_2, the fracture toughness was highest at 12 mole% CeO_2 with 1 µm grain size. Figure 5.5b shows the results of hydrothermal ageing at 150°C for Ce and Y modified TZP. While 12 mole% and 14 mole% Ce-TZP showed no increase in monoclinic fraction during ageing, Y-TZP containing 2 mole% and 3 mole% Y_2O_3 showed a rapid increase. Similarly, after thermal cycling between room temperature and 500°C for 1000 hours, Ce-TZP showed no strength degradation.

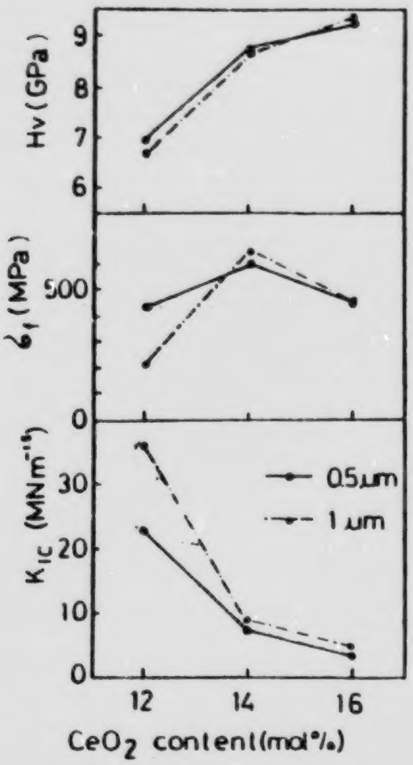

Figure 5.5a

Relation between mechanical properties and CeO_2 content. (K_{IC}— fracture toughness obtained from indentation microfracture method, δ_f— three-point bending strength, and Hv— Vickers hardness.)

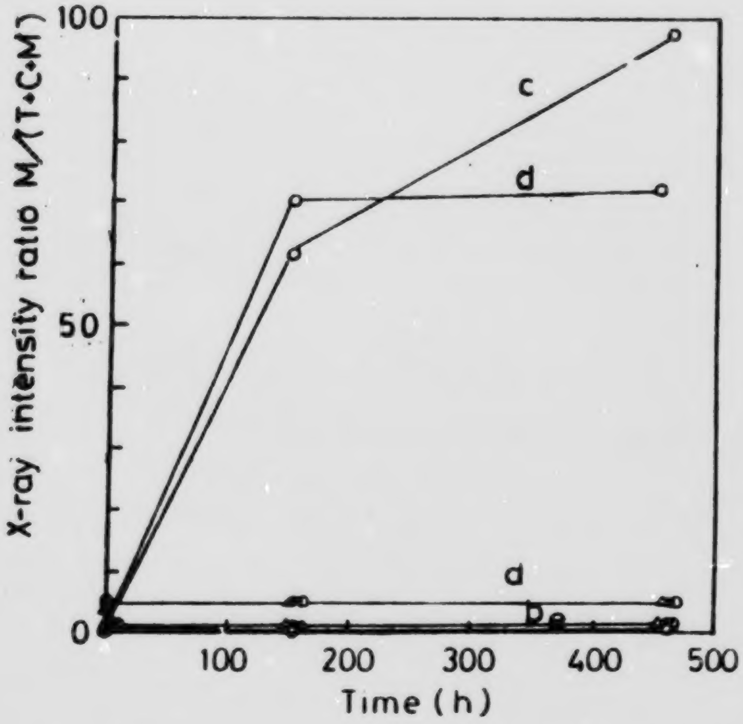

Figure 5.5b.

Result of hydrothermal aging at 150°C for pure Ce-TZP, (a—Ce-TZP (12 mol% CeO_2), b—Ce-TZP (14 mol% CeO_2), c—Y-TZP (2 mol% Y_2O_3), d—Y-TZP (3 mol% Y_2O_3), e—Y-TZP (4 mol% Y_2O_3)) grain-size of Ce-TZP—–○– 0.5 μm, –Δ– 1 μm –•– 2.5 μm, and grain-size of Y-TZP—0.2 μm.

Figure 5.2 also gives fracture toughness results for 12 wt% CeO_2-zirconia samples, sintered from Unitec powder. Although extremely high value of $K_{Ic} > 20$ MPa.m^{½} is indicated in the figure, it should be noted that this value may be in error due to extreme plasticity shown by this material. The micro-indentation technique used for K_{Ic} measurement is probably not valid under these conditions. Even at 60 kg applied load on the indenter, only very small cracks appeared. nowhere close to the required $c > 2a$ condition.

5.1.3 Alumina Toughened Zirconia (ATZ)

Japanese have used the term "alumina toughened zirconia" to describe the improved strength, toughness and stability observed when alumina was added to TZP composition. Figure 5.6 and 5.7 (from Tsukuma, Ueda and Shimada, 1985) demonstrate the improvement of strength and toughness observed when alumina is added to Y-TZP material and hot isostatically pressed at 1500°C. Strengths in excess of 2.4 GPa, highest ever achieved for a ceramic material, are observed in this system. As shown in Figure 5.7, the two techniques of fracture toughness measurements, micro-indentation (MI) and Chevron-notched beam (CNB) do not show the same trend with increasing alumina addition. The toughness obtained with Chevron-notched beam technique increased with addition of alumina upto 20 wt%, consistent with strength data shown in Figure 5.5. On the other hand, fracture toughness obtained from micro-indentation technique decreased with increasing alumina content, consistent with the relation between

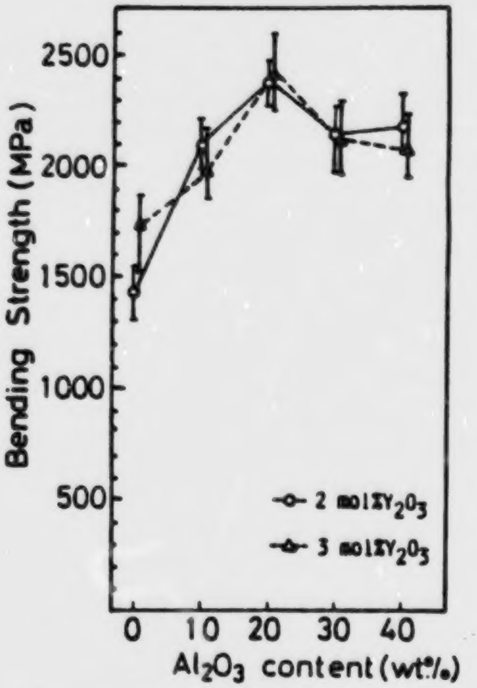

Figure 5.6

Dependence of bending strength on Al_2O_3 content for Y_2O_3-PSZ containing (O) 2 mol% Y_2O_3 and (Δ) 3 mol% Y_2O_3. Error bars indicate maximum and minimum strength values; 6 bars were tested for each sample.

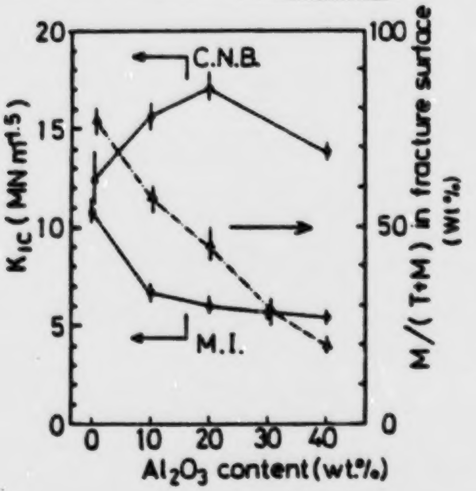

Figure 5.7

Fracture toughness and fraction of monoclinic phase resulting from stress-induced transformation of ZrO_2+2 mol% Y_2O_3 and ZrO_2+2 mol% Y_2O_3-Al_2O_3 composites. (M.I. = microindentation technique and C.N.B. = chevron-notched beam technique.)

the fraction of stress-induced transformation and alumina content (shown in Figure 5.7). This may be due to the fact that fracture toughness measured by the CNB method is related to crack initiation, whereas that obtained from MI method is related to crack propagation. Thus, CNB results suggest that the addition of alumina contributed significantly to the improvement of fracture toughness through its effect on crack initiation.

Alumina appears to have beneficial effect on high temperature strength of Y-TZP, as shown in Figure 5.8. The bending strength of all samples decreased drastically when temperature increased to 400°C due to the reduction in the contribution of phase transformation toughening. Then, the strength remains constant or slightly increases upto 600°C. In the range 600° to 1000°C, the strength of materials with and without small amounts of alumina (2Y, 2Y10A and 2Y20A) decreased gradually with increasing temperature, whereas the material containing a large amount of alumina (40 wt% Al_2O_3) showed nearly a constant high strength of about 1000 MPa upto 1000°C.

As indicated in Section 1.5, these exceptional strengths are being achieved at moderate toughness. The additon of alumina to Y-TZP matrix, somehow, appears to decrease the critical defect size. This toughening effect of alumina on zirconia (ATZ) is not well understood.

Fracture toughness, measured by micro-indentation technique in this program, is shown in Figure 5.2 for PSZ-3Y and PSZ-3Y-20A. The 3Y-20A is a 80 wt% zirconia (3 mole% yttria)-20 wt% alumina

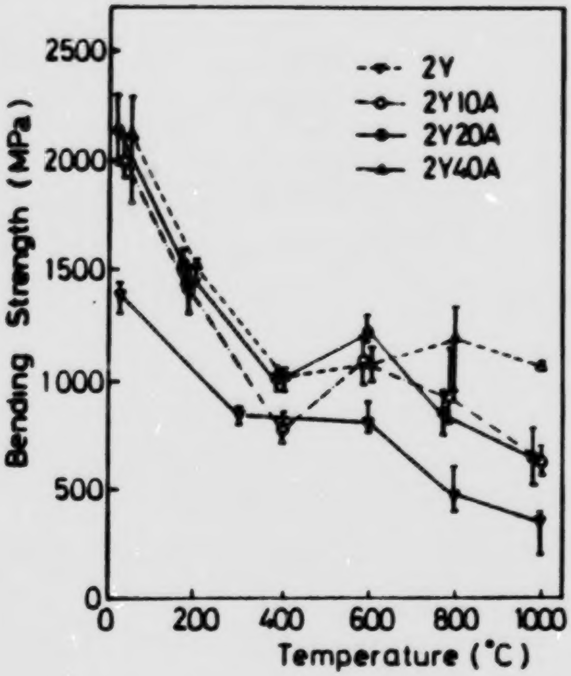

Figure 5.8

Temperature dependence of bending strength of isostatically hot-pressed ZrO_2 (2 mol% Y_2O_3)/Al_2O_3 composites (error bars indicate maximum and minimum strength values).

powder commercially sold by Toyo Soda, which was cold pressed and sintered. As shown in Table 5.1, all of the zirconia was in tetragonal form. The room temperature fracture toughness of about 9 MPa.$m^{½}$ was slightly better than 3Y material alone, and in between the values shown in Figure 5.7 by the two methods.

5.2 Zirconia Toughened Alumina (ZTA) With Yttria

As discussed in Chapter 1, the martensitic t-->m transformation in zirconia can be used to improve the toughness and strngth of ceramic matrices. The alumina matrix is particularly suitable due to higher elastic modulus (390 GPa compared to 207 GPa for zirconia) and chemical compatibility. Pure zirconia can be retained at the room temperature in metastable t-form by the physical constraint of the matrix phase. However, only a limited amount of very fine zirconia particles (less than the critical size) can be retained in t morphology without the addition of "stabilizers" such as yttria toázirconia. On the other hand, increasing yttria additions to zirconia reduces its transformability and eventually stabilizes the cubic phase which have a negative effect on the toughness and strength. Hence, there must be a optimum yttria content. The following series of experiments were performed tc determine the optimum yttria content and to determine the effect of zirconia content on alumina matrix :

* Series 1 - Volume fraction of zirconia constant at 20%.
Vary mole % Y_2O_3 in zirconia.

* Series 2 - From above, fix the mole% yttria in zirconia at the optimum concentration. Vary the volume fraction of zirconia.

5.2.1 Series 1 Experiments

In this series, the volume fraction of zirconia added to alumina was kept constant at 20 vol%. The yttria content of zirconia was varied between 0 tc 3 mole% by wet milling alumina powder with the following commercial zirconia powders :

1. ToyoáSoda TZ-0Y (0 m% Y_3O_3)
2. Zircar ZYP (1 m% Y_2O_3)
3. ToyoáSoda TZ-2Y (2 m% Y_2O_3)
4. ToyoáSoda TZ-3Y (3 m% Y_2O_3)

As described in Chapter 3, the wet mixing can be accomplished in acidic or basic regions, although acidic regions yielded somewhat better dispersion. Fine high quality aluminas such as CR-10 and AKP-30 gave best results with minimum grinding. However, lower priced aluminas, such as A-16SG, can be used with long ball milling time.

Figure 5.9 and Table 5.1 give XRD phase analysis of retained tetragonal phase in sintered samples of 20 v% zirconia ZTA. With noáyttria addition, all zirconia was in monoclinic morphology. The tetragonal fraction increased toáabout 12% at 1 m% yttria and toá100% at 2 and 3 m% Y_2O_3.

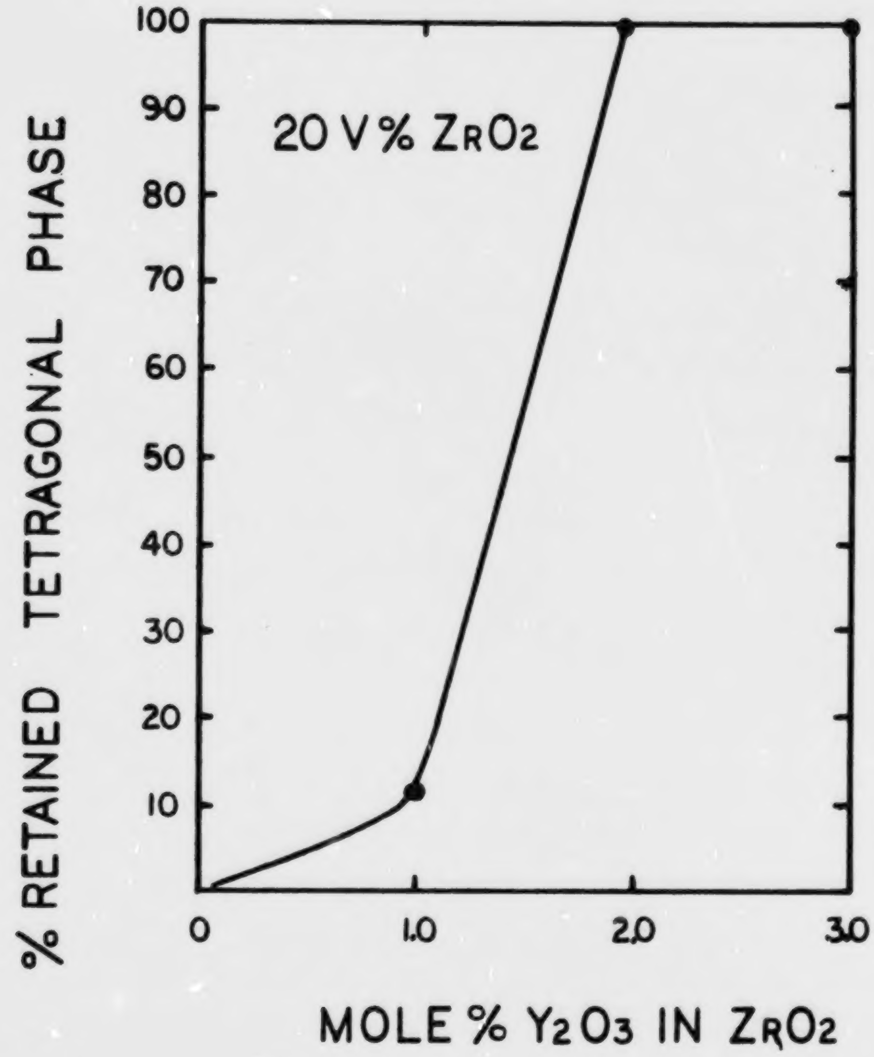

Figure 5.9. % Retained tetragonal phase as a function of mole% yttria.

15

Title	Scale	Date	Initial	Dwg.No.	Rev.
				59	

Figure 5.10 shows the fracture toughness values obtained as a function of yttria content for 20 v% zirconia ZTA. With increasing yttria content upto 2 m%, the fracture toughness increased mainly due to an increase in the number density of tetragonal particles (as shown in Figure 5.9). The decrease in K_{Ic} observed above 2 m% yttria reflects the decrease in transformability of t-phase similar to the effect observed in pure Y-TZP materials (see Section 5.1.1). This is due to reduced change in chemical free energy of transformation from t to m phase with increasing yttria stabilizer additions.

Figure 5.10 also includes fracture toughness results reported by Becher and Tennery (1983). Although they used a different technique to determine K_{Ic} (Double Cantilever Beam - DCB), the results are in good agreement. Lange (1982) also reported optimum results for ZTA with yttria content of 2 m% in zirconia.

With no yttria added, all zirconia particles transformed to monoclinic phase, which must result in extensive microcracking. These samples were difficult to polish due to surface chipping. However, polished areas gave high toughness values due to crack deflection (microcrack toughening) by the micro-indentation technique. Nevertheless, it is believed that this material will have low strength and low resistance to crack initiation.

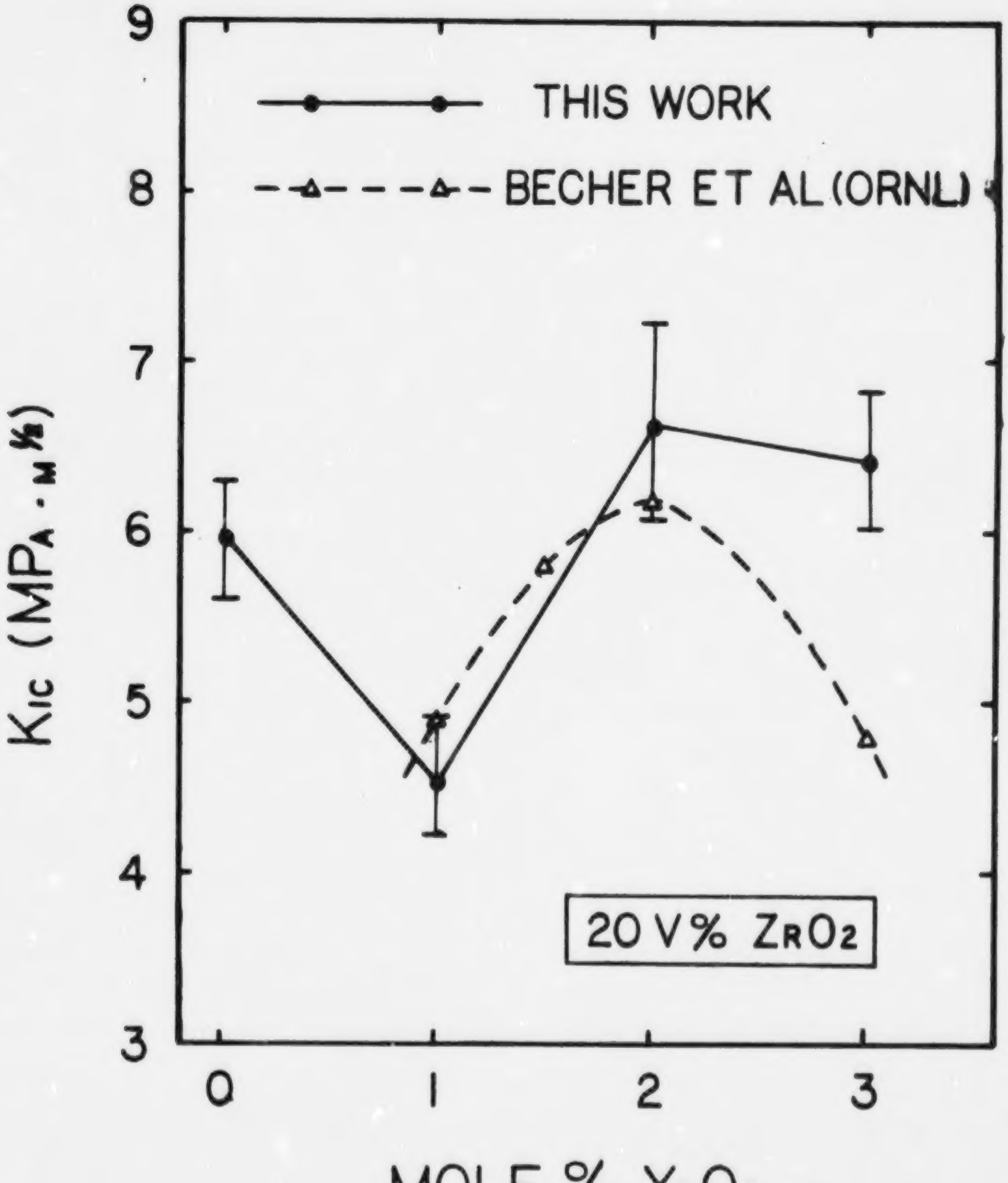

Figure 5.10. Fracture toughness as a function of yttria content for 20 vol% zirconia ZTA.

16

THE ELECTROFUEL MANUFACTURING CO. 9 Hanna Avenue Toronto, Ontario, Canada M6K 1W8

Title	Scale	Date	Initial	Dwg.No.	Rev.
				5.10	

5.2.2 Series 2 Experiments

Yttria content of zirconia was kept constant at the optimum value of 2 m% (determined above), and, the volume percent of zirconia in alumina matrix was varied between 0 and 30% in this series. As shown in Table 5.1, the entire zirconia was retained in tetragonal form. The measured fracture toughness increased continuously from about 4 MPa.m$^{1/2}$ for pure alumina to about 7.5 MPa.m$^{1/2}$ for ZTA with 30 vol% zirconia, as shown in Figure 5.11. As can be seen from the figure, the K_{Ic} results are again in excellent agreement with those reported by Becher and Tennery (1983). This increase of K_{Ic} is obviously due to increase in the volume of t-zirconia present. There is obviously a limit to the increase in fracture toughness obtainable, and, according to Lange (1982), the maximum toughness is observed around 45 v% zirconia (see Figure 5.12). However, in practical applications, the gain in toughness at higher zirconia content is offset by reduction in hardness and increased cost. On the other end of the spectrum, 20 wt% alumina addition to 2-3 m% yttria-zirconia was shown in Section 5.1.3 to be a reasonably tough high strength material.

Lange (1982) has shown that the strength of ZTA increases with zirconia (see Figure 5.13) in proportion to its increase in toughness. Further increase in strength is possible by the introduction of surface compressive stresses through grinding, as shownn in the figure.

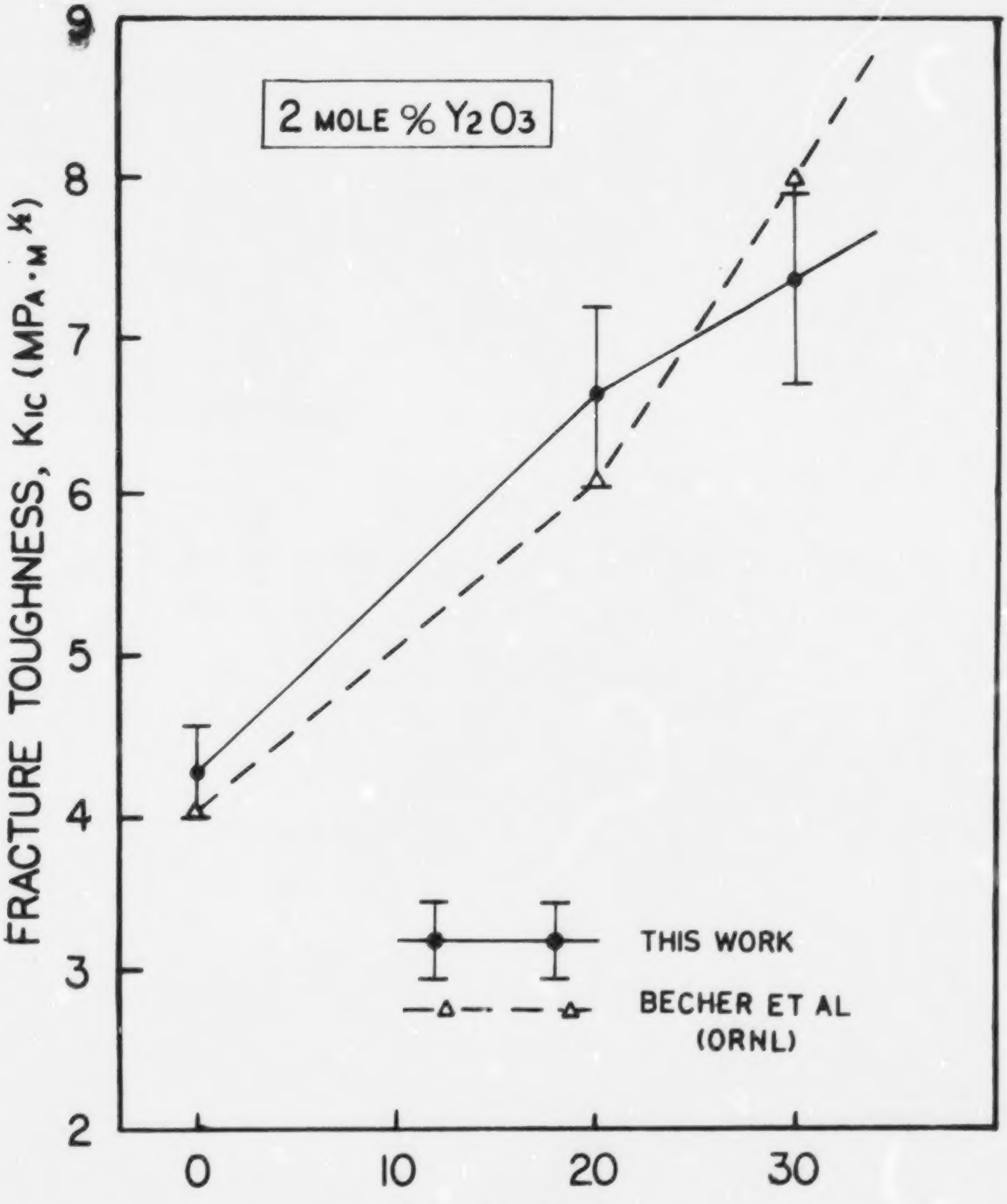

Figure 5.11. Fracture toughness as a function of zirconia content for ZTA containing 2 mole% yttria in zirconia.

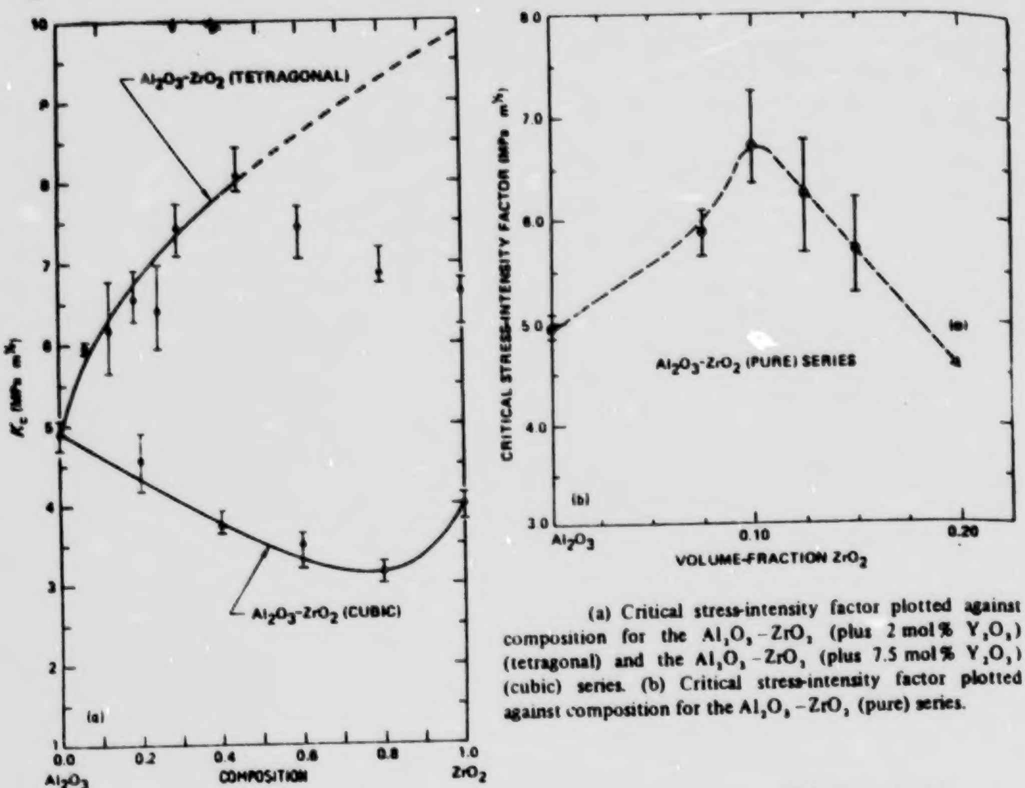

(a) Critical stress-intensity factor plotted against composition for the $Al_2O_3-ZrO_2$ (plus 2 mol% Y_2O_3) (tetragonal) and the $Al_2O_3-ZrO_2$ (plus 7.5 mol% Y_2O_3) (cubic) series. (b) Critical stress-intensity factor plotted against composition for the $Al_2O_3-ZrO_2$ (pure) series.

Figure 5.12

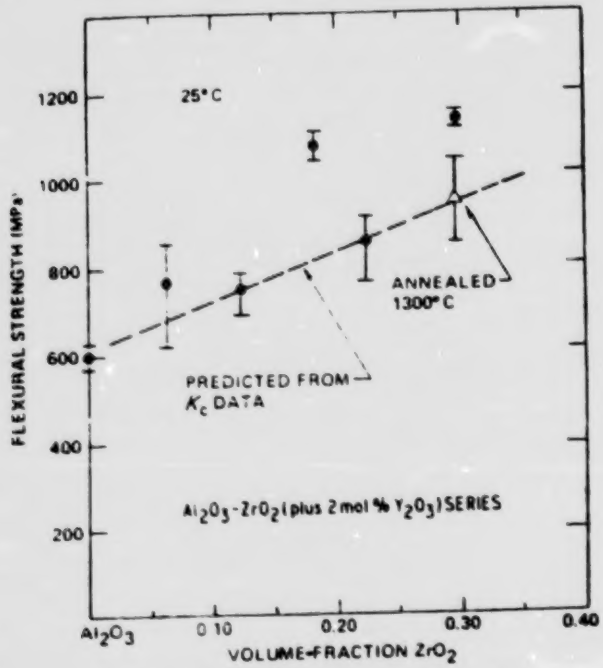

Figure 5.13

Flexural strength plotted against composition for the $Al_2O_3-ZrO_2$ (plus 2 mol% Y_2O_3) series.

5.3 Zirconia Toughened Alumina (ZTA) Without Yttria

As discussed earlier, the constraint of high modulus alumina matrix is able to retain tetragonal zirconia phase at room temperature without the additon of any stabilizer (yttria). The amount that can be retained depends on the particle size of zirconia, its volume fraction, whether present as intra- or intergranular particles, the elastic modulus of the matrix, etc.

Table 5.2 gives the critical grain size of zirconia particles in alumina matrix as a function of volume fraction of zirconia (reported by Lange and Green, Zirconia I, 1980). The critical grain size is the diameter below which zirconia particles will be retained in tetragonal form. Thus, critical grain size decreases from > 2.3 μm for 5 v% zirconia to about 0.74 μm for 20 v% zirconia.

Figure 5.14 shows the amount of tetragonal phase retained (obtained from XRD analysis) as a function of volume fraction of zirconia in ZTA without yttria additions. The results are probably affected by the surface grinding with 600 grit SiC paper before the measurements, which may have transformed some tetragonal particles. The results are also affected by the initial zirconia powder particle size, grinding time of the powders, processing temperature, etc. Figure 5.14 reports the results with Alcoa A-16SG alumina powder, Magnesium Electron SC-15 and ball milling time of 16 hours.

Table 5.2

Critical grain size for Al_2O_3/ZrO_2 composites

Vol fraction ZrO_2	Heat treatment		Critical grain size (μm)
	Temp. (°C)	Time (h)	
0.05*	1650	12	>2.3
0.10	1650	4	1.36
	1650	8	1.35
	1650	12	1.41
0.15	1650	4	0.85
	1650	8	0.84
	1650	12	0.85
0.20†	1650	4	0.74

*Monoclinic ZrO_2 not detectable by X-ray diffraction. †Longer heat treatment produced too much monoclinic ZrO_2 for reliable results.

Figure 5.14

PERCENT RETAINED TETRAGONAL PHASE IN ZTA AS A FUNCTION OF VOL. % ZrO_2 (PURE)

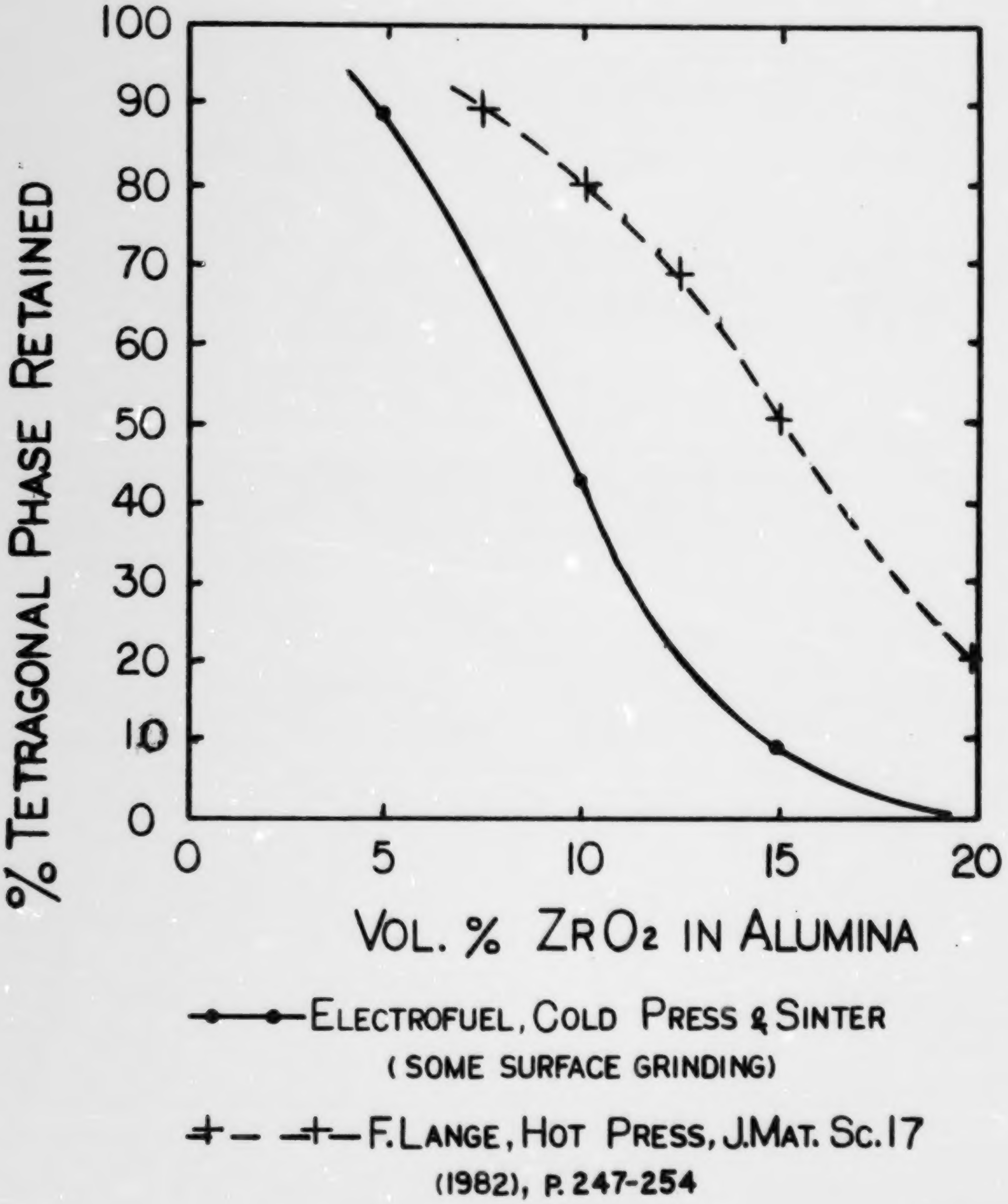

From Figure 5.14 it can be seen that percent retained tetragonal phase reduced from 90% at 5 v% zirconia to 0% at 20 v% zirconia. The figure also includes Lange's results (1982) for comparison, and, it can be seen that he was able to retain a higher fraction of t-phase by using fine powders and hot pressing. We were also able to retain higher tetragonal content by cold press and sinter process using fine alumina (CR-10, AKP-30) and zirconia (TZ-0Y, Hershaw, Dynazircon F) powders.

Figure 5.15 shows the fracture toughness obtained as a function of volume fraction of zirconia. The fracture toughness increases to a maximum of 7.5 MPa.m$^{1/2}$ at 10 v% zirconia and then drops off. This trend is in good agreement with results reported by Becher and Tennery (1983), although absolute values of K_{IC} do not agree as well as in the case of ZTA containing yttria (see Figure 5.11). This difference is probably due to different techniques of fracture toughness measurements. Double Cantilever Beam technique used by Becher and Tennery is probably more related to crack initiation, whereas micro-indentation method used here is more related to crack propagation. Hence, the contribution of microcrack toughening probably results in higher K_{IC} values by micro-indentation technique.

The fracture toughness increases with initial additions of pure zirconia to alumina due to increase of number density of t-zirconia. The decrease in K_{IC} values above 10 v% zirconia is associated with an increase in number density of monoclinic zirconia particles at the alumina grain boundaries. As the number

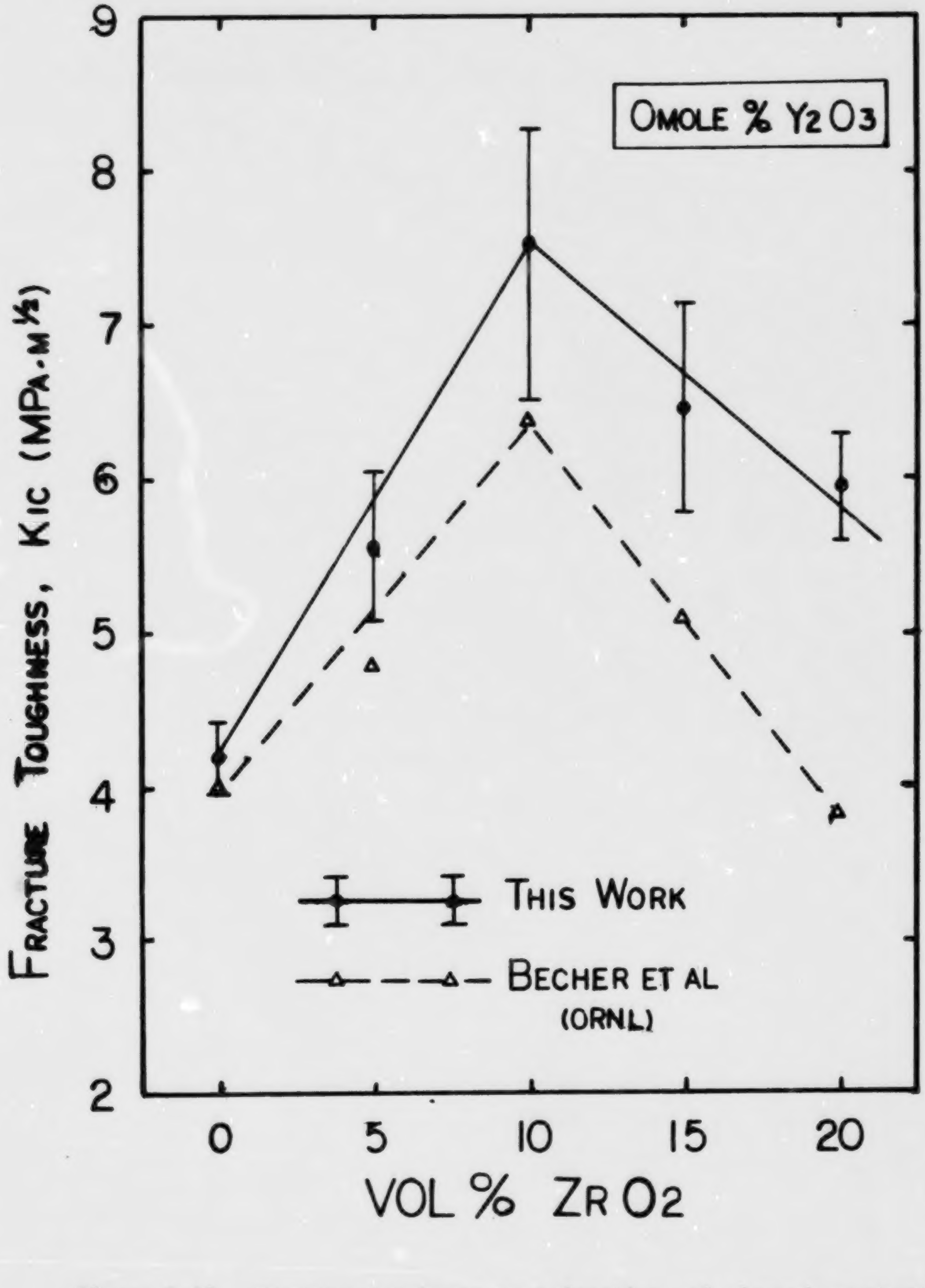

Figure 5.15. Fracture toughness as a function of zirconia content for ZTA with pure zirconia additions.

of larger monoclinic zirconia particles increases, microcracks are generated in the alumina grain boundaries between the m-particles and begin to link together. Thus, even if micro-indentation technique gives higher toughness reults with 20 v% pure zirconia ZTA material as compared to pure alumina, its strength will be poor. This kind of material with low strength but high toughness are useful in certain applications, such as thermal shock resistant material. For critical structural applications, maximum zirconia volume fraction should be limited to about 10% where a substantial fraction of zirconia is retained in tetragonal form.

Rühle, Claussen and Heuer (1986) have shown that transformation and microcrack toughening are complementary processes in zirconia toughened alumina. They have reported strength and fracture toughness of 15 v% zirconia (pure) ZTA in which t-phase concentration was varied by varying the zirconia particle size (by varying the milling time). The results are shown in Figure 5.16. It can be seen that with increasing t-zirconia content, i.e. finer zirconia particle size, toughness drops slightly, but, the strength increases substantially with increasing milling time. At 86% t-phase, strength over 1 GPa and toughness over 5 $\mathrm{MPa.m}^{1/2}$ were achieved for 15 v% pure zirconia addition.However, even with 23% t-phase, strength (700 MPa) and toughness (6 $\mathrm{MPa.m}^{1/2}$) were higher than pure alumina ($K_{Ic} \approx 3.5$ $\mathrm{MPa.m}^{1/2}$).

From Figure 5.16, it appears that although strength is favourably affected by transformation toughening, the toughness increase by these two mechanisms are comparable. This is why commercial ZTA

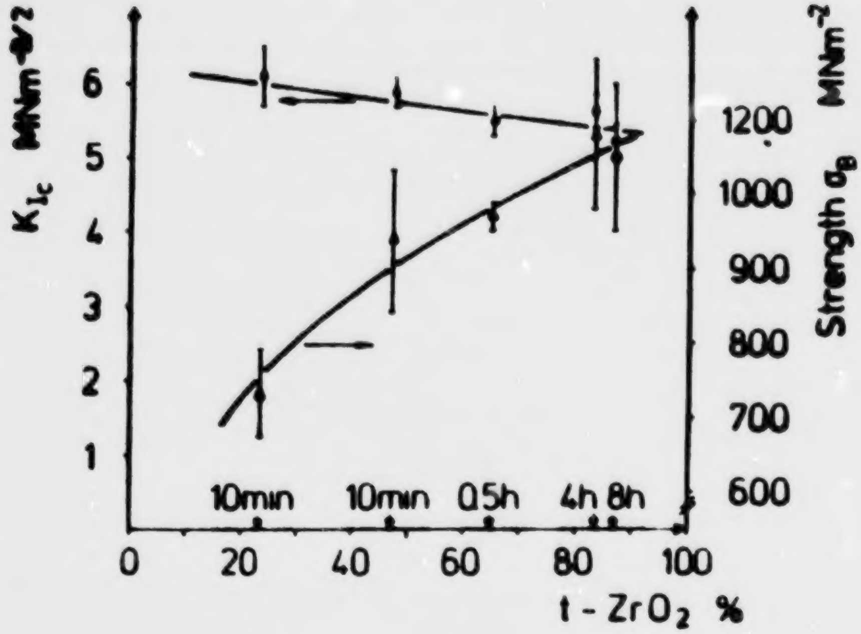

Strength and fracture toughness of 15 vol% ZTA as a function of t-ZrO$_2$ volume fraction

Figure 16

commonly contains both t- and m-zirconia. Invariably there will be a distribution of zirconia particle sizes. If all the particles are in t-symmetry, there would be a number of particles which would be too small to transform; while, if they all have m-symmetry, they would invariably provoke spontaneous microcracking and cause weakening. Thus, optimally fabricated ZTA should contain a mixture of t- and m-phases, and, the proportion must be tailored to the application.

The effect of microcracking by m-phase on the elastic modulus of ZTA is illustrated in Table 5.3. It can be seen that with increasing % m-phase, the modulus reduces to about 60% of the modulus without microcracking.

5.4 ZTA Reinforced With SiC Whiskers

A limited number of zirconia toughened alumina reinforced with SiC whiskers were hot pressed.

5.5 Hardness

Vickers hardness of zirconia toughened alumina ceramics were determined from pure alumina to partially stabilized zirconia. The results are shown in Figure 5.17 along with values reported by Lange (1982) for 20 Kg load. The hardness values more or less fall on a straight line suggesting that the hardness obeys a linear "rule of mixtures" for this material. Hardness of 15 and 20 vol% pure zirconia ZTA samples were low, probably due to high density of microcracks.

Figure 5.17 HARDNESS OF ZTA AS A FUNCTION OF COMPOSITION

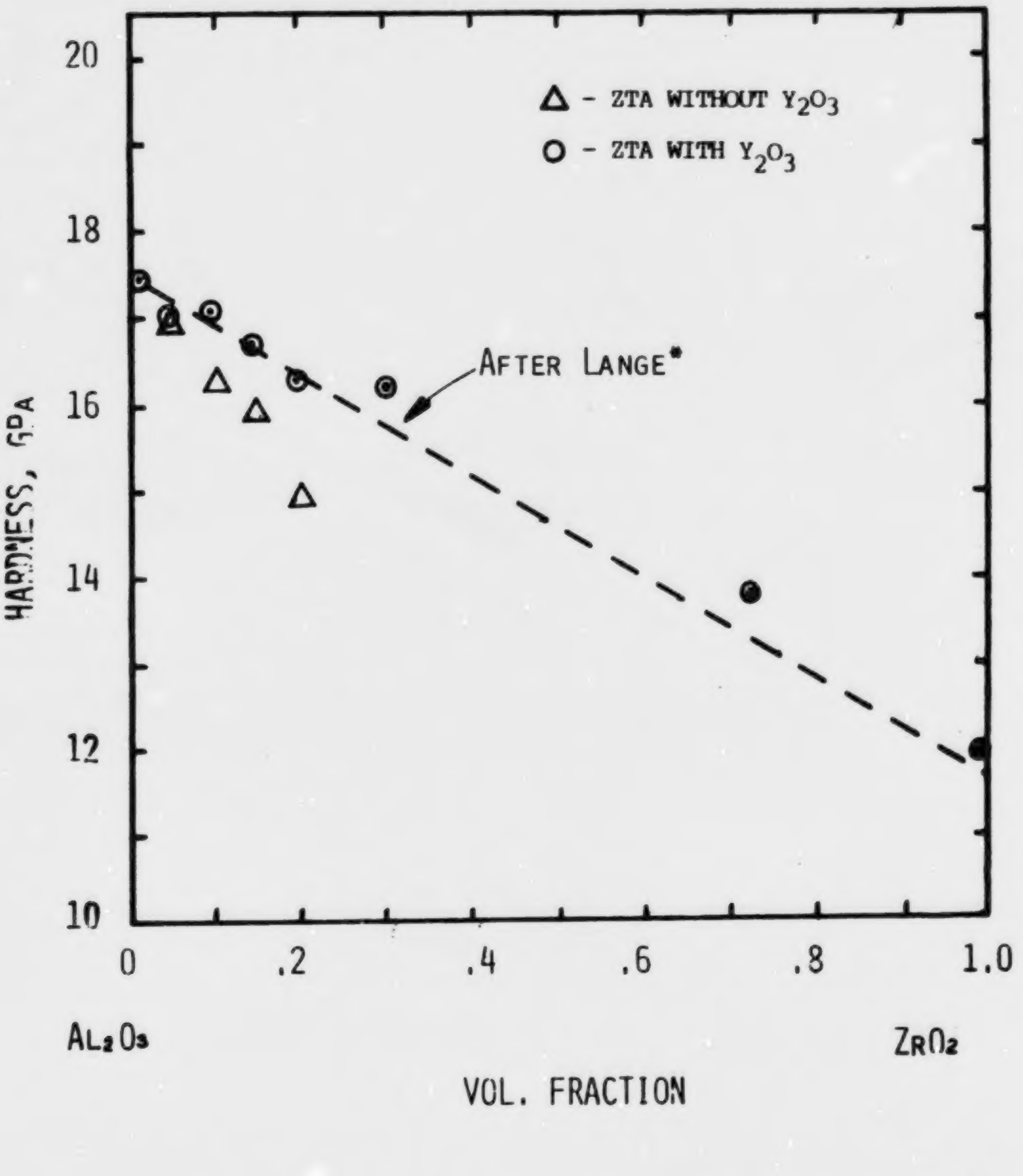

* F.F.LANGE, J.MAT.SC., 17(1982)P.247-254.

Table 6.3

Elastic modulus of Al_2O_3/ZrO_2 composites heat-treated at 1650°C for 12 h

Vol fraction ZrO_2	% Monoclinic	E (GPa)	E_0* (GPa)	E/E_0
0.01	0	381	390	0.98
0.05	0	375	383	0.98
0.075	13	370	378	0.98
0.10	47	282	374	0.75
0.125	92	231	369	0.63
0.150	92	229	364	0.63
0.20	95	227	355	0.64

*E_0 is the expected modulus without microcracks as measured with a series of Al_2O_3/ZrO_2 (+2 mol% Y_2O_3) in which the ZrO_2 is retained in its tetragonal structure (Ref. 2).

5.6 Hardness-Fracture Toughness Relationships

In wear and structural applications, a combination of hardness, fracture toughness and strength is important. In the literature, a number of emperical relationships between the properties and a measure of performance has been suggested. For example, in an application involving impact wear, it has been proposed :

$$\text{Volume wear} = \text{const} \ (H^{-1/2} . K_{Ic}^{-4/3}) \ldots\ldots\ldots\ldots (5.1)$$

where H is the Vickers hardness and K_{Ic} is the fracture toughness. On the other hand when abrasive wear is involved, the functional relationship is :

$$\text{Volume wear} = \text{const} \ (H^{-1/2} . K_{Ic}^{-3/4}) \ldots\ldots\ldots\ldots (5.2)$$

For each application there is an optimum combination of the two properties along with strength. Figure 5.18 shows the relationship between the hardness and fracture toughness of two types of zirconia toughened aluminas studied. As the fracture toughness increases with the addition of zirconia, the hardness of the composite falls. When pure zirconia is added to alumina matrix, much smaller addition is required to get a specified fracture toughness than when adding zirconia with 2 m% yttria. Therefore, for the same increase in toughness, decrease in hardness is less for pure zirconia additions than for zirconia plus yttria additions, as shown in Figure 5.18. It would appear that ZTA with pure zirconia addition gives better combination of properties. However, what is missing is the strength/fracture

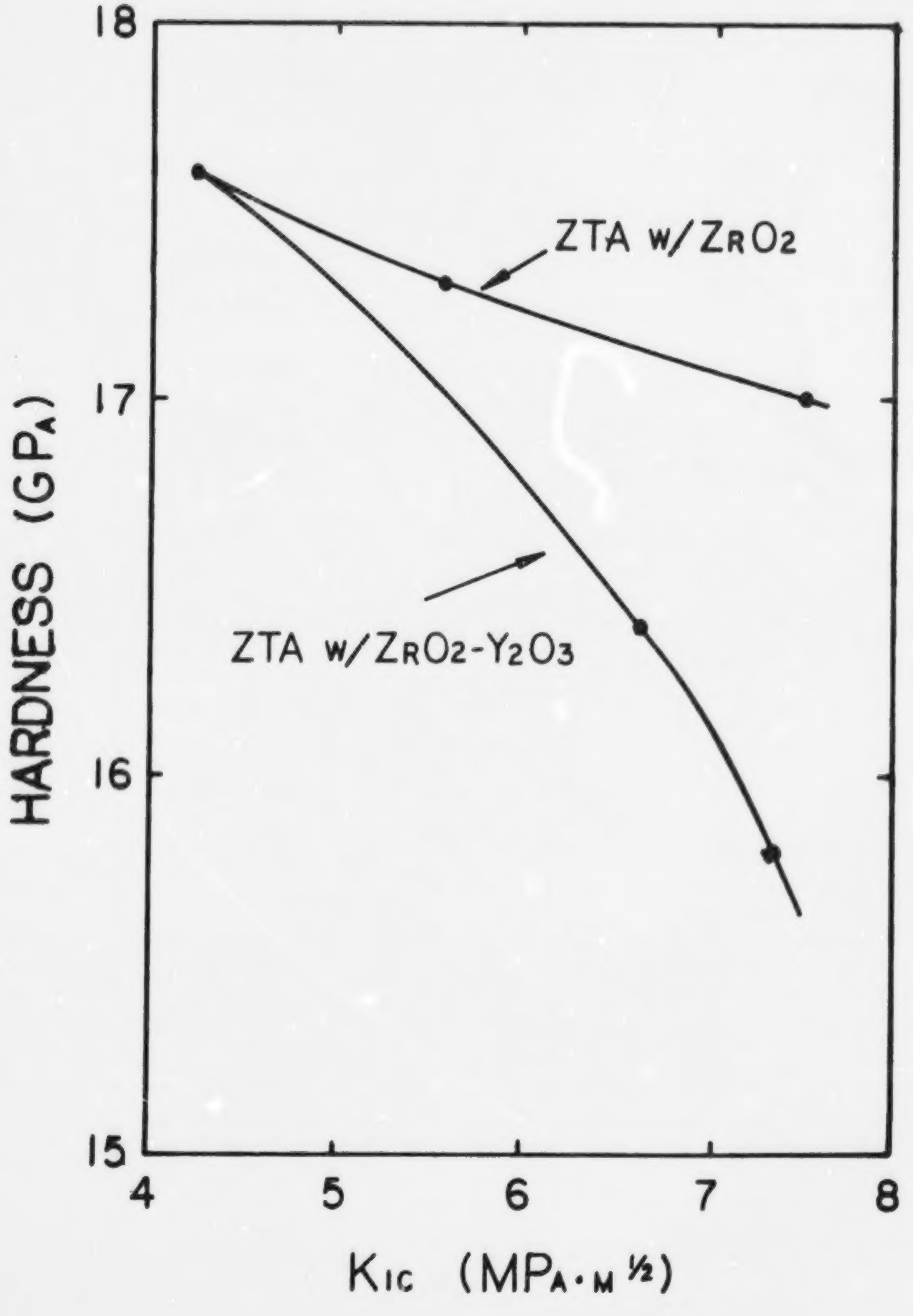

Figure 5.18. Hardness - fracture toughness relationship.

toughness data, that was presented in Chapter 2, Figure 2.2. ZTA with zirconia-yttria additions will normally give a better strength-toughness combination than ZTA with only zirconia addition. Therefore, it is the required combination of the three properties (strength, toughness and hardness) that will determine the combination.

5.7 Toughness vs Cost

Improvement in toughness of ceramic materials was the prime objective of this program. It has been demonstrated that toughness of alumina could be improved by about 100% by addition of zirconia. But at what cost? An underlying objective of this program was to determine feasibility of making toughened ceramic components for commercialization. The commercial feasibility will depend to a great extent on the cost performance ratio of the product. Figure 5.19 gives the material cost/lb (powder costs) as a function of fracture toughness required in the component. The material cost per pound is based on the following figures : alumina - $1/lb; pure zirconia - $8/lb; and, 2 m% yttria-zirconia - $30/lb. To obtain a required toughness, the amount of zirconia addition and the price of pure zirconia is lower than in the case of zirconia-yttria materials. Hence, the price of yttria containing ZTA rises more steeply than pure zirconia containing ZTA. Therefore, in applications wherein very high strengths are not demanded, ZTA with pure zirconia additives could become cost effective.

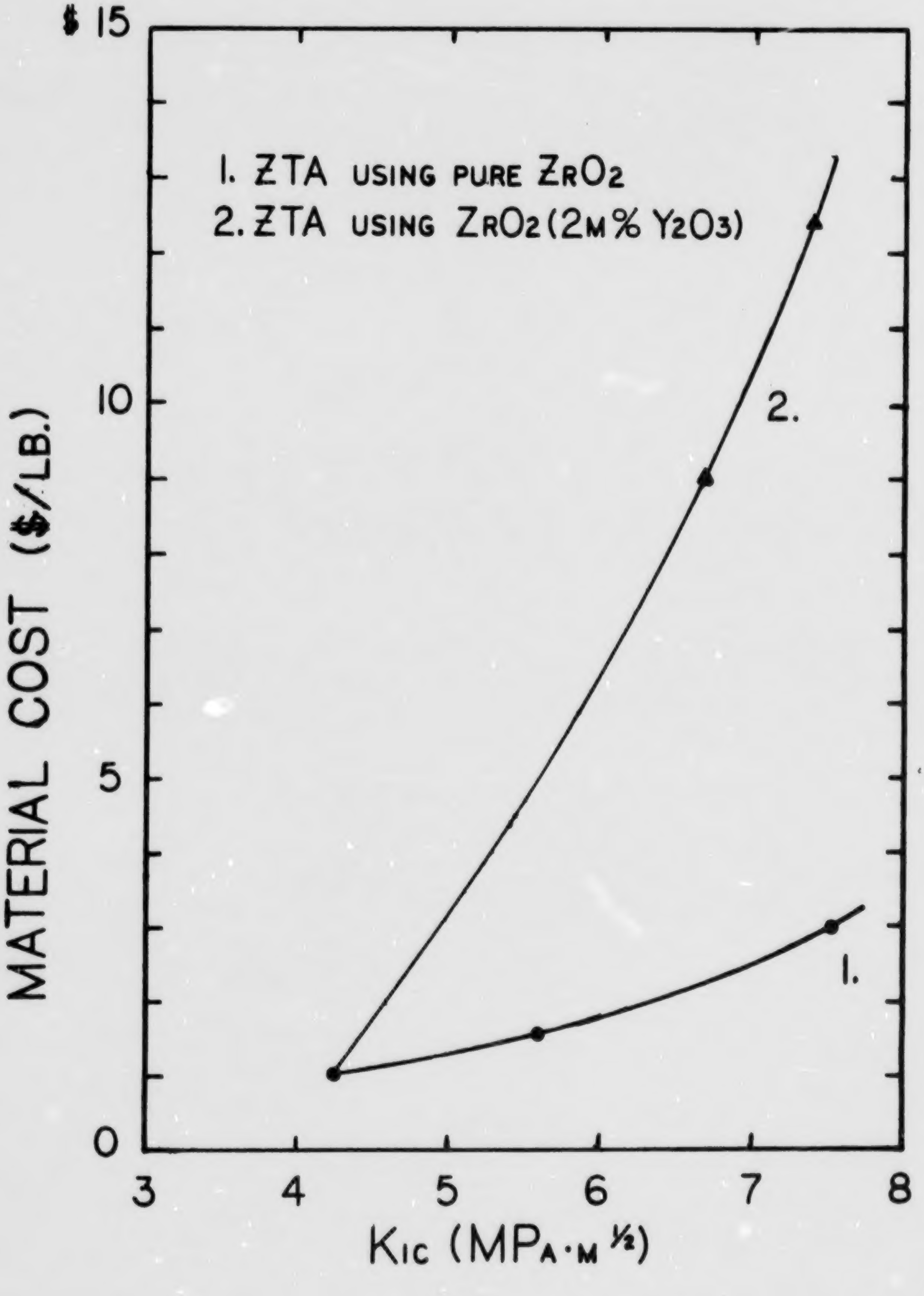

Figure 5.19. Material cost as a function of fracture toughness.

Title	Scale	Date	Initial	Dwg.No.	Rev.

6. CONCLUSIONS

The following conclusions were drawn from the work carried out in this program :

1. An extensive literature survey on zirconia transformation toughened ceramics was completed, and, a critical assessment of publications was presented in a 86-page report entitled "Literature Review on Tough Ceramics".

2. Four different commercial alumina powders : Alcoa A-16SG (modified Bayer), Ceralox HPA (chemical), Sumitomo AKP-30 (organometallic) and Baikowski CR-10 (alum) were considered. Although A-16SG is the cheapest powder, it has some impurities and "hard" agglomerates, and hence, it should be used in non critical room temperature applications. Hard agglomerates can be broken down with extended milling operation. AKP-30 and CR-10 are fine pure powders which give good products. However, they are expensive and should be considered for critical applications. Ceralox HPA is fairly pure and fine powder which yields a good cost to performance ratio.

3. The following commercially pure zirconia powders were used : Magnesium Electron SC-15,Daiichi Kigenso DK-1,Dynamit Nobel F, Harshaw Electronic Grade and Toyo Soda TZ-0. While Toyo Soda TZ-0 is the most expensive, it is not the finest or the purest material available. On the other hand, least pure or coarsest powder SC-15 is not the cheapest. Harshaw Electronic Grade and DK-1 give the best cost to performance ratic of the pure zirconia powders evaluated.

4. Alumina powders could be dispersed in water away from its isoelectric point, which varies in the pH range of 6.5 to 9.0. It was found to be well disperesd in the acid region at pH < 4.0 and in the basic region at pH > 10.5.

5. Zirconia appears to have three isoelectric points at pH of 3.0, 5.5 and 6.5. Therefore, it can also be dispersed in acid and basic regions. Best dispersion in conjunction with alumina was obtained in acid region at pH ≈ 2.5. It could also be dispersed in the basic region at pH ≈ 10.5.

6. Isoelectric point of silicon carbide whiskers is about pH ≈ 4.0. They were best dispersed in alumina-zirconia mixtures in the basic region at pH ≈ 10.5.

7. A technique of slip casting alumina-zirconia powders was developed and green densities around 60% were obtained.

8. The density-pressure curve for cold pressing alumina-zirconia powders were determined, from which the pressure required to get the minimum acceptable green density of the compact was obtained. At higher pressures cold pressing defects such as end capping and delamination appeared.

9. Pressureless sintering schedules for alumina, zirconia and ZTA were developed to yield final product densities over 96%.

10. One of the factors affecting the final sintered density was the initial green density of the compact. It was found that green density over 55% was required to obtain sintered density over 96%.

11. Linear shrinkage during sintering varied from 16% for pure alumina to 26% for zirconia containing 2 m% yttria. Higher shrinkage was observed for powders containing monoclinic zirconia which was retained as higher density tetragonal phase on sintering.

12. Vickers hardness number varied with load becoming relatively constant above a load of 5 Kg, above which most of the measurements were made.

13. Tetragonal zirconia polycrystal samples partially stabilized with yttria (Y-TZP) were successfully produced with toughness as high as 10 MPa.$m^{1/2}$ and density higher than 97% from commercial powders. The yttria content was varied from 1 mole% to 6 mole%. The 1 m% yttria material showed 100% m-phase and cracked extensively. The highest toughness was observed for 2 mole% yttria (˜á10 MPa.$m^{1/2}$, and, it is reduced to 8 MPa.$m^{1/2}$ for 3 mole% yttria and 6 MPa.$m^{1/2}$ for 6 mole% of yttria. The reduction of toughness with increasing yttria content is due the decrease in the negative free energy of transformation (transformability) of t to m phase. At 6 mole% yttria cubic phase appears, and hence, the munber of transformable t-phase is reduced.

14. Ce-TZP samples containing 12 wt% of CeO_2 were sintered from commercial powders to high densities (97% +). This material showed exceptional fracture toughness properties ($K_{IC} > 20$ MPa.m$^{1/2}$) which gave very small cracks even at 60 Kg load.

15. Alumina toughened zirconia containing 20 wt% alumina and 3 m% yttria were sintered from commercial powders. Good toughness values of about 9 MPa.m$^{1/2}$ were observed.

16. In the case of ZTA containing 20 vol% zirconia, the optimum yttria content in ZrO_2 was determined to be 2 mole%, at which composition the maximum toughness value of about 6.5 MPa.m$^{1/2}$ was observed. At this composition, 100% of zirconia was tetragonal; below this composition, monoclinic phase was present (depending on zirconia particle size). Above 2 mole% yttria, 100% t-phase was obtained, but the transformability of zirconia was reduced. This is in good agreement with literature data.

17. In the case of ZTA containing 2 mole% yttria added to zirconia, the fracture toughness increased with increasing addition of zirconia, from about 4 MPa.m$^{1/2}$ for pure alumina to about 7.5 MPa.m$^{1/2}$ for ZTA with 30 vol% zirconia. This is due to increasing number density of tetragonal zirconia particles present. The results are again in good agreement with literature data.

18. In the case of ZTA containing no yttria additions, the constraint by the alumina matrix (with higher elastic modulus) was sufficient to retain some zirconia particles in tetragonal form. Depending on zirconia grain size and volume fraction, upto 90% tetragonal phase could be retained.

19. In ZTA containing no yttria, the fracture toughness increased with volume fraction of zirconia upto 10 v% after which it declined. The maximum K_{Ic} of about 7.5 MPa.m$^{1/2}$ was obtained at 10 vol% of zirconia, where t-phase content was about 45-70%. This is in good agreement with results of Becher and Tennery (1983).

20. The increase in K_{Ic} with initial addition of pure zirconia in ZTA is due to increase in number density of t-phase. The decrease of K_{Ic} above 10 vol% zirconia is associated with an increase in m-phase at grain boundaries of alumina which results in extensive microcracking and hence weakening of the material.

21. Vickers hardness of ZTA decreased linearly with increasing zirconia volume fraction.

22. With the addition of zirconia to alumina, the fracture toughness increased, and the hardness reduced for both ZTA with and without yttria. However, the hardness-toughness relationships were different for the two systems. In the case of pure zirconia additions, higher K_{Ic} values were observed for smaller zirconia additions, and hence, higher hardness resulted for the same toughness (upto certain toughness values). However, the strength of these materials may be lower.

23. The optimum ZTA composition must be designed according to the application. In critical applications requiring high strength and toughness, large number density of t-phase can be obtained by a combination of zirconia grain size, yttria content, raw material and processing characteristics. However, in many wear applications requiring good toughness-hardness combination, optimum addition of pure zirconia may give the best cost performance ratio.

7. FUTURE DIRECTIONS

The research carried out in this program has resulted in the development of ZTA based materials which can be formulated to meet most structural applications. The worldwide alumina based structural ceramics is estimated to be in the $300 M range. The ZTA based ceramics can ideally be introduced in the present high value alumina market. In a later Chapter (Chapter 8 - Appendix), about 10 potential application areas have been identified, which consist of the high value alumina market.

The future direction of this technology is the need for further research and technology development (Phase II) targetted towards one or at most two major applications, such that a particular application oriented product is developed. Presently we have identified two products : a) Nozzles, and b) Cutting tools, where using ZTA would have substantial advantages.

In cutting tools, Electrofuel is committed to producing alumina/silicon carbide whisker based composite for high nickel based alloys, and a silicon nitride based composite for cast iron. Part of the commitment to cutting tools includes setting up the infra-structure for distributing and marketing of cutting tools. The development of a ZTA based cutting tool would be complementary to this effort.

APPENDIX A : APPLICATIONS

The market for high alumina ceramics is estimated to be $1.3B and a substantial portion of it is in the electronics sector. Although ceramics like aluminum nitride is slowly taking up a large chunk of the market share enjoyed by alumina as substrates, toughened alumina will not have any effect on this large electronic market. However, wear and structural industry also uses a significant amount of high alumina (over $300 M), and this is the area where toughened alumina is expected to have a major impact mainly on the top end of this market.

As discussed in Section 1.6, zirconia toughened alumina has the potential to improve the performance of high purity alumina in structural and wear applications. In the last 5 decades, high alumina ceramics have found uses in various fields, as shown in Figure A1. Figure A2 illustrates the growth of the annual production volume of high alumina ceramics in Japan, USA and Europe, and, this exponential growth has continued in the 1980s. However, there is a considerable difference between the three regions on the distribution of the production volume in the major fields of application : mechanical engineering (structural), electronics and other (medical, armour, etc.) applications (see Figue A3). While electronics application dominates Japanese production of alumina , the mechanical engineering applications take the lion's share of European production.

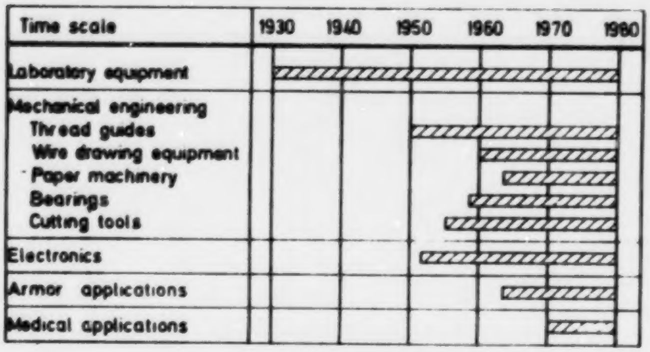

Fig. A1 Advance of utilization of high alumina ceramics in various fields of application

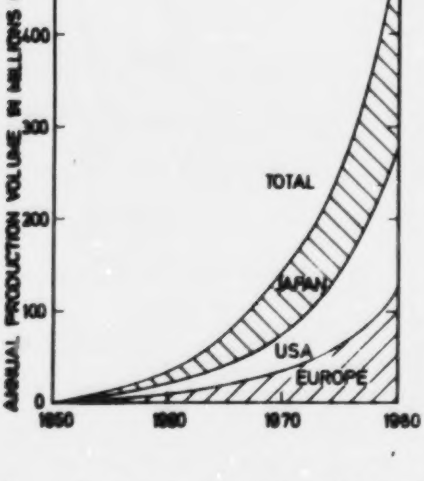

Fig. A2 Development of world production volume of high alumina ceramics

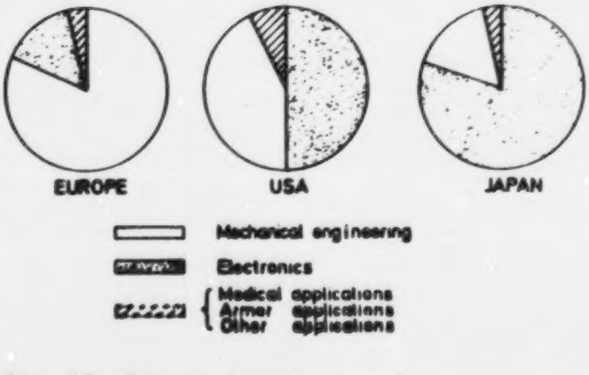

Fig. A3 Present distribution of production volume of high alumina ceramics to various fields of application

Since the introduction of sintered alumina ceramic cutting tool "Degussit" in Germany during W.W.II, the structural applications of high performance alumina has grown rapidly. The structural applications include not only those listed under "mechanical engineering" in Figure A1, but also armour and medical applications. In many of these applications, the performance of alumina, though considerably superior to the metals it replaces, is barely adequate, and, we believe that replacement with zirconia toughened ceramics will result in a better cost performance ratio. The following is a brief description of applications, which we have identified as areas wherein ZTA can favourably replace alumina :

1. Cutting tools
2. Dies
3. Textile thread guides
4. Wire drawing
5. Pulp and paper
6. Pump seals and bearings
7. Printed circuit industry
8. Armour
9. Engine components
10. Nozzles for slurries, sand blasting, etc.

A1 Cutting Tools

Since the introduction of alumina cutting tools during W.W.II, cuting speeds have gone up by an order of magnitude, from around 200 m/min to 2000 m/min (see Figure A4). This is possible due to higher retained strength of ceramics at elevated temperatures

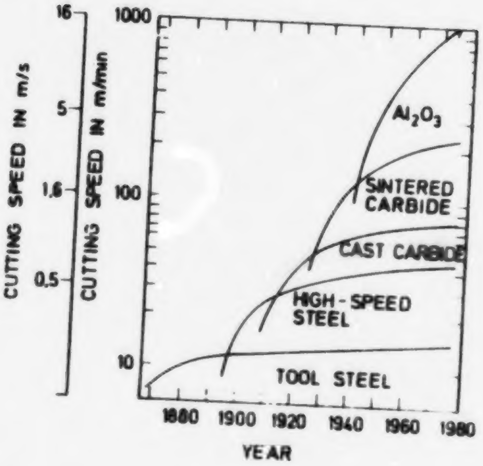

Fig. A4 Progression of cutting speed depending on the time (after H.Tully)

compared to high speed steels and cemented carbides, as shown in Figure A5. It should be noted that even at 1100° C, alumina retains strength equal to steel at room temperature, while carbide and steel have negligible strength at this temperature. Due to considerably higher cutting speeds possible with alumina tools, total machining costs can be dramatically reduced at high speeds. Figure A6 illustrates the production costs of a turning operation when machining steel with carbide (pca) and alumina (pce). The curves for production costs (pce and pca) are obtained from a combination of the curves of the machine costs and of the tool costs (tce and tca). It can be seen that when using carbide tools, the production costs (pca) show a sharp minimum, rising steeply with increasing cutting speeds above 200 m/min. On the other hand, with alumina cutting tools,the production costs (pce) decreases rapidly with increasing cutting speeds upto 600 m/min and then flattens out.

Zirconia toughened cutting tools (with 16 vol% zirconia) have been shown to improve tool lifetime by a factor of 3 compared to alumina in interrupted cutting, as illustrated in Table A1. During interrupted cutting, each revolution imposes repeated severe mechanical impacts on toll bits. However, as shown in the table, it is important toáobtain 1:1 ratio of monoclinic and tetragonal zirconia particles to yield a right combination of microcrack toughening and surface strengthening mechanisms.

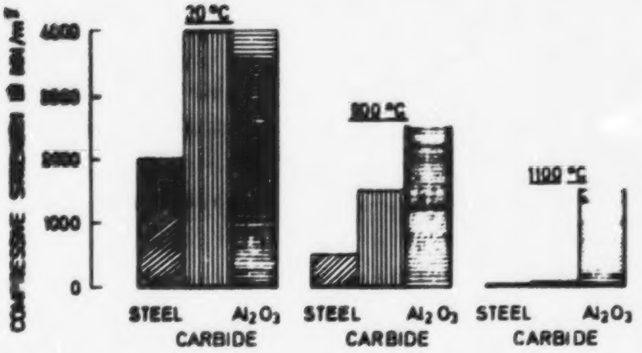

Fig. A5 Compressive strength of steel, cemented carbide, and high-purity alumina ceramics at various temperatures

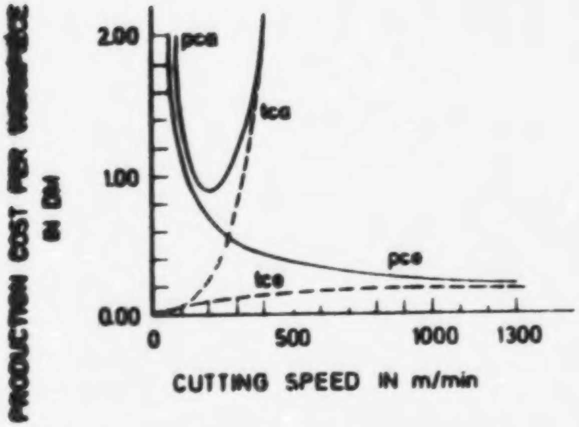

Fig. A6 Production costs depending on the cutting speed; pca: production costs carbides; tca: tool costs carbides; pce: production costs ceramics; tce: tool costs ceramics [5.63]

Table A1 Lifetime and Wear Data for Al_2O_3 and ZrO_2 Tool Bits[*]

	Cutting Mode					
	Continuous[†]			Interrupted[†]		
	A	$A + m-Z$	$A + (m,t-Z)$	A	$A + m-Z$	$A + (m,t-Z)$
No. of passes	25			25	53	70
Flank wear (mm)	0.20	0.78	0.23	0.20		

[*] Reference 38.

[†] $A = Al_2O_3$; $A + m-Z = Al_2O_3 + 16$ vol% $m-ZrO_2$; $A + (m,t-Z) = Al_2O_3 + 16$ vol% $(m-+t-ZrO_2)$; m/t, ~1.

A2 Dies for Extrusion, Drawing and Pressing

Recently there is a surge of interest in metal matrix composites (MMC) in which metal is reinforced by stiff ceramic fibres. These materials (e.g. aluminum reinforced by alumina or SiC fibres) are often hot extruded. The extrusion dies used to produce the MMC usually operates at 425° C and speciality steel dies have a lifetime of only 20 extrusions instead of the required 1000 extrusions. Zirconia toughened alumina can be an useful die material. The MMC extrusion dies are a new industry and a growing one. For example, in the automobile sector, Toyota has substituted MMC pistons in six of their seven categories of diesel engines, and it is expected that American manufacturers will also be introducing similar materials.

Some discussions have taken place with Dr.Suzuki of Nippon Light Metal. The company has developed a process for the manufacture of alumina fibres. They expect their material to be superior to that produced by ICI (Saffil fibres) or by DuPont, and are presently involved in using their material for metal matrix composites, the principal MMC material being Al/alumina fibres. The trading company C.Itoh handles Nippon Light Metal's products and is also a distributor of Electrofuel's products.

In applications involving dies for compacting hard abrasive powders, presently cemented carbide liners are used in place of tool steel. Zirconia toughened ceramics should result in much better performance due to increased hardness and wear resistance.

A3 Textile Thread Guides

One of the first large-scale applications for high alumina ceramic parts was thread guides for textile machines. Increasing working speeds as well as the introduction of synthetic fibres called for deviation elements and guide elements with increased wear resistance and, in some cases, increased strength. Previously applied materials such as hardened steel, glass or glazed porcelain were unsuitable due to their poor abrasion property. They wore out within a very short period of time when extremely abrasive synthetic threads were drawn across the surface with a speed in the order of 1000 m/min. High strength alumina have successfully been able to withstand these wear conditions, and have increased the lifetime of thread guides manyfolds.

We strongly feel that alumina based ceramic materials with higher toughness and strength, for example ZTA, has an excellent potential in this market since it would not only improve the service life of these parts but also increase the speed of operation in the textile industry.

Figure A7 presents a collection of thread guides made of high alumina ceramics, such as deviationn elements, stretch pins and thread breaks. Figures A8 and A9 showáthread guides in operation.

A4 Wire Drawing

Another area where wear properties play a major role is the wire drawing industry. Wire drawing operations, particularly the manufacture of steel and copper wire, require wear resistant materials for drawing and diverting elements. Therefore, step

Fig. A7 Collection of thread guides made of high alumina ceramics

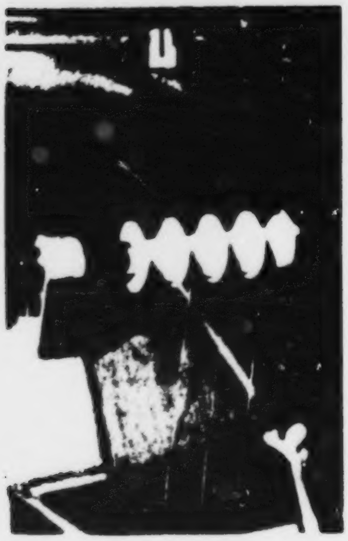

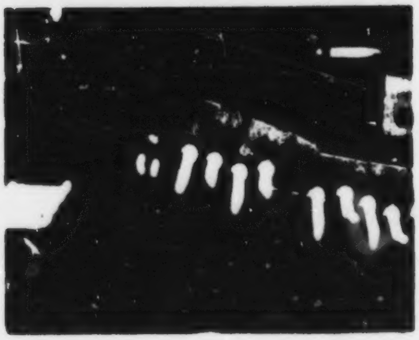

Figs. A8 and A9 Thread guides made of high alumina ceramics in operation cones, capstans, pulleys, rollers, and other wire drawing elements made of high strength alumina ceramics have proved quite successful in this field.

Drawing speeds can go up to 3600 m/min when using modern wire drawing machines. Under these conditions extreme wear caused by slip can occur making metallic wear resistant materials unworthy of use. More than 1000 tons of copper wire in the diameter range 1 to 2 mm have to be manufactured without any sign of wear on the surface of the step cones. Another important factor is the smoothness of the cone surface. High strength alumina ceramics have been successful in taking care of these requirements. Figure A10 shows wire drawing step cone made of high alumina ceramics.

This is another industry where high strength and toughened alumina appears to have the potential of a significant market share.

A5 Pulp and Paper

The efficieny and economy of paper manufacturing has improved considerably during the last 20 years by the application of high strength alumina ceramics. The development of paper machines has taken place in two steps :

(1) Replacement of dynamic dewatering elements as the table rolls by stationary elements.
(2) Increasing wear resistance of stationary elements by the replacement of high density polyethylene and wood by high strength alumina ceramics.

Covers and wire, which are two important components of the sheet forming machine, are exposed to considerable friction and wear, and previously employed polyethylene or wood materials showed extensive

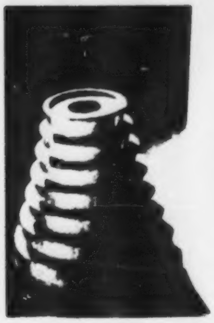

Fig. A10 Wire drawing step cones made of high alumina ceramics

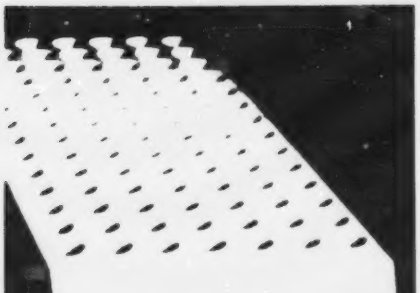

Fig. A11 High alumina ceramic cover for flat suction boxes

wear even after a few hours of operation. Use of high alumina ceramic components have considerably eliminated the disadvantages of wear, lower production speeds and equipment downtime in the paper industry. Figure A11 is a photograph of covers made of high alumina ceramics.

Toughened alumina ceramics may become a material of choice for such covers and other wear parts of the paper industry to further improve the life of these components.

A6 Pump Seals and Bearings

Pump seals, seal rings, sleeve bearings, and plain bearings are examples of components that are subjected to high friction and wear by interaction with other components. Bearings are a typical example of a combined exposure to corrosion and wear. In this special case, ceramic bearings, particularly high alumina ceramics, meet these requirements to a much greater extent than metals. Therefore, ceramic bearings are preferably applied to pumps for chemically aggressive fluids, sea water, or dirty water, as well as to high pressure pumps. The main field of application, however, are pumps for central heatings. Figure A12 shows bearings and seal rings made of high alumina ceramics.

Since high hardness, high strength and toughness are factors governing the life and performance of seals and bearings, toughened alumina ceramics may have a substantial impact on this particular industry.

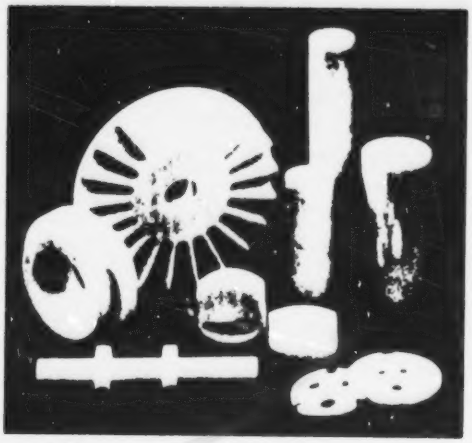

Fig. A12 Bearings and seal rings made of high alumina ceramics

A7 Printed Circuit Industry

It appears that the major section of the world's printed circuit industry is centred around the Singapore/Malaysia area. Electrofuel recently made contact with a company called Advanced Materials Inc. based in Singapore, and a potential market for ZTC was identified by AMI.

Presently, the gold wire interconnects in a semi-conductor chip is made by a machine which feeds the thin gold wire (25 micron) through an alumina based tip. The special alumina tip costs about $10 and lasts for a very short time, as they tend to break with the applied mechanical shock. The present market for this material is about $40 million worldwide and ZTA could significantly improve the performance of this product.

A8 Armour

Successful applications of high alumina ceramics as armour material date back to the early 1960s due tc its strength and light weight. According to experimental data, there are considerable differences in the armouring mechanism between metals and ceramics. Whereas the bullet-absorbing effect of metallic materials is based on plastic deformation, the mechanism taking place in brittle materials can be described as a conversion of the kinetic energy of the bullet into fracture energy absorbed by the ceramic material. Another important property requirement is high hardness to allow bullet tips to become blunt on striking the armour surface, leading to an increase in effective cross-section of the bullet and accordingly to a reduction of the compressive stress acting on the ceramic. For this reason it is necessary for ceramics to have high hardness and compressive strength as well as high Young's modulus for use as armour material.

Toughened alumina ceramics due to their very high hardness and toughness (higher energy absorption) is expected to have a significant impact on this market.

A9 Engine Components

Partially stabilized zirconia (PSZ) has long been considered for engine applications due to its good thermal insulation property and its thermal expansion coefficient being quite close to cast iron. Zirconia toughened alumina due to its high hardness and toughness is a good candidate for wear applications in an engine. A list of potential applications for ZTA is shown in Table A2 (reproduced from Advanced Ceramics-Impact on Ontario Industry, Min. Northern Dev. and Mines, 1988, p 61). Realizing that ZTA will lose its toughness and strength at elevated temperatures, it must be applied to the cooler parts of the engine.

TABLE A2 PROTOTYPE APPLICATIONS FOR ZIRCONIA TOUGHENED ALUMINA.

Application	Component	Advantage
Auto/truck gas and diesel engines	Rocker arm roller Valve lifter roller	Reduced friction and wear vs metal or ceramic insert flat followers. Simplicity over metal roller/needle bearing assembly.
	Valve guide Valve seat	Improved wear and corrosion resistance vs metal components.
	Valve	Help maintain designed engine performance over a longer interval than metal components
	Wrist pin	Inertia weight reduction Potential of operating with reduced lubrication.
Truck diesel engine	Crown on aluminum piston	Inertia weight reduction over mechanical strength of ceramic/aluminum composite over aluminum alone.
Ballistic armor	Ceramic tile	Improved strength to weight ratio over conventional alumina bodies. Improved ballistic threat level capability.
Production tooling e.g. Inserts hot metal pins in TV tube face plates	Pinchucks	High compressive strength. High thermal shock resistance in 400 to 2500°F range for thousands of 20 sec cycles, (fast heat up, fast cool down). High oxidation resistance.

Source: Champion Spark Plug Co.

A10 Nozzles for Slurries and Sand Blasting

Nozzles, generally made out of cast iron or metal alloys, are quite extensively used for slurry and sand blasting operations. However, due to low hardness and poor wear properties, their service life is extremely short. Alumina and other ceramic nozzles such as boron carbide, etc., have replaced these conventional materials and considerably improved the service life due to its superior hardness and wear properties. However, the wear in these hard materials is by impact damage of the particles and hence an improved toughness should further improve their wear behaviour. In this regard ZTA materials with a good combination of hardness and toughness should considerably improve nozzle life. Figure A13 shows a typical sand blasting nozzle sold by Montreal Carbide who have expressed interest for a possible Canadian source to manufacture nozzles that have long service life and are cost productive.

Large volumes

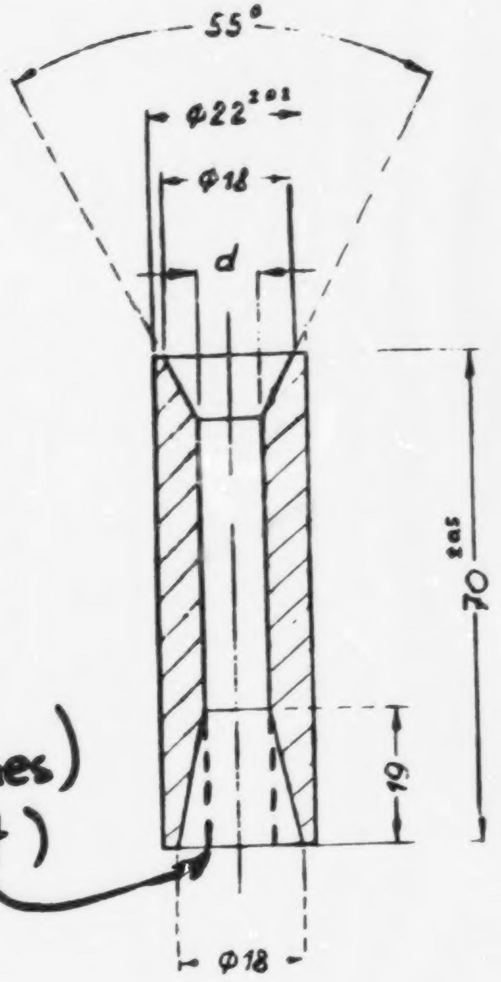
55°
φ22±01
φ18
d
70±05
19
φ18

2 TYPES EXIST
#4135 (w 2 cones)
#4165 (straight)

d =	9.5	11	12.5

Fig.A13. Sand blasting nozzle insert made in ceramic.

	Tag	Name	Maßstab
Bearb	22.8.84		1:1
Sandstrahdüseneinsatz			
Fa. Montreal Carbide			4135

BIBLIOGRAPHY

1 Fisher,G. ZIRCONIA: CERAMIC ENGINEERING'S TOUGHNESS CHALLENGE, Am.Ceram.Soc.Bull.,1986,pp.1355-60

2 Yangyun,S; Brook,R.J. PREPARATION OF ZIRCONIA-TOUGHENED CERAMICS BY REACTION SINTERING, Science of Sintering,1985,17(1),pp.35-47

3 Lange,F.F.; Shubert,H.; Claussen,N.: Ruhle,M. EFFECTS OF ATTRITION MILLING AND POST-SINTERING HEAT TREATMENT ON FABRICATION. MICROSTRUCTURE AND PROPERTIES OF TRANSFORMATION TOUGHENED ZrO_2. J.Mater.Sci..1986.21.pp.768-774

4 Becher.P.F. SUBCRITICAL CRACK GROWTH IN PARTIALLY STABILIZED ZrO_2 (MgO). J.Mater.Sci..1986.21.pp.297-300

5 Wieninger,H.; Kromp.K.: Pabst.R.F. CRACK RESISTANCE CURVES OF ALUMINA AND ZIRCONIA AT ROOM TEMPERATURE. J.Mater.Sci..1986.21.pp.411-418

6 Jayaratna,M.; Yoshimura,M.; Somiya,S. HOT PRESSING OF Y_2O_3-STABILIZED ZrO_2 WITH Cr_2O_3 ADDITIONS, J.Mater.Sci.,1986,21,pp.591-596

7 Garvie,R.C.; Swain,M.V. THERMODYNAMICS OF THE TETRAGONAL TO MONOCLINIC PHASE TRANSFORMATION IN CONSTRAINED ZIRCONIA MICROCRYSTALS. J.Mater.Sci.,1985,20,pp.1193-1200

8 Tsukuma,K.; Shimada.M. STRENGTH. FRACTURE TOUGHNESS AND VICKERS HARDNESS OF CeO_2-STABILIZED TETRAGONAL ZrO_2 POLYCRYSTALS (Ce-TZP). J.Mater.Sci..1985.20.pp.1178-1184

9 Itoh.T. STABILITY OF TETRAGONAL PHASE IN ZrO_2 POWDER. J.Mater.Sci.Lett..1986.5.pp.107-108

10 Itoh,T. PARTICLE AND CRYSTALLITE SIZES OF ZrO_2 POWDER OBTAINED BY THE CALCINATION OF HYDROUS ZIRCONIA. J.Mater.Sci.Lett.,1985,4,pp.431-433

11 Hori,S.; Kurita,R.; Yoshimura,M.; Somiya,S. SUPPRESSED GRAIN GROWTH IN FINAL-STAGE SINTERING OF Al_2O_3 WITH DISPERSED ZrO_2 PARTICLES, J.Mater.Sci.Lett.,1985,4,pp.1067-1070

12 Hori.S.: Yoshimura.M: Somiva.S.: Kurita.R.: Kaji.H. MECHANICAL PROPERTIES OF ZrO_2-TOUGHENED Al_2O_3 CERAMICS FROM CVD POWDERS. J.Mater.Sci.Lett..1985.4.pp.413-416

13 Pena,P. et al. MULTICOMPONENT TOUGHENED CERAMIC MATERIALS OBTAINED BY REACTION SINTERING, J.Mater.Sci.,1985.20,pp.2011-2022

14 Van de Graaf,M.A.C.G. et al. MICROSTRUCTURE AND SINTERING KINETICS OF HIGHLY REACTIVE ZrO_2-Y_2O_3 CERAMICS. J.Mater.Sci.,1985,20,pp.1407-1418

15 Drennan,J. THE OBSERVATION OF b-ALUMINA TYPE PHASES IN ZIRCONIA-TOUGHENED ALUMINA (ZTA), J.Mater.Sci.Lett..1985.4.pp.725-727

16 Osendi,M.I. et al. SOLID SOLUTION EFFECTS ON THE FRACTURE TOUGHNESS OF MULLITE-ZrO_2 COMPOSITES. J.Mater.Sci.Lett..1985.4.pp.1026-1028

17 Murase,Y. et al. STABILITY OF ZrO_2 PHASES IN ULTRAFINE ZrO_2-Al_2O_3 MIXTURES. J.Am.Ceram.Soc.,1986.69(2).pp.83-87

18 Nogami,M.; Tomozawa,M. ZrO_2-TRANSFORMATION-TOUGHENED GLASS-CERAMICS PREPARED BY THE SOL-GEL PROCESS FROM METAL ALKOXIDES, J.Am.Ceram.Soc.,1986,69(2),pp.99-102

19 Sakka,Y. et al. ENHANCEMENT OF MgO EVAPORATION FROM MgO-STABILIZED ZrO_2 BY GRAIN-BOUNDARY DIFFUSION, J.Am.Ceram.Soc..1986.69(2),pp.111-113

20 Heuer,A.H. et al. TRANSFORMATION TOUGHENING: AN OVERVIEW, J.Am.Ceram.Soc.,1986.69(2)

--▸21 Hori,S. et al. STRENGTH-TOUGHENESS RELATIONS IN SINTERED AND ISOSTATICALLY HOT-PRESSED ZrO_2-TOUGHENED Al_2O_3. J.Am.Ceram.Soc..1986.69(3).pp.169-72

22 Marshall,D.B. STRENGTH CHARACTERISTICS OF TRANSFORMATION-TOUGHENED ZIRCONIA, J.Am.Ceram.Soc.,1986,69(3),pp.173-80

23 Chen,I; Reyes Morel,P.E IMPLICATIONS OF TRANSFORMATION PLASTICITY IN ZrO_2-CONTAINING CERAMICS: I, SHEAR AND DILATATION EFFECTS,

J.Am.Ceram.Soc.,1986.69(3).pp.181-89

Chen.I IMPLICATIONS OF TRANSFORMATION PLASTICITY IN ZrO_2-CONTAINING CERAMICS: II. ELASTIC-PLASTIC INDENTATION.
J.Am.Ceram.Soc..1986.69(3).pp.189-94

25 Ruhle,M. et al. TRANSFORMATION AND MICROCRACK TOUGHENING AS COMPLEMENTARY PROCESSES IN ZrO_2-TOUGHENED Al_2O_3. J.Am.Ceram.Soc.,1986.69(3),pp.195-97

26 Matsui,M. et al. STRESS-INDUCED TRANSFORMATION AND PLASTIC DEFORMATION FOR Y_2O_3-CONTAINING TETRAGONAL ZIRCONIA POLYCRYSTALS.
J.Am.Ceram.Soc.,1986,69(3),pp.198-202

27 Rose,L.R.F.; Swain,M.V. TWO R CURVES FOR PARTIALLY STABILIZED ZIRCONIA,
J.Am.Ceram.Soc.,1986,69(3),pp.203-207

28 Rose.L.R.F. KINEMATICAL MODEL FOR STRESS-INDUCED TRANSFORMATION AROUND CRACKS. J.Am.Ceram.Soc..1986.69(3).pp.208-212

29 Rose.L.R.F. EFFECTIVE FRACTURE TOUGHNESS OF MICROCRACKED MATERIALS.
J.Am.Ceram.Soc..1986.69(3).pp.212-14

30 Marshall.D.B.; James.M.R. REVERSIBLE STRESS-INDUCED MARTENSITIC TRANSFORMATION IN ZrO_2, J.Am.Ceram.Soc..1986,69(3).pp.215-17

31 Lambropoulos,J.C. EFFECT OF NUCLEATION ON TRANSFORMATION TOUGHENING,
J.Am.Ceram.Soc..1986.69(3).pp.218-22

32 Green,D.J.; Maloney,B.R. INFLUENCE OF SURFACE STRESS ON INDENTATION CRACKING, J.Am.Ceram.Soc.,1986.69(3),pp.223-25

33 Burns,S.J.; Swain,M.V. FRACTURE TOUGHNESS OF MgO-PARTIALLY-STABILIZED ZrO_2 SPECIMENS WITH K_R-CURVE BEHAVIOR FROM TRANSFORMATION TOUGHENING,
J.Am.Ceram.Soc..1986.69(3).pp.226-30

34 Kibbel,B.; Heuer.A.H. EXAGGERATED GRAIN GROWTH IN ZrO_2-TOUGHENED Al_2O_3,
J.Am.Ceram.Soc..1986.69(3).pp.231-36

35 Lange,F.F. et al. DEGRADATION DURING AGING OF TRANSFORMATION-TOUGHENED ZrO_2-Y_2O_3 MATERIALS AT 250°C, J.Am.Ceram.Soc.,1986,69(3),pp.237-40

→ 36 Lange,F.F. TRANSFORMATION-TOUGHENED ZrO_2: CORRELATIONS BETWEEN GRAIN SIZE CONTROL AND COMPOSITION IN THE SYSTEM ZrO_2-Y_2O_3. J.Am.Ceram.Soc.,1986,69(3),pp.240-42

37 Chaim,R. et al. PHASE EQUILIBRATION IN ZrO_2-Y_2O_3 ALLOYS BY LIQUID-FILM MIGRATION. J.Am.Ceram.Soc.,1986,69(3),pp.243-48

38 Hogg,C.L. et al. GRAIN-BOUNDARY CAVITATION AND BLOATING OF ISOSTATICALLY HOT-PRESSED MAGNESIA-PARTAILLY-STABILIZED ZIRCONIA ON AIR ANNEALING, J.Am.Ceram.Soc.,1986,69(3),pp.248-51

? → 39 Mazerolles,L. et al. INTERFACES IN ORIENTED Al_2O_3-ZrO_2(Y_2O_3) EUTECTICS, J.Am.Ceram.Soc.,1986,69(3),pp.252-55

40 Kraus-Lanteri,S.P. et al. STRUCTURE OF INCOHERENT ZrO_2/Al_2O_3 INTERFACES, J.Am.Ceram.Soc.,1986,69(3),pp.256-58

41 Kelly,P.M.; Ball,C.J. CRYSTALLOGRAPHY OF STRESS-INDUCED MARTENSITIC TRANSFORMATIONS IN PARTIALLY STABILIZED ZIRCONIA. J.Am.Ceram.Soc.,1986,69(3),pp.259-64

42 Yuan,Q. et al. PREPARATION AND PROPERTIES OF ZIRCONIA-TOUGHENED MULLITE CERAMICS, J.Am.Ceram.Soc.,1986,69(3),pp.265-67

43 Yuan,Q. et al. PROCESSING AND MICROSTRUCTURE OF MULLITE-ZIRCONIA COMPOSITES PREPARED FROM SOL-GEL POWDERS. J.Am.Ceram.Soc.,1986,69(3),pp.268-69

44 Schubert,H. ANISOTROPIC THERMAL EXPANSION COEFFICIENTS OF Y_2O_3-STABILIZED TETRAGONAL ZIRCONIA, J.Am.Ceram.Soc.,1986,69(3),pp.270-71

45 Catlow,C.R.A. et al. EXAFS STUDY OF YTTRIA-STABILIZED ZIRCONIA. J.Am.Ceram.Soc.,1986,69(3),pp.272-77

46 Mackrodt,W.C.; Woodrow,P.M. THEORETICAL ESTIMATES OF POINT DEFECT

ENERGIES IN CUBIC ZIRCONIA, J.Am.Ceram.Soc..1986.69(3).pp.277-80

47 Dominguez-Rodriguez,A. et al. PLASTIC DEFORMATION AND SOLID-SOLUTION HARDENING OF Y_2O_3-STABILIZED ZrO_2. J.Am.Ceram.Soc.,1986,69(3),pp.281-84

48 Dominguez-Rodriguez,A. et al. HIGH-TEMPERATURE PRECIPITATION HARDENING OF TWO-PHASE Y_2O_3-PARTIALLY-STABILIZED ZrO_2 SINGLE CRYSTALS: A FIRST REPORT. J.Am.Ceram.Soc..1986.69(3).pp.285-87

49 Claussen.N. et al. TETRAGONAL ZIRCONIA POLYCRYSTALS REINFORCED WITH SiC WHISKERS. J.Am.Ceram.Soc..1986.69(3).pp.288-92

50 McCoy.M. et al. CRYSTALLIZATION OF $MgO-Al_2O_3-SiO_2-ZrO_2$ GLASSES. J.Am.Ceram.Soc..1986.69(3).pp.292-96

51 McPherson.R. PREPARATION OF MULLITE-ZIRCONIA COMPOSITES FROM GLASS POWDER, J.Am.Ceram.Soc..1986,69(3).pp.297-98

52 Kagawa,M. et al. SURFACE CHARACTERIZATION OF ULTRAFINE ZrO_2-SiO_2 POWDERS BY ELECTROPHORETIC MOBILITY MEASUREMENTS, J.Am.Ceram.Soc.,1986,69(3),pp.C50-C51

53 Jaeger,H. et al. STRUCTURAL CHARACTERIZATION OF HIGH-TEMPERATURE ZIRCONIA CERAMICS BY PERTURBED ANGULAR CORRELATION SPECTROSCOPY. J.Am.Ceram.Soc..1986.69(6).pp.458-63

54 Swain,M.V.; Rose.L.R.F. STRENGTH LIMITATIONS OF TRANSFORMATION-TOUGHENED ZIRCONIA ALLOYS. J.Am.Ceram.Soc..1986.69(7).pp.511-18

55 Masaki,T. MECHANICAL PROPERTIES OF Y_2O_3-STABILIZED TETRAGONAL ZrO_2 POLYCRYSTALS AFTER AGEING AT HIGH TEMPERATURE. J.Am.Ceram.Soc..1986,69(7).pp.519-22

7.8 n. [illegible] 56 Witek,S.R.; Butler,E.P. ZIRCONIA PARTICLE COARSENING AND THE EFFECTS OF ZIRCONIA ADDITIONS ON THE MECHANICAL PROPERTIES OF CERTAIN COMMERCIAL ALUMINAS, J.Am.Ceram.Soc.,1986,69(7),pp.523-29

57 Hoagland,R.G.; Hirth,J.P. DILATANT CENTER-CRACK TIP INTERACTION EFFECTS,

J.Am.Ceram.Soc..1986.69(7).pp.530-33

58 Schmauder,S.; Schubert,H. SIGNIFICANCE OF INTERNAL STRESSES FOR THE MARTENSITIC TRANSFORMATION IN YTTRIA-STABILIZED TETRAGONAL ZIRCONIA POLYCRYSTALS DURING DEGRADATION. J.Am.Ceram.Soc.,1986,69(7),pp.534-40

59 Drennan,J.; Hannink,R.H.J. EFFECT OF SrO ADDITIONS ON THE GRAIN-BOUNDARY MICROSTRUCTURE AND MECHANICAL PROPERTIES OF MAGNESIA-PARTIALLY-STABILIZED ZIRCONIA. J.Am.Ceram.Soc.,1986,69(7),pp.541-46

60 Muddle,B.C.; Hannink,R.H.J. CRYSTALLOGRAPHY OF THE TETRAGONAL TO MONOCLINIC TRANSFORMATION IN MgO-PARTIALLY-STABILIZED ZIRCONIA. J.Am.Ceram.Soc..1986,69(7).pp.547-55

61 Hughan.R.R.; Hannink.R.H.J. PRECIPITATION DURING CONTROLLED COOLING OF MAGNESIA-PARTIALLY-STABILIZED ZIRCONIA. J.Am.Ceram.Soc..1986.69(7).pp.556-63

62 Lanteri.V. et al. MORPHOLOGY OF TETRAGONAL PRECIPITATES IN PARTIALLY STABILIZED ZrO_2, J.Am.Ceram.Soc..1986.69(7),pp.564-69

63 Wen,S. et al. TRANSMISSION ELECTRON MICROSCOPIC OBSERVATION OF THE MARTENSITIC PHASE TRANSFORMATION IN TETRAGONAL ZrO_2, J.Am.Ceram.Soc.,1986,69(7),pp.570-72

64 Weller,M.; Schubert,H. INTERNAL FRICTION. DIELECTRIC LOSS. AND IONIC CONDUCTIVITY OF TETRRAGONAL ZrO_2-3% Y_2O_3 (Y-TZP). J.Am.Ceram.Soc..1986.69(7),pp.573-77

65 Dworak.U. et al. DILATATION BEHAVIOR OF TWO DIFFERENTLY HEAT-TREATED COMMERCIAL MAGNESIA-PARTIALLY-STABILIZED ZIRCONIAS. J.Am.Ceram.Soc..1986.69(7).pp.578-79

66 Readev,M.J.; Readev,D.W. SINTERING OF ZrO_2 IN HCl ATMOSPHERES. J.Am.Ceram.Soc..1986,69(7).pp.580-82

67 Yoshimura,M. et al. DISSOLUTION AND REACTION OF YTTRIA-STABILIZED ZIRCONIA SINGLE CRYSTALS IN HYDROTHERMAL SOLUTIONS.

J.Am.Ceram.Soc..1986.69(7).pp.583-84

68 Masaki.T. MECHANICAL PROPERTIES OF TOUGHENED ZrO_2-Y_2O_3 CERAMICS. J.Am.Ceram.Soc..1986.69(8).pp.638-40

69 Sato.T. et al. TRANSFORMATION OF YTTRIA-DOPED TETRAGONAL ZrO_2 POLYCRYSTALS BY ANNEALING UNDER CONTROLLED HUMIDITY CONDITIONS. J.Am.Ceram.Soc..1986.69(12).pp.C320-C322

70 Miyayama,M. et al. EFFECTS OF Al_2O_3 ADDITIONS ON RESISTIVITY AND MICROSTRUCTURE OF YTTRIA-STABILIZED ZIRCONIA. Am.Ceram.Soc.Bull..1985,64(4),pp.660-64

71 Sato,T.; Shimada,M. TRANSFORMATION OF CERIA-DOPED TETRAGONAL ZIRCONIA POLYCRYSTALS BY ANNEALING IN WATER. Am.Ceram.Soc.Bull..1985.64(10).pp.1382-84

72 Tsukuma.K. & Ueda.K. HIGH-TEMPERATURE STRENGTH AND FRACTURE TOUGHNESS OF Y_2O_3-PARTIALLY-STABILIZED ZrO_2/Al_2O_3 COMPOSITES. J.Am.Ceram.Soc..1985.68(2).pp.C56-C58

73 Tsukuma.K. MECHANICAL PROPERTIES AND THERMAL STABILITY OF CeO_2 CONTAINING TETRAGONAL ZIRCONIA POLYCRYSTALS. Am.Ceram.Soc.Bull..1986.65(10).pp.1386-89

74 Ishizawa,H. et al. HOMOGENEOUS Y_2O_3-STABILIZED ZrO_2 POWDER BY SPRAY PYROLYSIS METHOD. Am.Ceram.Soc.Bull..1986,65(10).pp.1399-1404

75 Excell.J.A. & Marmach.M. REVERSIBLE CRYOGENICALLY INDUCED TETRAGONAL TO MONOCLINIC PHASE TRENSFORMATION IN Mg-PSZ. Am.Ceram.Soc.Bull..1986.65(10).pp.1404-7

76 Swain.M.V. INELASTIC DEFORMATION OF Mg-PSZ AND ITS SIGNIFICANCE FOR STRENGTH-TOUGHNESS RELATIONSHIP OF ZIRCONIA TOUGHENED CERAMICS. Acta Metall..1985.33(11).pp.2083-2091

77 Cambier.F. et al. FORMATION OF MICROSTRUCTURAL DEFECTS IN MULLITE-ZIRCONIA AND MULLITE-ALUMINA-ZIRCONIA COMPOSITES OBTAINED BY REACTION-

SINTERING OF MIXED POWDERS. Br.Ceram.Trans.J..1984.83.pp.196-200

78 Norman,C.J. et al. THE PREPARATION OF ZIRCONIA POWDERS. Br.Ceram.Trans.J.,1984,83

79 Stevens.R.; Yuksel.A. GRAIN-GRAIN BOUNDARY PRECIPITATION PHENOMENA AND RELATED MECHANICAL PROPERTIES IN DENSE (HOT-PRESSED) MgPSZ. Br.Ceram.Trans.J..1984.83.pp.146-150

80 De Portu.G.; Hennev.J.W. THE MICROSTRUCTURE AND MECHANICAL PROPERTIES OF MULLITE-ZIRCONIA COMPOSITES. Br.Ceram.Trans.J..1984.83(3).pp.69-72

81 Kemer,E.L.; Johnson,D.L. MICROWAVE PLASMA SINTERING OF ALUMINA, Am.Ceram.Soc.Bull.,1985,64(8).pp.1132-36

82 Fegley Jr.,B. et al. PROCESSING AND CHARACTERIZATION OF ZrO_2 AND Y-DOPED ZrO_2 POWDERS. Am.Ceram.Soc.Bull..1985.64(8),pp.1115-20

83 Matsumoto.R.L.K. STRENGTH RECOVERY IN DEGRADED YTTRIA-DOPED TETRAGONAL ZIRCONIA POLYCRYSTALS. J.Am.Ceram.Soc..1985.68(8).pp.C213

84 Matsui.H. et al. MICROSTRUCTURE AND MECHANICAL PROPERTIES OF Al_2O_3. Si_3N_4. SiC. AND ZrO_2(PSZ) CERAMICS FOR SLURRY VALVES. Zairyo.1986.35(388).pp.41-7

85 Koehler.E.K. THE STRUCTURE AND PROPERTIES OF REFRACTORY ZIRCONIA CERAMICS: III. STUDIES OF TECHNICAL PROPERTIES OF MATERIALS AND TECHNOLOGICAL ELABORATIONS.. Ceram.Int.,1985.11(1).pp.3-12

86 Ado,G. et al. MECANISME DE FRITTAGE SOUS CHARGE DU NITRURE D'ALUMINIUM ET DE L'OXYNITRURE AlON-g. Rev.Chim.Miner..1985,22(4),pp.473-83

87 Lefort,P. et al. SUR LA FORMATION DU NITRURE D'ALUMINIUM A PARTIR D'ALUMINE EN PRESENCE DE CARBONE. Rev.Chim.Miner..1985.22(4).pp.534-45

88 Gauthier.G. et al. INFLUENCE DE TRES FAIBLES TENEURS D'AJOUTS (CaO ET Y_2O_3) SUR LA DENSIFICATION DU NITRURE D'ALUMINIUM PAR FRITTAGE SOUS CHARGE ENTRE 1650 ET 1750°C. C.R.Acad.Sci..Ser.2.1985.301(3).pp.135-8

89 Jones,R.L. et al. SULFATION OF CeO_2 AND ZrO_2 RELATING TO HOT CORROSION, J.Electrochem.Soc.,1985,132(6),pp.1498-501

90 Claussen,N. FRACTURE TOUGHNESS OF Al_2O_3 WITH AN UNSTABILIZED ZrO_2 DISPERSED PHASE, J.Amer.Ceram.Soc.,1976,59(1-2),pp.49-51

91 Claussen,N. INDUCED TRANSFORMATIONS OF TETRAGONAL ZrO_2 PARTICLES IN CERAMIC MATRICES. J.Amer.Ceram.Soc..1978,61(1-2).pp.85-86

92 Claussen,N. & Jurgen,J. MECHANICAL PROPERTIES OF SINTERED AND HOT-PRESSED Si_3N_4-ZrO_2 COMPOSITES. J.Amer.Ceram.Soc..1978.61(1-2),pp.94-95

93 Claussen,N. & Jurgen.J. MECHANICAL PROPERTIES OF SINTERED, IN SITU-REACTED MULLITE-ZIRCONIA COMPOSITES,J.Amer.Ceram.Soc.,1980,63(3-4),pp.228-29

1 Kronert,W. et al. SEM INVESTIGATIONS ON THE MORPHOLOGY AND SINTERING OF HIGH PURITY ALUMINA FROM DIFFERENT MANUFACTURING PROCESSES.
CeramicPowders,edited by Vicenzini,P.,1983,Elsevier,pp.391-400

2 Li,W.I. et al. PREPARATION OF SOME HIGH PURITY ULTRAFINE NON-OXIDE POWDERS,
CeramicPowders,edited by Vicenzini,P.,1983,Elsevier,pp.403-412

3 Claussen,N. et al. RAPID SOLIDIFICATION OF Al_2O_3-ZrO_2 CERAMICS,
CeramicPowders,edited by Vicenzini,P.,1983,Elsevier,pp.489-497

4 Reynen,P. et al. THE USE OF EMULSIONS IN THE PREPARATION OF CERAMIC POWDERS,
CeramicPowders,edited by Vicenzini,P.,1983,Elsevier,pp.499-504

5 Roettenbacher,R.; Schmidberger,R. PREPARATION OF SPECIAL CERAMICS FOR HIGH TEMPERATURE APPLICATIONS.
CeramicPowders,edited by Vicenzini,P.,1983,Elsevier,pp.539-546

6 Meriani,S.; Soraru,G. ULTRA FINE CERIA ZIRCONIA POWDERS OBTAINED VIA METALLORGANIC PRECURSORS,
CeramicPowders,edited by Vicenzini,P.,1983,Elsevier,pp.547-554

7 Kungang,C. et al. DENSE CONDUCTIVE b"-Al_2O_3 CERAMICS BY GEL METHOD,
CeramicPowders,edited by Vicenzini,P.,1983,Elsevier,pp.587-592

8 Pampuch,R.; Haberko,K. AGGLOMERATES IN CERAMIC MICROPOWDERS AND THEIR BEHAVIOUR ON COLD PRESSING AND SINTERING.
CeramicPowders,edited by Vicenzini,P.,1983,Elsevier,pp.623-634

9 Lange,F.F. FORMATION OF CRACK-LIKE VOIDS AND AGGLOMERATE MOBILITY DUE TO DIFFERENTIAL SINTERING.
CeramicPowders,edited by Vicenzini,P.,1983,Elsevier,pp.635-649

10 van de Graaf,M.A.G.G. et al. MICROSTRUCTURAL DEVELOPMENT DURING PRESSING AND SINTERING OF ULTRA FINE ZIRCONIA POWDERS,

CeramicPowders.edited by Vicenzini.P..1983.Elsevier.pp.783-794

11 Kato.A. et al. SINTERING BEHAVIOR OF b"-ALUMINA POWDERS PREPARED BY SPRAY-PYROLYSIS TECHNIQUE.
CeramicPowders.edited by Vicenzini.P..1983.Elsevier.pp.835-841

12 Bennison.S.J.; Harmer.M.P. MICROSTRUCTURAL STUDIES OF ABNORMAL GRAIN GROWTH DEVELOPMENT IN Al_2O_3.
CeramicPowders.edited by Vicenzini.P..1983.Elsevier.pp.929-938

13 Kosmac,T. et al. MICROSTRUCTURE AND MECHANICAL PROPERTIES OF Al_2O_3-ZrO_2 COMPOSITES, J.Amer.Ceram.Soc..1982,65(5),pp.C66-67

14 Watanabe,T.; Shoubu.K. MECHANICAL PROPERTIES OF HOT-PRESSED TiB_2-ZrO_2 COMPOSITES. J.Amer.Ceram.Soc..1985.68(2).pp.C34-36

15 Tsukuma.K. et al. STRENGTH AND FRACTURE TOUGHNESS OF ISOSTATICALLY HOT-PRESSED COMPOSITES OF Al_2O_3 AND Y_2O_3-PARTIALLY-STABILIZED ZrO_2. J.Amer.Ceram.Soc..1985.68(1).pp.C4-5

16 Feolev Jr.,B. et al. PREPARATION OF ZIRCONIA-ALUMINA POWDERS BY ZIRCONIUM ALKOXIDE HYDROLYSIS.
J.Amer.Ceram.Soc..1985.68(2).pp.C60-62

17 Schioler.L.J. WORKSHOP STUDIES CERAMIC ENGINES - CURRENT STATUS AND FUTURE, Am.Ceram.Soc.Bull..1985,64(2).pp.269-70

18 *** BASIC SCIENCE DIVISION. Am.Ceram.Soc.Bull..1977,56(3),pp.289

19 Yoshimura.M.; Somiya.S. FABRICATION OF DENSE. NONSTABILIZED ZrO_2 CERAMICS BY HYDROTHERMAL REACTION SINTERING.
Am.Ceram.Soc.Bull..1980.59(2).pp.246

20 Evans.J.R.G. et al. THERMAL SHOCK OF b-ALUMINA WITH ZIRCONIA ADDITIONS. J.Mater.Sci..1984.19.pp.4068-4076

21 Lange.F.F. TRANSFORMATION TOUGHENING PART 1 SIZE EFFECTS ASSOCIATED WITH THE THERMODYNAMICS OF CONSTRAINED

TRANSFORMATIONS. J.Mater.Sci..1982.17.pp.225-234

22 Lange,F.F. TRANSFORMATION TOUGHENING PART 2 CONTRIBUTION TO FRACTURE TOUGHNESS. J.Mater.Sci..1982.17.pp.235-239

23 Lange.F.F. TRANSFORMATION TOUGHENING PART 3 EXPERIMENTAL OBSERVATIONS IN THE ZrO_2-Y_2O_3 SYSTEM. J.Mater.Sci..1982.17.pp.240-246

24 Lange,F.F. TRANSFORMATION TOUGHENING PART 4 FABRICATION. FRACTURE TOUGHNESS AND STRENGTH OF Al_2O_3-ZrO_2 COMPOSITES. J.Mater.Sci..1982.17,pp.247-254

25 Lange,F.F. TRANSFORMATION TOUGHENING PART 5 EFFECT OF TEMPERATURE AND ALLOY ON FRACTURE TOUGHNESS. J.Mater.Sci..1982.17.pp.255-262

26 Yoshikawa.N.; Ikeda.S. HIGH-STRENGTH PARTIALLY STABILIZED ZIRCONIA COMPACT OBTAINED BY CENTRIFUGAL CONSOLIDATION. J.Mater.Sci.Lett.,1986.5.pp.849-51

27 Hori.S. et al. CHANGE OF TETRAGONAL ZrO_2 CONTENT IN ZrO_2-TOUGHENED Al_2O_3 BY HOT ISOSTATIC PRESSING. J.Mater.Sci.Lett..1984.3.pp.242-44 Al_2O_3, ZrO_2

28 Swain,M.V. et al. MATERIAL DEVELOPMENT AND EVALUATION OF PARTIALLY STABILIZED ZIRCONIA FOR EXTRUSION DIE APPLICATIONS. Proc.Br.Cer.Soc..1982.32.pp.343-53

29 Hunold.K. HOT ISOSTATIC PRESSING OF HIGH TEMPERATURE CERAMICS. InterCeram,1985.34(2).38.pp.40-3

30 Kobavashi,K. et al. PHASE CHANGE AND MECHANICAL PROPERTIES OF ZrO_2-Y_2O_3 SOLID ELECTROLYTE AFTER AGEING. SolidStateIonics.1981.(3/4).pp.489-93

31 Niihara.K. et al. EVALUATION OF K_{IC} OF BRITTLE SOLIDS BY THE INDENTATION METHOD WITH LOW CRACK-TO-INDENT RATIOS. J.Mater.Sci.Lett..1982.1.pp.13-16

32 Scott,H.G. PHASE RELATIONSHIPS IN THE ZIRCONIA-YTTRIA SYSTEM. J.Mater.Sci..1975.10.pp.1527-35

33 Gupta,T.K. et al. STABILIZATION OF TETRAGONAL PHASE IN POLYCRYSTALLINE ZIRCONIA. J.Mater.Sci..1977.12.pp.2421-26

34 Gupta.T.K. et al. EFFECT OF STRESS-INDUCED PHASE TRANSFORMATION ON THE PROPERTIES OF POLYCRYSTALLINE ZIRCONIA CONTAINING METASTABLE TETRAGONAL PHASE. J.Mater.Sci..1978.13.pp.1464-70

35 Rieth.P.H. et al. FABRICATION AND FLEXURAL STRENGTH OF ULTRAFINE-GRAINED YTTRIA-STABILIZED ZIRCONIA. Am.Ceram.Soc.Bull..1976.55(8).pp.717-21.27

36 Lewis III.D. et al. PROCESSING DEFECTS IN PARTIALLY STABILIZED ZIRCONIA, Am.Ceram.Soc.Bull..1980.59(2).pp.244-5

37 Munz,D. et al. FRACTURE TOUGHNESS DETERMINATION OF Al_2O_3 USING FOUR-POINT-BEND SPECIMENS WITH STRAIGHT-THROUGH AND CHEVRON NOTCHES, J.Amer.Ceram.Soc..1980.63(5-6).pp.300-5

38 Becher,P.F. TRANSIENT THERMAL STRESS BEHAVIOR IN ZrO_2-TOUGHENED Al_2O_3, J.Amer.Ceram.Soc..1981.64(1).pp.37-39

39 Kosmac.T. et al. X-RAY DETERMINATION OF TRANSFORMATION DEPTHS IN CERAMICS CONTAINING TETRAGONAL ZrO_2. J.Amer.Ceram.Soc..1981.64(4).pp.C72-73

40 Kirchner.H.P. et al. CRACK BRANCHING IN TRANSFORMATION-TOUGHENED ZIRCONIA. J.Amer.Ceram.Soc..1981.64(9).pp.529-33

41 Mussler,B. et al. DEPENDENCE OF FRACTURE TOUGHNESS OF ALUMINA ON GRAIN SIZE AND TEST TECHNIQUE. J.Amer.Ceram.Soc..1982,65(11).pp.566-72

42 Claussen,N. et al. SLOW GROWTH OF MICROCRACKS: EVIDENCE FOR ONE TYPE OF ZrO_2 TOUGHENING. J.Amer.Ceram.Soc..1982,65(11).pp.C190-91

43 Green.D.J. CRITICAL MICROSTRUCTURES FOR MICROCRACKING IN Al_2O_3-ZrO_2 COMPOSITES. J.Amer.Ceram.Soc..1982.65(12).pp.610-14

44 Heuer.A.H. et al. STABILITY OF TETRAGONAL ZrO_2 PARTICLES IN CERAMIC MATRICES. J.Amer.Ceram.Soc..1982.65(12),pp.642-50

45 Butler.E.P.: Heuer.A.H. X-RAY MICROANALYSIS OF ZrO_2 PARTICLES IN ZrO_2-TOUGHENED Al_2O_3. J.Amer.Ceram.Soc..1982.65(12).pp.C206-7

46 Ingel.R.P. et al. TEMPERATURE DEPENDENCE OF STRENGTH AND FRACTURE TOUGHNESS OF ZrO_2 SINGLE CRYSTALS. J.Amer.Ceram.Soc..1982.65(9).pp.C150-2

47 Dole.S.L.: Hunter Jr..O. ELASTIC PROPERTIES OF HAFNIUM AND ZIRCONIUM OXIDES STABILIZED WITH PRASEODYMIUM OR TERBIUM OXIDE. J.Amer.Ceram.Soc..1983.66(3).pp.C47-49

48 Lange.F.F. PROCESSING-RELATED FRACTURE ORIGINS: I. OBSERVATIONS IN SINTERED AND ISOSTATICALLY HOT-PRESSED Al_2O_3/ZrO_2 COMPOSITES. J.Amer.Ceram.Soc..1983.66(6).pp.396-98

49 Shimada.M. et al. TEMPERATURE DEPENDENCE OF YOUNG'S MODULUS AND INTERNAL FRICTION IN ALUMINA. SILICON NITRIDE. AND PARTIALLY STABILIZED ZIRCONIA CERAMICS. J.Amer.Ceram.Soc..1984.67(2).pp.C23-24